Antiferromagnetism and Superconductivity in Correlated Electron Systems

by

Hiroshi Shimahara

Submitted in partial fulfillment of the requirements for the degree of Doctor of Science in Doctoral Program in University of Tsukuba

January, 1990

PREFACE

Effects of electron correlations on superconductivity have been studied since the BCS theory (1957). In the original BCS theory, in which the electron-phonon interaction is regarded to be a unique mechanism for superconductivity, the repulsive Coulomb interaction between electrons is considered only to suppress superconductivity. However later Kohn and Luttinger (1965) pointed out a possibility of superconductivity not induced by the electron-phonon interaction. The first experimental support of this kind of superconductivity was the discovery of anisotropic superfluidity in liquid He^3 in 1972. This experiment strongly suggested a triplet pairing superfluidity enhanced by exchange of the ferromagnetic spin-fluctuations, namely, the paramagnon exchange interaction. The paramagnon theory and other spin-fluctuation theories are very successful in explaining properties of nearly ferromagnetic metals and liquid He^3.

Furthermore, antiferromagnetic spin-fluctuations has also been studied recently by many authors. This is because there is a possibility that the antiferromagnetic spin-fluctuations enhance superconductivity in heavy fermion compounds and quasi-one-dimensional organic superconductors. Further, the high temperature superconductivity in copper oxides has also been arousing the current interest in superconductivity enhanced by some magnetic interaction. Although these three types of superconductors have many different properties in many respects,

they have common important features in their superconductivity. The most remarkable similarities are that all of them are nearly antiferromagnetic, and that evidences for anisotropic superconductivity such as d-wave pairing have been found in many experiments.

Thus electron systems with short range repulsive interactions have been studied extensively in connection with interplay and competition between magnetism and superconductivity. These systems are regarded as important models which exhibit various correlation effects in wide range of interaction strength; from weak limit to strong limit. For the organics it is almost established that the conduction electrons are in weak correlation regime, and their antiferromagnetism is due to spin density wave (SDW). The SDW and magnetic field induced SDW in the organics have been understood by means of mechanism of the Fermi-surface nesting. In the heavy fermion compounds, various physical quantities are well-described in the Fermi-liquid theory as well, although f-electrons in them are strongly interacting with each other and hence the effective mass of quasi-particles is extraordinary large. For the oxides, on the other hand, large sublattice magnetization has been observed in their antiferromagnetic phase. Thus it has been argued that the electrons are strongly correlated in these compounds, and strong coupling models have been studied for them.

The problem of magnetism itself besides the interplay with the superconductivity is also of interest. Magnetic properties of the Hubbard model have been a longstanding problem in solid state physics. Many researchers have studied ferromagnetism and

antiferromagnetism, as well as the Mott-Hubbard transition in this model. After the mean-field theories by Slater (1936), Stoner (1938), and Penn (1966), much work has been carried out to take into account the electron correlation effects by such as Hubbard (1963~1964), Gutzwiller (1963~1965), and Kanamori (1963). The paramagnon theory mentioned before is another approach to treat electron correlation effects, which is effective to describe nearly ferromagnetic systems.

This thesis reports our study on magnetism and superconductivity both in the weak coupling regime and strong coupling regime. For the weak coupling regime, we study the weak coupling Hubbard model, while for the strong coupling regime, we analyse the t-J model. The t-J model can be derived from the extended Hubbard model describing electrons on the CuO_2 planes of the oxides in a strong coupling limit. It can be also derived from the strong coupling single band Hubbard model. Our study is performed in two ways, that is, a weak coupling theory similar to the paramagnon theory in nearly antiferromagnetic systems and a Green's function decoupling theory based on a strong coupling model. We will contrast and compare the results obtained in the weak coupling and the strong coupling systems. We discuss our result in relation to the characteristic properties in the organics and the oxides.

For the organics we obtain a theoretical phase diagram which qualitatively agrees with the experimental phase diagrams. For the t-J model, we reproduce rapid change of the magnetism from localized one to itinerant one and drastic suppression of the antiferromagnetic transition temperature when the electron

concentration deviates from half-filling slightly. On the other hand, for superconductivity, it is suggested that high temperature superconductivity is difficult to occur in the single band Hubbard model with only nearest neighbour hopping both in the weak and the strong coupling regimes. However it is also found that superconductivity is remarkably enhanced by electron hopping between next nearest neighbour sites in quasi-two-dimensional Hubbard model in the weak coupling regime. This result seems to suggest that some kind of frustration to the antiferromagnetism may enhance superconductivity.

H.Shimahara

Institute of Physics, University of Tsukuba

30 December 1989

Acknowledgment

I would like to thank Professor Satoshi Takada for valuable instruction, suggestion, and stimulating discussions.

I would like to thank Prof. Fumihiko Takano for valuable discussions, instruction, and advices. I wish to thank Dr. Kenn Kubo for valuable discussions and helpful instruction. I also wish to thank Prof. Hajime Takayama for valuable discussions.

I would like to thank Prof. Katsurou Sawada for helpful instructions and advices.

I am very grateful to other members of Institute of Physics in University of Tsukuba for discussions, instructions, and encouragement.

I would like to express my sincere thanks to Dr. Morinori Yaotome for encouragement and valuable instruction in Aoyama High School.

I wish to acknowledge financial support of Iwanami-Fujukai.

Lastly I would like to thank my parents for encouragement.

List of papers published for the requirement of the Degree.

(1) Local Interactions and van Hove Singularities in High-T_c Superconductors.

H.Shimahara and S.Takada: Jpn.J.Appl.Phys. **26**(1987)L1674.

(2) Superconductivity and Spin-Density-Wave in Two-Dimensional Hubbard Model.

H.Shimahara and S.Takada: J.Phys.Soc.Jpn. **57**(1988)1044.

(3) Long-Range Spin-Fluctuations and Superconductivity in Quasi-One-Dimensional Organic Compounds.

H.Shimahara: J.Phys.Soc.Jpn. **58**(1989)1735.

(4) Long-Range Spin-Fluctuations and Superconductivity in the Quasi-One-Dimensional Hubbard Model.

H.Shimahara: in Proceeding of the Physics and Chemistry of Organic Superconductors, edited by G.Saito and S.Kagoshima (Springer-Verlag, Berlin, Heidelberg, New York, to be published)

(5) Magnetic Properties of the Strong Coupling Hubbard Model.

H.Shimahara, S.Misawa, and S.Takada: J.Phys.Soc.Jpn. **58**(1989)801.

(6) Magnetic Properties and Superconductivity of the Strong Coupling Hubbard Model.

H.Shimahara, S.Misawa, and S.Takada: J.Phys.Soc.Jpn. **58** (1989) 4168.

(7) Magnetic Properties and Superconductivity of the t-J model.

H.Shimahara, S.Misawa, and S.Takada: Proceeding of the Tsukuba Seminar on High-T_c Superconductivity, edited by K.Masuda, T.Arai, I.Iguchi, and R.Yoshizaki (Univ.Tsukuba, Tsukuba, 1989), pp.73~78.

CONTENTS

Chapter 1.

Introduction

§1.1 Heavy Fermion, Organic, and Oxide Superconductors

Magnetic properties and superconductivity of electron systems with short range repulsive interaction have been studied for a long time and also have attracted current interest in connection with the exotic superconductors such as heavy-fermion compounds,[1-4] organic superconductors,[5-11] and copper oxide high-T_c superconductors.[12-17] They exhibit some similar characteristics, such as the anisotropy of the pair wave functions and proximity of the antiferromagnetic (AF) and the superconducting phases, although they exhibit many differences in many other properties, such as effective mass, transition temperatures, conductivity, and itinerant or localized nature, which fact arises from the differences in dimensionality, lattice structure, interaction strength, hopping parameters, electron concentration, and so on. The striking similarities are observed in the following experiments and give rise to a new aspect in the problem of the competition and the interplay between magnetism and superconductivity.

Anisotropic superconductivity has been suggested by the experiments of NMR relaxation rate[18-21] and accoustic atttenuation rate,[22-24] in the heavy fermion compounds UBe_{13},[18,22] $CeCu_2Si_2$,[19] and UPt_3,[23,24] and the quasi-one-dimensional (quasi-1D) organic superconductor $(TMTSF)_2ClO_4$.[20,21] The nuclear relaxation rates of the oxides La-Sr-Cu-O,[25] Y-Ba-Cu-O,[26-29] and Bi-Pb-Sr-Ca-Cu-O [30] also exhibit power law behaviour just below T_c, which also suggests a gapless anisotropic superconductivity.

The measurements of the lower critical magnetic field[31-34] and the specific heat[35] also suggest the anisotropic superconductivity in the heavy fermion compound $U_{1-x}Th_xBe_{13}$,[31,35] and in the oxides Y-Ba-Cu-O. It is found from their temperature dependence that another superconducting transition appears to occur at a temperature below the true superconducting transition temperature. This can be explained by assuming some kind of abrupt change of the gap function, which seems to imply an anisotropic superconductivity.[36,37]

Furthermore, the proximity of the superconductivity and the AF instability is observed in many compounds such as the heavy fermion compounds UPt_3[38,39] and $CeCu_2Si_2$, the quasi-1D organics $(TMTSF)_2X$ (with $X=PF_6$, AsF_6, SbF_6, TaF_6)[6-8] and $(DMET)_2X$ (with $X=Au(CN)_2$, AuI_2, $AuCl_2$)[9-11] and the oxides La-Sr-Cu-O,[40] Nd-Ce-Cu-O,[41] Y-Ba-Cu-O,[42] and Bi-Sr-Ca-Y-Cu-O.[43] Phase diagrams of the normal, the AF, and the superconducting phase were obtained for them. In the phase diagrams of the organics, the superconducting and the SDW phase exist on the border of each other, while in most of the other phase diagrams, there is a normal region between the AF and the superconducting phase.

For $(TMTSF)_2X$ and $(DMET)_2X$ families, the existence of the SDW is remarkable because most of the other quasi-1D organics such as TTF·TCNQ exhibit Peierls transition but neither superconductivity nor SDW.[7] On the other hand, in Ba-Pb-Bi-O [44,45] and Ba-K-Bi-O,[46,47] superconductivity occurs near the CDW instability, while superfluidity in liquid He^3 occurs near ferromagnetic instability.[48,49]

These experimental facts have been arousing much interest in the superconductivity enhanced by some magnetic interaction induced by electron correlations. Moreover, this is supported by the fact that the isotope effect of the copper oxide superconductors[50-53] does not exhibit the behaviour expected from theories based on phonon mediated pairing. Thus a number of theoretical studies[54-64] have been devoted to magnetism and superconductivity of the Hubbard model, which is the simplest but could nevertheless describe various situations of correlated electrons.

However these three compounds have differences as well. For example, for the the organic superconductors $(TMTSF)_2X$ and $(DMET)_2X$ families, the itinerant property of electrons seems to be established by conductivity measurements,[5] observations of itinerant antiferromagnetism,[5-11,65,66] and others.[6-8] On the other hand for the oxide superconductors, analyses based on the one particle picture for the experiments sometimes give inconsistent results, and it has been suggested that some strong correlation models seem to be appropriate[67] from the hole coefficient measurement,[68-72] the observations of large sublattice-magnetization,[73-75] photo-emission spectro-scopies.[76-79] In

addition, for the heavy fermion systems, although the quasi-particles are extremely heavy owing to strong correlations, the Fermi-liquid theory gives a consistent picture to the analyses of the experimental results of specific heat, susceptibility, and so on.[4)]

Thus in a context of the Hubbard model, the weak coupling model would be appropriate to the organics, while the strong or intermediate coupling model and the t-J model would be useful in the study of the oxides. In fact, the weak coupling Hubbard model has been successful in explaining the SDW in the organics in many respects,[80-82)] and the t-J model have been derived from the extended Hubbard model on the CuO_2 plane, so-called d-p model, in a limiting case appropriate for the oxides.[83,84)] As for the oxides, it has been also argued that some essential nature of realistic lattice structure of Cu_2O plane may be needed to be taken into account in reproducing the high-T_c superconductivity,[85-92)] and thus the d-p model[89,90)] and coupled spin-fermion systems[91)] have been studied.

Furthermore the quasi-low-dimensionality is another important point of this problem. The quasi-low-dimensionality causes the following two specific features. First, in the itinerant electron system, shape of the Fermi-surface and density of states (DOS) are quite important to the physical properties at low temperatures. In particular in low-dimensional systems, van Hove singularities and Fermi-surface nesting are characteristic. Secondly, another specific feature is that the low-dimensionality suppresses magnetic ordering and superconductivity, when the corresponding quasi-long-range order grows.

As for the quasi-1D organics, which would be an itinerant systems, the above two points have to be investigated. However, as far as at the low temperatures which the SDW and the superconductivity concern, it is almost established that the three-dimensional (3D) interactions are strong enough to suppress the thermal fluctuations and that the system is essentially 3D in critical phenomena.[80,92] On the other hand, for the oxides, it has been suggested that there is a quasi-long-range AF order[93,94] above the low temperature phases, which fact reflects the weak inter-plane coupling.[95] In addition, it would be plausible that the suppression of antiferromagnetism and that of superconductivity due to the quasi-low-dimensionality are quite different, because there is a Kosteritz-Thouless transition to superconductivity but no antiferromagnetic transition in two dimensional systems at finite temperatures.

In this paper, we study the magnetic properties and the superconductivity in the Hubbard model and the t-J model in itinerant and localized electron regimes in connection with the organics and the oxides.

Here it should be added that there are many other organic superconductors, such as (BEDT·TTF)$_2$X family,[8,96] in which the AF phase has not been observed. These compounds exhibit many interesting features, but we does not examine them in this paper. Furthermore, as for the oxides, the two-band nature may be essential for the high-T_c superconductivity as mentioned above. However we mainly study single band models in this thesis.

In the rest of this chapter, we briefly review theories of correlated electron systems, especially those of the Hubbard

model. In chapter 2, we study electron systems on square lattices with n.n. and n.n.n. hopping from the side of the weak coupling theory. First, we examine the free electrons system and the electron system with some local attraction. Second, we examine the Hubbard model by means of a perturbation theory and effect of the n.n.n. hopping. The chapter 2 contains our papers published in ref.97 and 98 and unpublished results. In chapter 3, we study the superconductivity enhanced by the AFSF in quasi-1D organic compounds. For example, a theoretical phase diagram and momentum dependence of gap function are obtained. The study of this chapter has been presented in our papers of ref.99. In chapter 4, the t-J model is studied in an improved Hubbard III approximation, which is valid for the strong correlation regime. For example, we calculate susceptibility, antiferromagnetic and superconducting transition temperatures. This chapter contains our three papers of ref.100 and unpublished results. The last chapter is devoted to summary and discussion.

§1.2 Hubbard model

The Hubbard model is a longstanding subject of interest as a fundamental model of correlated electron systems, and a number of studies have been made for the problems on Mott-Hubbard transition, magnetic properties, and superconductivity in this model, by means of mean field approximation,[101-103] Green's function decoupling schemes,[104-108] variational methods,[109-116] perturbation in weak correlation regime,[117-125] exact diagonalization of finite size systems,[126,127] quantum simulations,[128-135] exact solution for one-dimensional systems,[136-143] and others.[144-157] The Hubbard Hamiltonian is defined by

$$H = \sum_{i,j,\sigma} t_{ij} c^{\dagger}_{i\sigma} c_{j\sigma} + U \sum_{i} n_{i\alpha} n_{i\beta} , \qquad (1.1)$$

where U denotes the on-site Coulomb repulsion implying the electron screening by the electrons which do not participate in the formation of the electron band. Justification of this model is given in ref.104.

In the strong coupling regime it reduces to the t-J model up to the order of t^2/U:

$$H = \sum_{i,j,\sigma} t_{ij} \tilde{c}^{\dagger}_{i\sigma} \tilde{c}_{j\sigma} + \sum_{i,j} 2J_{ij} (S_i \cdot S_j - \frac{1}{4} n_i n_j) , \qquad (1.2)$$

where we assume $t_{ij}=-t$ for nearest neighbor (n.n.) sites (i,j) and otherwise zero and we define $\tilde{c}_{i\sigma} \equiv (1-n_{i-\sigma}) c_{i\sigma}$, $n_{i\sigma} \equiv c^{\dagger}_{i\sigma} c_{i\sigma}$, $S_i \equiv \sum_{\sigma',\sigma''} 1/2 \cdot c^{\dagger}_{i\sigma'} \sigma_{\sigma'\sigma''} c_{i\sigma''}$, $n_i \equiv n_{i\alpha} + n_{i\beta}$, and $J_{ij} \equiv J \equiv t^2/U$ for n.n. sites (i,j) and otherwise $J_{ij} \equiv 0$. This model describes the

electron motions which is restricted by the strong Coulomb repulsion, as well as the kinetic exchange interactions. More generally the t-J model can describe other strongly correlated electron systems such as the d-p model in some strong coupling limit,[83,84] although then the expression of J is no longer t^2/U.

The physics of the Hubbard model varies with its lattice structure, values of the parameters t_{ij} and U, and electron concentration. For example, as the interaction U becomes stronger and as the electron number approaches half-filling, the electrons become to have localized nature, that is, the length of the phase coherence of the quasi-particles becomes shorter. In particular in the strong correlation limit, namely in the half-filled and sufficiently large U regime, the electrons are completely localized and the system is insulating even before undergoing AF ordering. This metal-insulator transition called Mott-Hubbard transition is reproduced with Hubbard's decoupling scheme[106] and Brinkman and Rice's theory.[112]

On the other hand, as the interaction U becomes weaker or as the electron number reduces from the half-filling, the electrons tend to be itinerant.

In the localized electron case, the antiferromagnetism is a localized one, in which the spin-moment is large, and then the spin-susceptibility in the paramagnetic phase increases with decreasing temperature. In particular, at half-filling and in large U limit, the Hubbard Hamiltonian reduces to the AF Heisenberg Hamiltonian:

$$H = \sum_{i,j} 2J_{ij}\mathbf{S}_i \cdot \mathbf{S}_j \ . \qquad (1.3)$$

This model has its own vast field of theoretical study.[158-166] The mean-field approximation gives the susceptibility which obeys the Curie-Weiss law.

On the other hand, in the itinerant electron case, the antiferromagnetism is itinerant one, i.e. SDW, and the spin-susceptibility would become a Pauli-paramagnetic one.

Moreover, property of superconductivity in correlated electron systems would also change depending on whether the electrons are itinerant or localized. In the itinerant systems, i.e. in metallic systems, superconductivity occurs easily in the presence of some attractive interaction, as the BCS theory showed.[167] In this case, long-range nature and retardation of the interaction are essential for the appearance of superconductivity, and it is well-known that the coherence length of pair wave function is semi-macroscopically large.

However as the electrons become more localized, the coherence length becomes shorter. The coherence length is roughly v_F/T_c in the BCS theory, where v_F is the Fermi-velocity and T_c is the superconducting transition temperature. In the localized electron case, v_F may not be well-defined and it should be noted that the coherence length could not be estimated by v_F/T_c no longer. Furthermore, as the insulating phase is approached with the Coulomb interaction strengthened or half-filling approached, the superconducting phase would disappear.

Both in the itinerant and the localized case, mechanisms of the superconductivity enhanced by some magnetic interaction have been studied by many authors.[54-58,60-64,119,120] In the

former case, it has been pointed out that the AF spin-fluctuations asisted by the Fermi-surface nesting may enhance the superconductivity near the SDW instability,[55-57,60] while in the later case, the kinetic or super-exchange interaction leads to the n.n. attractive interaction.[61-64] Further, a new type of superconducting transition from the insulating phase has been argued.[61-63]

§1.3 Antiferromagnetism.

A physical origin of the antiferromagnetism in itinerant systems such as metal Cr and Mn is Fermi-surface nesting, and that in localized ones, which is observed in insulators such as transition metal oxides MnO, FeO, CoO, and NiO, is kinetic or super exchange interaction, as mentioned before. These pictures, which are quite different from each other, can be studied as opposite limiting cases of some unified mechanism in the Hubbard model, and the AF transition temperature T_{AF} would take a maximum in the intermediate region. In fact in the quantum simulation of the Hubbard model on a cubic lattice for the half-filled band case by Hirsch,[131] T_{AF} takes maximum value about W/18 around U~5W/6, where W denotes band width 12t.

For the half-filled band sector, existence of the antiferromagnetic long-range-order (LRO) is plausible for bipartite lattice structures except 1D case, in which the ground state was proved to be antiferromagnetic without LRO.[136,137]

In the weak coupling regime perfect nesting of Fermi-surface necessarily leads to the AF instability in repulsive systems, although even then existence of the AF LRO is not obvious in 2D cases. However for the half-filled Hubbard model on a square lattice with only n.n. hopping, Hirsch suggested that the AF LRO exists for all values of U using Monte-Carlo simulation.[129] On the other hand, in the strong coupling regime, our model reduces to the AF Heisenberg model. The existence of the AF LRO in the AF Heisenberg model was rigorously proved by Kennedy et al. for the 3D (quasi-2D) systems with the exchange coupling $J_x=J_y$, $J_z=rJ_x$

with $0.16 \leq r \leq 1$.[158] The AF transition temperature was estimated by high-temperature series expansion as $T_{AF} \cong 3.83t^2/U$ for the cubic lattice.[159] For the 2D AF Heisenberg model, the exact diagonalization study of the finite size system ($\leq$16sites) on the square lattice by Oitmaa and Betts indicates the LRO.[160] Further the Monte-Carlo simulation (12x12) by Reger et al. supports the existence of the LRO and they estimated the staggered magnetization as $m=0.30\pm0.02$,[161] which is consistent with the result of spin-wave theory[162] and an analysis of the perturbation expansion from the Ising limit by Huse.[163]

It is almost established that La_2CuO_4, which has the one electrons par lattice site on the CuO_2 layer, can be described very well by quasi-2D spin-1/2 AF Heisenberg model with n.n. exchange interaction, and the inter-plane coupling is estimated to be very weak.[95] Observed values of the staggered magnetization[73-75] agree with the theories mentioned above.[161-163] Such a large value of the staggered magnetization is in contrast to that in SDW phase.

On the other hand, for unbipartite lattice structure there would be a critical U value below which the system does not undergo the AF LRO, even at half-filling. The n.n.n. hopping worsens the Fermi-surface nesting in weak coupling regime and suppresses the SDW transition. On the other hand in strong coupling regime, it leads to an AF coupling between spins on n.n.n. site and causes frustration to AF correlations. In fact, Lin et al. showed that the critical U exists in the 2D Hubbard model on a square lattice with n.n. and next-nearest-neighbour (n.n.n.)

hoppings by their mean-field approximation and Monte-Carlo simulation.[132)]

Moreover, even in the system of bipartite structures, reduction of the electron number from half-filling leads to incomplete nesting of the Fermi-surface in weak coupling regime, and suppresses the SDW transition. In strong coupling regime, the holes doped to the half-filled band would move around and destroy the AF ordering.

We demonstrate these behaviour of SDW in chapter 2 and those of localized antiferromagnetism in chapter 4.

§1.4 Ferromagnetism

Now we briefly review theories on the ferromagnetism. On this problem much work has been made. For the Hubbard model, the mean-field approximation gives Stoner's condition[101,102]: $U\rho(\varepsilon_F)>1$ for the ferromagnetism, where $\rho(\varepsilon_F)$ is a DOS at the Fermi-level. This condition shows that the ferromagnetism occurs when the on-site Coulomb interaction is sufficiently strong in the itinerant model. However the Stoner's theory could not reproduce the Curie-Weiss law, which is observed in almost all ferromagnets such as transition metals Fe, Co, Ni, and gives extraordinary large values of Curie-temperature T_C.

In the next stage, the electron correlations were taken into account. Hubbard proposed a decoupling scheme based on the equation of motion of the Green's function in real space, and developed it.[104-106] Moreover, Gutzwiller proposed a variational method,[109-111] and Kanamori did the t-matrix approximation.[144] They found approximate conditions for the ferromagnetism which takes into account the electron correlations.

Another important development is a train of spin-fluctuation theories[117-125,145] such as paramagnon theories[117-120] for Pd and liquid He^3 and self-consistent renormalization (SCR) theory[123,125] for weak ferromagnets $ZrZn_2$ and Sc_3In. Doniach and Englesberg[117] studied a nearly ferromagnetic Fermi-liquid and found enhancement of the temperature linear term and the appearance of $T^3\ln(T)$ term in low temperature specific heat. The paramagnon effect on superconductivity will be reviewed later. The result of the paramagnon theory is fairly good for very low

temperatures, but worsens as the temperature becomes higher, because this theory neglects mode-mode coupling of the spin-fluctuation. The weak ferromagnet $ZuZn_2$ [168] and Sc_3In [169] exhibit low Curie temperature T_C=25K and 6K, small magnetization par atom $0.12\mu_B$ and $0.04\mu_B$, respectively, and also exhibit Curie-Weiss law from just above T_C to much higher temperature $\sim 10T_C$ with much larger coefficient than that predicted from the magnetic moment at low temperatures. For this problem, Moriya and Kawabata proposed the SCR theory in which the spin-fluctuations are treated in a modified random phase approximation, and they explained the above properties of the weak ferromagnet. In particular they showed the new mechanism of the Curie-Weiss law not based on the localized spin model, which explains why almost all ferromagnets exhibit the Curie-Weiss law, whether it is weak ferromagnet or strong one.

Furthermore, Moriya and Takahashi showed an unified description of the weak and the strong ferromagnetism using a functional integral method.[146]

Thus the theory of itinerant ferromagnetism has been very progressed, but it is still open whether the ferromagnetic LRO does exist or not in the Hubbard model especially for the bipartite lattice structures. Nagaoka[149] proved that the ferromagnetic ground state occurs in the case of $U\to\infty$ and if the electron number N_e and the number of the lattice sites N_s satisfies the following condition: $N_e=N_s\pm 1$ for simple cubic (s.c.), body centered cubic (b.c.c.), and square lattices, and $N_e=N_s+1$ for hexagonal closed packed (h.c.p.) and face centered cubic (f.c.c.) lattices, where the electron transfer matrix

elements t_{ij} are non-vanishing only between nearest-neighbor sites (i,j) and assumed to be positive $t_{ij}=t>0$ for h.c.p. and f.c.c. structures. The Nagaoka's theorem is rigorous but as for the thermodynamic limit its meaning is not clear. Fukuyama et al. showed that the susceptibility is not singular at T=0 for any electron numbers within a coherent potential approximation (CPA).[151] Takahashi studied the Hubbard model of $U=\infty$ on finite lattices ($\leq$ 12 sites) with only n.n. hopping.[127] His result is also negative to the ferromagnetism for bipartite lattice except the case in which the Nagaoka's theorem holds. Moreover he found that the n.n.n. hopping strengthened the ferromagnetism in a b.c.c. case. Even in a high-temperature expansion up to the ninth order in the strong coupling limit by Kubo et al.,[152-154] they could not give a definite answer whether the susceptibility is diverge or not for bipartite lattices. Furthermore, by means of a Monte-Carlo simulation, Lin and Hirsch[132,129] have showed that ferromagnetic LRO is difficult to exist in the Hubbard model on a square lattice with n.n. and n.n.n. hoppings, but the n.n.n. hopping enhances the ferromagnetic correlation. On the other hand, the ground states of the finite size Hubbard models with $U\to\infty$ on f.c.c., h.c.p. and triangular lattice are completely ferromagnetic in most cases for t>0, while they are almost always paramagnetic for t<0, according to the exact diagonalization study by Takahashi. This is consistent with the high-temperature expansion and the Nagaoka's theorem.

Thus the ferromagnetic LRO would exist in the Hubbard model on f.c.c. and h.c.p. lattice with t>0, if the on-site repulsion is sufficiently strong, although it would not exist for t<0.

However it is not settled whether the ferromagnetic LRO exists or not in the single band Hubbard model on bipartite lattice structures, even in the strong coupling limit, although metal ferromagnet Fe has b.c.c. lattice structures. Here we should note that the real transition metals have a band degeneracy, which may play some important role in the ferromagnetism.[170,101,105,110)]

§1.5 Superconductivity

Recently, superconductivity in correlated electron systems have been attracting much attention in connection with the interplay with the magnetism in the heavy-fermion systems, the organics, and the oxides, and thus many theories have been proposed on the basis of the Hubbard model. However the existence of the superconductivity in the Hubbard model is controversial at the present stage, and as for the single band Hubbard model with only n.n. hopping, it is very negative.

For example, according to the quantum simulations by Imada et al.[85,86] and Hirsch et al.,[87] the pairing susceptibility is not enhanced as the Coulomb interaction U increases. Moreover exact diagonalization studies for 8 site Hubbard model[88] also show the result against the superconductivity. They are very suggestive but not definite consequence on the superconductivity at the ground states or low temperatures. This is mainly because of the finite size of the systems examined, even by the use of a new method proposed by Sorella,[133] although that is very effective method to this problem. Generally, the superconducting transition temperature is much smaller than AF one, and the size effect ought to become large as the temperature is lowered. For example, even in non-interacting case, the pairing susceptibility is logarithmically enhanced as the temperature is lowered, but discreteness of the DOS due to the finite size introduces some artificial lower energy-cutoff which is much larger than the temperature at which superconductivity occurs in ordinary materials.

However, the result of the simulation studies strongly suggest that the high-temperature superconductivity could not be reproduced in the single band Hubbard model with only n.n. hopping. In chapter 2, we also demonstrate in the same case that the superconducting transition temperatures are very low within a perturbation theory.

Now we mention about an interplay between the magnetism and the superconductivity. The magnetic instability and the superconducting one conflict with each other. However it has been pointed out by many authors that some magnetic interaction may enhance the superconductivity, as mentioned before.

For example, in the Fermi-liquid theory, exchanges of the charge- and spin-fluctuations may induce the superconductivity. This kind of superconductivity has been first studied by Kohn and Luttinger,[171] and later the paramagnon-mediated superconductivity has been studied.[119,120]

The paramagnon theory has clarified the roles of exchange of ferromagnetic spin-fluctuations in the nearly ferromagnetic materials such as Pd and He^3. Doniach and Engelsberg[117] showed that the factor of linear T term of the low temperature specific heat is enhanced by the paramagnon exchange interaction and also $T^3\ln(T)$ term appears. Berk and Schrieffer[118] showed that the ferromagnetic spin correlations suppress the singlet pairing superconductivity and argued that this is a reason for no superconductivity in Pd. Later Anderson et al.[119] and Nakajima[120] found that the paramagnon exchange interaction enhance triplet p-wave pairing.

On the other hand, it was found by Moriya[121] that for nearly AF metals, any $T^3\ln(T)$ term does not appear and linear-T term is not anomalously enhanced in specific heats, as in those of the nearly ferromagnetic systems. Further Beal-Monod et al.[58] have argued that in rotational invariant systems, the AF fluctuation does not enhance singlet pairings as well as triplet pairings.

However, Scalapino et al.[56] and Miyake et al.[57] have showed that the AF spin-fluctuations (AFSF) enhance the d-wave pairing superconductivity in a cubic lattice system near the SDW instability, mainly in connection with the heavy fermion systems. Norman[59] has applied this mechanism to the heavy fermion UPt_3 systems and estimated T_c=0.1K~0.2K from the neutron data. As Emery discussed,[55] the similar effects are possible in the Bechgaard salts. We also study this mechanism in the quasi-1D organic superconductors in chapter 3. There we obtain the phase diagrams which agrees with the experiments. Bourbonnais et al.[172] have studied the case in which the three dimensionality is weak and then the RPA is invalid. They also found the sensitive decrease of T_c. These two studies indicate the importance of long-range nature of the AFSF along the conductive chains to superconductivity in the quasi-1D systems.

There are two experimental supports of the AFSF exchange mechanism in the quasi-1D organic compounds, that is, the phase diagrams of the SDW and the superconductivity and the temperature dependence of NMR relaxation rate. We discuss this problem in detail in chapter 3.

On the other hand, this mechanism would not be applied to the copper oxide superconductors because the antiferromagnetism in them is not SDW from the experiments of the magnetic moments and others. Nevertheless, it is still possible that the spin-fluctuations which are localized in real space enhance the superconductivity as mentioned before. Thus it would be useful to examine this mechanism from the side of the weak coupling theories, for obtaining some suggestions.

In this itinerant mechanism, in which the AFSF are enhanced by the Fermi-surface nesting, shape of the Fermi-surface and DOS would sesitively change physical properties. Thus the nearly half-filled square lattice system is of much interest because it has following specific features of 2D systems, that is, logarithmic van Hove singularities in the DOS and perfect nesting of the Fermi-surface for half-filled band.

In chapter2, we study this mechanism on the basis of the 2D Hubbard model and examine the specific features of the two-dimensionality and an effect of n.n.n. hopping, which acts as a frustration to the antiferromagnetism as mentioned before. For example, there we found that the n.n.n. hopping remarkably enhance the superconductivity.

Furthermore much work has been made for this mechanism in the 2D Hubbard model,[60,173-176] and the d-p model,[177,178] and so on.[179] Yonemitsu[174] has studied an effect of vertex corrections and found that the next order correction to the RPA would enhance the superconductivity. Bickers et al.[175,176] have applied the conserving approximation and found the superconducting phase near the SDW phase in low temperature region. Further,

Schultz[60] has studied the scaling theory in the 2D Hubbard model near half-filling, and obtain the similar phase diagrams. Their phase diagrams agree with that of ours which is obtained in chapter 2.

On the other hand, in the strong coupling Hubbard model, it has been pointed out that the kinetic exchange interaction may enhance the superconductivity.[61,64] Here we should note that although the kinetic exchange acts as a n.n. attractive interaction between electrons, the strong on-site repulsion would drastically change the property of electrons, simultaneously. Thus we cannot conclude the superconductivity to occur only from the existence of the kinetic exchange interaction.

Thus the t-J model has been studied as an effective Hamiltonian of the strong coupling Hubbard model and the d-p model, as mentioned before.[61,64,85] We also study the t-J model on its magnetic properties and superconductivity in chapter 4. On the superconductivity, we found that the superconductivity is difficult to occur in small J systems and is possible in large J ones, and that a d-wave pairing is more favourable than an s-wave pairing, consistently with variational methods.[115]

Moreover many theories on a new type of superconductivity in the strong coupling regime, such as resonating valence band (RVB) theory,[61-63] have been studied for the high-T_c superconductors. Theory of anion superconductivity has been also studied recently.[180-182]

§1.6 One-Dimensional Hubbard Model

In the one-dimensional Hubbard model, the exact solution is known by the study of Lieb and Wu,[136] Yang,[138] and so on.[137,164] It was found that the ground state for the half-filling case is always insulating for any positive U, and that the total spin is minimized in the ground state. Further the thermodynamic properties have been investigated by many authors.[139-142] However in spite of the exact solution the physical properties of this model are far from completely known still now.

Recently the momentum distribution and the singularity of the spin-correlation function was studied. Ogata et al.[143] have studied the 1D Hubbard model in the large U-limit using the Bethe Ansatz wave function. For example, they have examined the singularity of the momentum distribution at Fermi-momentum k_F as well as the weak singularity at $3k_F$. They have fitted the power-law singularity around $k=k_F$ to their results for finite size systems ($\leq$ 32 sites), and estimated exponent is 0.13~0.15. Imada et al.[85] have applied the Monte-Carlo simulation technique improved by Sorella et al.[133] to the system of U=4t and 160 sites with 130 fermions, and found that the Fermi-jump in the momentum distribution appears within their accuracy due to the finite size of the systems. On the other hand, Sorella et al.[134] have also applied their Monte-Carlo simulation to the system of 36 sites at the largest size. They have suggested the non-Fermi-liquid nature of the marginal conducting state[183] of the system away from half-filling, through the finite size scaling, and have

also showed that the model can be scaled to the Tomonaga-Luttinger model even in the strong coupling regime, consistently with the study of Ogata et al. Their results appear to suggest the Fermi-liquid nature of quasi-low-dimensional systems even in the strong or intermediate coupling regime, as far as well away from half-filling.

References 1.

1. F.Steglich, J.Aarts, C.D.Bredl, W.Lieke, D.Meschede, W.Franz and H.Schäfer: Phys.Rev.Lett. **43**(1979)1892.
2. H.R.Ott, H.Rudigier, Z.Fisk, and J.L.Smith: Phys. Rev. Lett. **50**(1983)1595.
3. G.R.Stewart, Z,Fisk, O.Willis, and J.L.Smith: Phys.Rev.Lett. **52**(1984)679.
4. G. P. Meisner, A.L. Giorgi, A.C. Lawson, G.R. Stewart, J. O. Williams, M.S.Wire, and J.L.Smith: Phys. Rev. Lett. **53**(1984) 1829.
5. K.Bechgaard, C.S. Jacobsen, K. Mortensen, H.J. Pedersen, and N.Thorup: Solid State Commun. **33**(1980)1119.
6. R.Brusetti, M.R.Bault, D. Jerome, and K. Bechgaard: J. Phys. (Paris) **43**(1982)801.
7. P.Jerome and H.J.Schulz: Adv.Phys. **31**(1982)299; references therein.
8. S. Kagoshima and Y. Nogami: Parity, Vol.**03**, No.05 (1988) pp.2~7; references therein.
9. K. Kikuchi, K. Murata, Y. Honda, T. Namiki, K. Saito, K. Kobayashi, T. Ishiguro, and I. Ikemoto: J. Phys.Soc.Jpn. **56** (1987)2627.
10. K. Kikuchi, K. Murata, Y. Honda, T. Namiki, K. Saito, K. Kobayashi, and I. Ikemoto: J. Phys. Soc. Jpn. **56** (1987)3436.
11. K. Kikuchi, M. Kikuchi, T. Namiki, K. Saito, I. Ikemoto, K. Murata, T.Ishiguro, and K.Kobayashi: Chem.Lett.(Tokyo) **1987** (1987)931.
12. J.G.Bedonorz and K.A.Müller: Z.Phys.B **64**(1986)189.

13. C.W.Chu, P.H.Hor, P.L.Meng, L.Gao, Z.J.Huang, and Y.Q.Wang: Phys.Rev.Lett. **58**(1987)405.
14. H.Maeda, Y.Tanaka, M.Fukutomi, and T.Asano: Jpn.J.Appl.Phys. **27**(1988)L209.
15. Z.Z.Sleng and A.M.Hermann: Nature **332**(1988)138.
16. Y. Tokura, H. Takagi, and S. Uchida: Nature **377**(1989)345; H. Takagi, S.Uchida, and Y.Tokuro: Phys.Rev.Lett. **62**(1989)1197.
17. J.T.Markert and M.B.Maple: Solid State Commun. **70** (1989)145.
18. D.E.MacLaughlin, C.Tien, W.G.Clark, M.D. Lan, Z. Fisk, J. L. Smith, and H.R.Ott: Phys.Rev.Lett. **53**(1984)1833.
19. K. Kitaoka, K. Ueda, T. Kohara, K. Asayama, Y. Onuki, and T. Komatsubara: J.Magn. & Magn.Mater **52**(1985)341.
20. M.Takigawa, H.Yasuoka, and G.Saito: J.Phys.Soc.Jpn. **56**(1987) 873.
21. Y.Hasegawa and H.Fukuyama: J.Phys.Soc.Jpn. **56**(1987)877.
22. B.Golding, K.J.Bishop, B.Batlogg, W.H.Haemmerle, Z.Fisk, L. Smith, and H.R.Ott: Phys.Rev.Lett. **55**(1985)2479.
23. B.Batlogg, D.J.Bishop, B. Golding, E. Bucher, J. Hufnagl, Z. Fisk, J. L. Smith, and H. R. Ott: Phys. Rev. B **33**(1986)5906.
24. D.J.Bishop, C.M.Varma, B.Batlogg, E.Bucher, Z.Fisk, and J.L. Smith: Phys.Rev.Lett. **53**(1984)1009.
25. K.Ishida, Y.Kitaoka, and K.Asayama: J.Phys.Soc.Jpn. **58**(1989) 36.
26. I.Furo, A. Janossy, L.Mihaly, P.Banki, I.Pocsic, I. Bakonyi, I.Heinmaa, E.Joon, and E. Lipmaa: Phys. Rev. B **36**(1987)5690.
27. R.E.Walstedt, W.W.Warren,Jr., R.F.Bell, G.F. Brenneart, G.P. Espinosa, J.P.Remeika, R.J.Cava, and E.A.Reitman: Phys. Rev. B **36**(1987)5721.

28. Y.Kitaoka, S.Hiramatsu, T.Kondo, and K.Asayama: J. Phys.Soc. Jpn. **57**(1988)30.

29. Y. Kitaoka, S. Hiramatsu, Y. Kohori, K. Ishida, T. Kondo, H. Shibai, K.Asayama, H. Takagi, S. Uchida, H. Iwabuchi, and S. Tanaka: Physica **C153-155**(1988)83.

30. K.Fujiwara, Y.Kitaoka, K.Asayama, H.Sasakura, S.Minamigawa, K. Nakahigashi, S. Nakaishi, M. Kogachi, N. Fukuoka, and A. Yanase: J.Phys.Soc.Jpn. **58**(1989)380.

31. U. Rauchschwalbe, F. Steglich, G.R. Stewart, A.L. Georgi, P. Fulde, and K. Maki: Europhys.Lett. **3**(1987)751.

32. J.P.Ströbel, A.Thomä, B.Hensel, H. Adrian, and G. Saemann-Ischenko: Physica **C153-155**(1988)1537.

33. A.Umezawa, G.W.Crabtree, K.G.Vandervoort, U.Welp, W.K.Kwak, and J.Z.Liu: Proc.Int.Conf.M^2S·HTSC, (Stanford, 1989, to be published).

34. M.Sato, S.Shamoto, M.Sera, and H.Fujishita: to be published in Solid State Commun.

35. H.R. Ott, H. Rudigier, Z. Fisk, and J.L.Smith: Phys.Rev.B **31** (1985)1651.

36. M.Sigrist, T.M.Rice, and K. Ueda: Phys. Rev. Lett. **63** (1989) 1727.

37. D.S.Hirashima and T.Matsuura: preprint.

38. A.P.Ramirez, B.Batlogg, E.Bucher, and A.S.Cooper: Phys. Rev. Lett. **57**(1986)1072.

39. G. Aeppli, A. Goldman, G. Shirane, E. Bucher, and M.-Ch.Lux-Steiner: Phys.Rev.Lett. **58**(1987)808.

40. T.Fujita, Y.Aoki, Y.Maeno, J.Sakurai, H.Fukuba, and H.Fujii: Jpn.J.Appl.Phys. **26**(1987)L368.

41. Y. Kohori, T. Sugata, H. Takenaka, T. Kohara, Y.Yamada, J.T. Market, and M.B.Maple: J.Phys.Soc.Jpn. **58**(1989)3493.

42. N.Nishida, H.Miyatake, D.Shimada, S. Okuma, M. Ishikawa, T. Takabatake, Y.Nakazawa, Y.Kuno, R. Keitel, J.H. Brewer, T.M. Riseman, D.L.Williams, Y.Watanabe, T.Yamazaki, K. Nishiyama, K.Nagamine, E.J.Ausaldo, and E.Tarikai: Jpn.J.Appl.Phys. **26** (1987)1856.

43. N. Nishida, H. Miyatake, S. Okuma, T. Tamegai, Y. Iye, R. Yosizaki, K. Nishizawa, K. Nagamine: to be published in Physica C.

44. A. W. Sleight, J.L. Gillson, and P.E.Bierstedt: Solid State Commun. **17**(1975)27.

45. T.D. Thanh, A. Koma, and S. Tanaka: Appl.Phys. **22** (1980)205.

46. R.J. Cava, B.Batlogg, J.J.Krajewski, R.Farrow, L.W.Rupp,Jr., A.E. White, K. Short, W.F. Peck, and T. Kometani: Nature **332** (1988)814.

47. L.F.Mattheiss, E.M.Gyorgy, and K.W.Johnson,Jr.: Phys.Rev. B **37**(1988)3745.

48. D.D.Osheroff, W.J.Gully, R.C.Richardson, and D.M. Lee: Phys. Rev.Lett. **29**(1972)920.

49. D.D.Osheroff, R.C.Richardson, and D.M.Lee: Phys.Rev.Lett. **28** (1972)885.

50. B. Batlogg, R. J. Cava, A. Jayaraman, R. B. van Dover, G. A. Kourouklis, S. Sunshine, D.W. Murphy, L.W.Rupp, H.S.Chen, A. White, K.T.Short, A.M. Mujsce, and E. A. Rietman: Phys. Rev. Lett. **58**(1987)2333.

51. L.C.Bourne, M.F.Crommie, A.Zettl, H.-C.zur Loye, S.W.Keller, K.L.Leary, A.M.Stacy, K.J.Chang, M.L.Cohen, and D.E. Morris: Phys.Rev.Lett. **58**(1987)2337.

52. K.J.Leary, H.-C.zur Loye, S.W.Keller, T.A.Faltens, W.K.Ham, J.N.Michaels, and A.M. Stacy: Phys. Rev. Lett. **59**(1987)1236.

53 T.A.Faltens, W.K.Ham, S.W.Keller, K.J.Leary, J. N. Michaels, A.M.Stacy, H.-C. zur Loye, D.M.Morris, T.W.Barbee,III, L.C. Bourne, M.L.Cohen, S.Hoen, and A.Zettl: Phys. Rev. Lett. **58** (1987)1035.

54. P.W.Anderson: Phys.Rev.B **30**(1984)1549.

55. V.J.Emery: Synth.Met. **13**(1986)21.

56. D.J.Scalapino, E.Loh,Jr., and J. E. Hirsch: Phys. Rev. B **34** (1986)8190; **35**(1987)6694.

57. K.Miyake, S.Schmitt-Rink, and C.M.Varma: Phys.Rev.B **34**(1986) 6554.

58. M.T.Beal-Monod, C.Bourbonnais, and V.J.Emery: Phys.Rev.B **34** (1986)7716.

59. M.R.Norman: Phys.Rev.Lett. **59**(1987)232.

60. H.J.Schulz: Europhys.Lett. **4**(5)(1987)609.

61. P.W.Anderson: Science **235**(1987)1196. See also P.W.Anderson, Mater Res.Bull. **8**(1973)153.

62. P.W.Anderson, G.Baskaran, Z.Zou, and T.Hsu: Phys. Rev. Lett. **58**(1987)2790.

63. S.Kivelson, D.Rokhsar, and J. Sethna: Phys. Rev. B **35** (1987) 8865.

64. H.Fukuyama and K.Yoshida: Jpn. J. Appl. Phys. **26** (1987)L371.

65. J.C.Scott, H.J.Pedereen, and K.Bechgaard: Phys.Rev.Lett. **45** (1980)2125.

66. W.M.Walsh, F.Wudl, G.A.Thomas, D.Nalewajek, J.J.Hauser, P.A. Lee, and T.Poehler: Phys.Rev.Lett. **45**(1980)829.

67. H.Fukuyama and Y.Hasegawa: Physica B **148**(1987)204.

68. N.P.Ong, Z.Z.Wang, J.Clayhold, J.M.Tarascon, L.H.Greene, and W.R.McKnnon: Phys.Rev. B **35**(1987)8807.

69. S.Uchida, H.Takagi, H.Ishii, H.Eisaki, T.Yabe, S.Tajima, and S.Tanaka: Jpn.J.Appl.Phys. **26**(1987)L440.

70. T. Penney, M.W. Shafer, B.L. Olsen, and T.S. Plaskett: Adv. Ceramic.Mater **2**(1987)577.

71. B.W. Ricketts, R.B. Roberts, R. Driver, and H.K.Welsh: Solid State Commun. **64**(1987)1287.

72. S. W. Tozer, A. W. Kleinsasser, T. Penney, D. Kaisen, and F. Holtzberg: Phys.Rev.Lett. **59**(1987)1768.

73. D.Vaknin, S.K.Sinha, D.E.Moncton, D.C.Johnston, J.Newsam, C. R.Safinya, and H.King: Phys.Rev.Lett. **58**(1987)2802.

74. T.Freltoft, J.E.Fisher, G.Shirane, D.E.Moncton, S. K. Sinha, D.Vaknin, J.P.Remeika, A.S.Cooper, and D.Harshman: Phys.Rev. B **36**(1987)826.

75. B.X.Yang, S.Mitsuda, G.Shirane, Y.Yamaguchi, H.Yamauchi, and Y.Syono: J.Phys.Soc.Jpn. **56**(1987)2283.

76. B.Reihl, T.Riesterer, J.G.Bednorz, and K.A.Müller: Phys.Rev. B **35**(1987)8804.

76. T. Riesterer, J.G. Bednorz, K.A. Müller, and B. Reihl: Appl. Phys.A **44**(1987)81.

77. A. Fujimori, E. Takayama-Muromachi, Y. Uchida, and B. Okai: Phys.Rev. B **35**(1987)8814.

78. A.Fujimori, E.Takayama-Muromachi, and Y.Uchida: Solid State Commun. **63**(1987)857.

79. A. Bianconi, A. C. Costellano, M. De Santis, P. Delogn, A. Gargano, R.Giorgi: Solid State Commun. **63**(1987)1135.

80. K.Yamaji: J.Phys.Soc.Jpn. **51**(1982)2787.

81. Y.Hasegawa and H.Fukuyama: J. Phys. Soc. Jpn. **55** (1986)3978.

82. K.Yamaji: Syn.Met. **13**(1986)29; J.Phys.Soc.Jpn. **56**(1987)1841.

83. F.C.Zhang and T.M.Rice: Phys.Rev.B **37**(1988)3759.

84. H.Fukuyama, H. Matsukawa, and Y. Hasegawa: J.Phys.Soc.Jpn.**58** (1989)364.

85. M.Imada and Y.Hatsugai: J.Phys.Soc.Jpn. **58**(1989)3752.

86. M.Imada: J.Phys.Soc.Jpn. **57**(1987)42; **57**(1988)2689.

87. J.E.Hirsch and H.Q.Lin: Phys.Rev.B **37**(1988)5070.

88. H.Q.Lin, J.E.Hirsch, and D.J.Scalapino: Phys.Rev.B **37** (1988) 7359.

89. M.Ogata and H.Shiba: J.Phys.Soc.Jpn. **57**(1988)3074.

90. M.Imada: J.Phys.Soc.Jpn. **56**(1987)3793; **57**(1988)3128.

91. Y.Hatsugai, M.Imada, and N.Nagaosa: J.Phys.Soc.Jpn. **58**(1989) 1347; N.Nagaosa, Y.Hatsugai, and M.Imada: J.Phys.Soc.Jpn.**58** (1989)978.

92. P.M. Grant: J. Phys. Colloq. **44** (1983)C3-847: Phys.Rev. B **26** (1982)6888.

93. G. Shirane, Y. Endoh, R.J. Birgenean, M.A.Kastuer, Y.Hidaka, M.Oda, M. Suzuki, and T. Murakami: Phys. Rev. Lett. **59**(1987) 1613.

94. G. A. Kourouklis, A. Jayaraman, W. Weber, J.P. Remeika, G.P. Expinosa, A.S. Cooper, and R.G. Maines, Sr.: Phys. Rev. B **36** (1987)7218.

95. S.Chakuravarty, B.I.Halperin, and D.R.Nelson: Phys.Rev.Lett. **60**(1988)1057.

96. S.S.P.Parkin, E.M.Enngber, R.R.Schumaker, R.Lagier, V.Y.Lee, J.C.Scott, R.L.Greene: Phys.Rev.Lett. **50**(1983)270.
97. H.Shimahara and S.Takada: Jpn. J. Appl. Phys. **26** (1987)1674.
98. H.Shimahara and S.Takada: J. Phys. Soc. Jpn. **57** (1988) 1044.
99. H.Shimahara: J.Phys.Soc.Jpn. **58**(1989)1735; in Proceeding of the Physics and Chemistry of Organic Superconductors, edited by G. Saito and S. Kagoshima (Springer-Verlag, Berlin, Heidelberg, New York, to be published).
100. H.Shimahara, S.Misawa, and S.Takada: J. Phys. Soc. Jpn. **58** (1989)801; J.Phys.Soc.Jpn. **58**(1989)4168; Proceeding of the Tsukuba Seminar on High T_c Superconductivity, edited by K. Masuda, T. Arai, I. Iguchi, and R. Yoshizaki (Univ.Tsukuba, Tsukuba, 1989) pp.73~78.
101. J.C.Slater: Phys.Rev. **49**(1936)537,931.
102. E.C.Stoner: Proc.Roy.Soc. **A165**(1938)372.
103. D.R.Penn: Phys.Rev. **142**(1966)350.
104. J.Hubbard: Proc.Roy.Soc. **A276**(1963)238.
105. J.Hubbard: Proc.Roy.Soc. **A281**(1964)401.
106. J.Hubbard: Proc.Roy.Soc. **A277**(1964)237.
107. A.Kawabata: Prog.Theor.Phys. **48**(1972)1793.
108. C.Mehrotra and K.S.Viswanathan: Solid State Commun. **12**(1973) 129.
109. M.C.Gutzwiller: Phys.Rev.Lett. **11**(1963)159.
110. M.C.Gutzwiller: Phys.Rev. **134**(1964)A923.
111. M.C.Gutzwiller: Phys.Rev. **137**(1965)A1726.
112. W.F.Brinkman and T.M.Rice: Phys.Rev.B **2**(1970)4302.
113. K.Kubo and M.Uchinami: Prog.Theor.Phys. **54**(1975)1289.

114. H. Yokoyama and H. Shiba: J.Phys.Soc.Jpn. **56**(1987)1490,3570, 3582.

115. H.Yokoyama and H.Shiba: J.Phys.Soc.Jpn. **57**(1988)2482.

116. C.Gros, R.Joynt, and T.M.Rice: Z.Phys.B **68**(1987)425.

117. S.Doniach and S.Engelsberg: Phys.Rev.Lett. **17**(1966)750.

118. N.F. Berk and J.R. Schrieffer: Phys. Rev. Lett. **17**(1966)433.

119. P.W.Anderson and W.F.Brinkman: Phys.Rev. Lett. **30**(1973)1108.

120. S.Nakajima: Prog.Theor.Phys. **50**(1973)1101.

121. T.Moriya: Phys.Rev.Lett. **24**(1970)1433.

122. T.Moriya and T.Kato: J.Phys.Soc.Jpn. **31**(1971)1016.

123. T.Moriya and A.Kawabata: J. Phys. Soc. Jpn. **34**(1973)639; **35** (1973)669.

124. H.Hasegawa and T.Moriya: J.Phys.Soc.Jpn. **36**(1974)1542.

125. T.Moriya: J.Phys.Soc.Jpn. **40**(1976)933.

126. A.Kawabata: Solid State Commun. **32**(1979)893.

127. M.Takahashi: J.Phys.Soc.Jpn. **51**(1982)3475.

128. J.E.Hirsch: Phys.Rev.Lett. **51**(1983)1900.

129. J.E.Hirsch: Phys.Rev.B **31**(1985)4403.

130. J.E.Hirsch: Phys.Rev.Lett. **54**(1985)1317.

131. J.E.Hirsch: Phys.Rev.B **35**(1987)1851.

132. H.Q.Lin and J.E.Hirsch: Phys.Rev.B **35**(1987)3359.

133. S. Sorella, E. Tosatti, S. Baroni, R. Car, and M.Parrinello: Int.J.Mod.Phys.B **1**(1988)993.

134. S.Sorella, A.Parola, M.Parrinello, and E.Tosatti: preprint.

135. R.R.dos Santos: Phys.Rev. B **39**(1989)7259

136. E.Lieb and F.Wu: Phys.Rev.Lett. **20**(1968)1445.

137. E.Lieb and D.C.Mattis: Phys.Rev. **125**(1962)164.

138. C.N.Yang: Phys.Rev.Lett. **19**(1967)1312.

139. H.Shiba and P.A.Pincus: Phys.Rev.B **5**(1972)1966.

140. H.Shiba: Prog.Theor.Phys. **48**(1972)2171; Phys. Rev.B **6**(1972) 930.

141. M.Takahashi: Prog.Theor.Phys. **47**(1972)69.

142. J.Carmelo and D.Baeriswyl: Phys.Rev.B **37**(1988)7541.

143. M.Ogata and H.Shiba: preprint.

144. J.Kanamori: Prog.Theor.Phys. **30**(1963)275.

145. K. K. Murata and S. Doniach: Phys. Rev. Lett. **29** (1972) 285.

146. T. Moriya and Y. Takahashi: J. Phys. Soc. Jpn. **45** (1978)397.

147. M.Cyrot: Phys.Rev.Lett. **25**(1970)871; J.Phys.(Paris) **33**(1972) 125.

148. Y.Kakehashi and P.Fulde: Phys.Rev.B **32**(1985)1595.

149. Y.Nagaoka: Phys.Rev. **147**(1966)392.

150. D.C.Mattis and R.E.Peña: Phys.Rev.B **10**(1974)1006.

151. H.Fukuyama and H.Ehrenreich: Phys.Rev.B **7**(1973)3266.

152. K.Kubo and M.Tada: Prog. Theor. Phys. **69**(1983)1345; **71**(1984) 479.

153. K.Kubo and M.Tada: J.Mag.Mag.Mat. **31**(1983)327.

154. K.Kubo: Prog.Theor.Phys.Suppl. No.69(1980)290.

155. K.Kubo: Prog.Theor.Phys. **64**(1980)758.

156. S.A.Trugman: Phys.Rev.B **37**(1988)1597.

157. C.L.Kane, P.A.Lee, and N. Read: Phys. Rev. B **39** (1989) 6880.

158. T.Kennedy, E.H.Lieb, and B.S.Shastry: J.Stat.Phys. **53** (1988) 1019.

159. G.S.Rushbrooke, G.A.Baker,Jr., and P.J.Wood: in Phase Transitions and Critical Phenomena, edited by C. Domb and M. S. Green (Academic, New York), p.245.

160. J.Oitmaa and D.D.Betts: Can.J. Phys. **56** (1978)897; D.D.Betts and J.Oitmaa: Phys.Lett.A **62**((1977)277.

161. J.D.Reger and A.P.Young: Phys.Rev.B **37**(1988)5978.

162. P. W. Anderson: Phys. Rev. **86**(1952)694; R.Kubo: Phys.Rev. **87** (1952)568; R.B.Stimchcombe: J.Phys.C **4**(1974)789.

163. D.A.Huse: Phys.Rev.B **37**(1988)2380.

164. L.Hulthen: Arkiv.Mat.Astron.Fysik. **26** A No.11,(1938).

165. S.Liang, B.Doucot, and P.W.Anderson: Phys.Rev.Lett. **61**(1988) 365.

166. D.A.Huse and V.Elser: Phys.Rev.Lett. **60**(1988)2531.

167. J. Bardeen, L.N. Cooper, and J.R. Schrieffer: Phys. Rev. **108** (1957)1175.

168. B.T.Matthias and R.M.Bozorth: Phys.Rev.**100**(1958)604.

169. B.T.Matthias, A.M.Clogston, H.J. Williams, E. Corenzwit, and R.C.Sherwood: Phys.Rev.Lett. **7**(1961)7.

170. J.H.van Vleck: Rev.Mod.Phys. **25**(1953)220.

171. W.Kohn and J.M.Luttinger: Phys.Rev.Lett. **15**(1965)524.

172. C.Bourbonnais and L.G. Caron: Europhys. Lett. **5**(3)(1988)209.

173. N.E.Bickers, D.J. Scalapino, and R.T. Scalettar: Int.J.Mod. Phys. B **1**(1987)678.

174. K.Yonemitsu: submitted to J.Phys.Soc.Jpn.

175. N.E.Bickers, D.J.Scalapino, and S.R.White: Phys.Rev.Lett.**62** (1989)961.

176. N. E. Bickers and D. J. Scalapino: Ann. Phys. **193** (1989)206.

177. K. Miyake, T. Matuura, K. Sano, and Y. Nagaoka: Physica **148B** (1987)381; J.Phys.Soc.Jpn. **57**(1988)722.

178. K.Yonemitsu: preprint.

179. K.Yamaji: submitted to J.Phys.Soc.Jpn.

180. R.B.Laughlin: Science **242**(1988)525.

181. P.W. Anderson: in Frontiers and Borderlines in Many Particle Physics, edited by R. Schrieffer and R. A. Broglia (North-Holland, Amsterdam, to be published).

182. X.G.Wen, F.Wilczek, and A. Zee: Phys. Rev. B **39** (1989)11413.

183. J.Solyom: Adv.Phys. **28**(1979)201.

Chapter 2.

Spin-Density-Wave and Superconductivity in Quasi-Two-Dimensional Electron Systems

In this chapter, we study quasi-two-dimensional electron systems with local interactions. In particular we examine an interplay between SDW and superconductivity in weak coupling Hubbard model on a square lattice by means of a perturbation theory. In the weak coupling regime, spin-fluctuations strengthened by the Fermi-surface nesting may enhance a d-wave superconductivity as mentioned in chapter 1.

We obtain the phase diagram of the normal, the SDW and the superconducting phase, in which superconductivity occurs near the SDW boundary. The superconducting transition temperature (T_c) is found to be remarkably suppressed by the the electron self-energy and to be sensitive to the band parameters due to the Fermi-surface nesting and the presence of the van Hove singularity as well as to the band fillingness and the strength of the Coulomb interaction. As a consequence T_c is enhanced by the next-nearest-neighbour hopping integral. We discuss the relation between the present theory and the high-T_c superconductors. Moreover we also study the specific features of the quasi-two-dimensional band structures of the systems without interactions and with local attractive interactions.

§2.1 Introduction

Copper oxide superconductors, discovered recently,[1-6] have remarkably high transition temperatures (T_c) and several characteristic features[7-100] such as the small isotope effects,[7-10] the quasi-two-dimensional (quasi-2D) motion of conduction electrons,[11-17] the existence of a magnetic order in their families,[18-29] and others. Their origin have not been clarified theoretically yet, although much work has been devoted to this problem.[101] It is believed, however, that some electronic mechanism such as an antiferromagnetic (AF) interaction would be responsible for the pairing mechanism. Thus, the superconductivity in repulsive systems has attracted a current interest, and the quasi-2D Hubbard model has been studied in two different ways, that is, the strong interaction theory based on the localized electron picture and the perturbation theory of the itinerant electrons.

The first picture is supported by the experiments of the AF moment in La-Ba-Cu-O family,[19-24] and by the Hall coefficient measurement.[30-39] The resonating valence bond (RVB), which was first proposed by Anderson[102] and has been studied extensively,[103-106] is based on this picture.

On the other hand the itinerant electron pictures are supported by the experiments which show the temperature dependence of the susceptibility like that in the Pauli-paramagnetism,[18,40-46] and the metallic resistivity.[33-36,47-50] The values of the density of states which is estimated from the susceptibilities[42-46] and the specific heats[68-77] are roughly

consistent to the band calculations,[11-17] although they are much larger than that predicted by the photo emission spectroscopies.[59-65] From this view-point, superconductivity was investigated for heavy fermion systems by Scalapino et al.[107] and Miyake et al.,[108] in perturbative approach on the basis of the three-dimensional Hubbard model, in which they showed that AF spin-fluctuations enhance the d-wave superconductivity.

However, such perturbative approaches depend on some approximations such as a random phase approximation (RPA), the validity of which is not assured. Moreover the electron systems in the oxides would be in the intermediate region between the localized and the itinerant pictures. Then, more direct treatments have been proposed to examine the existence of the superconductivity in repulsive systems.

One of them is quantum simulations by Imada et al.[109,110] They calculated a pairing susceptibility and showed that it may be difficult for superconductivity to appear in the Hubbard model on a square lattice with only nearest neighbour (n.n.) hopping, while it is enhanced by the Coulomb repulsions in the extended Hubbard model on the CuO_2 lattice plane, which is more realistic to the recent oxides. Furthermore, an exact diagonalization in the present model was studied by Lin, Hirsch, and Scalapino.[111] They also conjectured the absence of the superconductivity in the 2D Hubbard model.

These results are full of suggestions to clarify the mechanism of the high-T_c superconductivity, but they have an inevitable limitation on the system size. In particular, in the

diagonalization methods, the system is too small to call it two-dimensional system. Hence they do not exclude the possibility of the superconductivity originating from the repulsive interactions in 2D Hubbard model. Thus we complement their results from the side of a perturbation theory in this chapter.

Another important aspect of this problem is competition and interplay between superconductivity and antiferromagnetism. The experiments for La-Ba-Cu-O system exhibit the possibility of the following two types of the phase diagrams on the plane of temperature and hole concentration. This kind of phase diagram was obtained first by measurements of the susceptibility,[18] which showed that the superconducting phase does not touch the antiferromagnetic phase. However, an recent NQR experiment[27] have shown that the AF phase extends close to the superconducting phase. Further for Y-Ba-Cu-O system, antiferromagnetism was observed in μ^+SR experiments by N.Nishida et al.[28] These experiments give rise to the problem on the interplay between antiferromagnetism and superconductivity and the possibility of the superconductivity enhanced by the AF spin-fluctuations. In this context, we think that it is important to clarify the effect of next-nearest-neighbour (n.n.n.) hopping on superconductivity, since the n.n.n. hopping acts as a frustration to antiferromagnetism.

On the other hand, the two-dimensional band structure is also one of the most important characteristics of the recent oxides. It is usually considered that the conduction band is an anti-bonding band formed by Cu-d-orbitals and O-p-orbitals on the CuO_2 plane.[11-17] This gives the two specific features in connection with the problem of the interplay mentioned above. One of

this is the logarithmic enhancement of the state density so-called van Hove singularity. Several band calculations for the stoichiometric La-Ba-Cu-O system shows that the van Hove singularity exists near or at the Fermi-energy.[11,12] In this case, various quantities also exhibit the logarithmic enhancement for low temperatures, and T_c is also enhanced,[112-114] due to the van Hove singularities. Another specific feature is the Fermi-surface nesting, which leads to the strong fluctuations and the Fermi-surface instability. Effects of those specific features on physical properties are sensitive to band parameters and band fillingness.

In this chapter, we study the spin-fluctuation mechanism of superconductivity by means of a perturbation theory in the 2D Hubbard model:

$$H = \sum_{i,j,\sigma} t_{ij} c^{\dagger}_{i\sigma} c_{j\sigma} + U \sum_{i} n_{i\alpha} n_{i\beta} , \qquad (2.1.1)$$

and examine the interplay with the SDW. Although the realistic situation is more complicated, we restrict ourselves to the single-band Hubbard model for simplicity. In particular we concentrate our attention on the characteristics of the present 2D system, that is, the Fermi-surface nesting and the van Hove singularity. Next we briefly study the extended Hubbard model on a CuO_2 plane, according to the suggestion[109,115,116] that the CuO_2 structure may enhance superconductivity.

In §2.2, the specific features of quasi-2D band structure are examined for non-interacting electron systems. In §2.3, we study the SDW transition of the quasi-2D systems with only n.n.

hopping and that with n.n. and n.n.n. hopping. We also study an effect of orthorhombic distortion of lattice. In §2.4, the superconductivity induced by local interactions and specific features due to the van Hove singularities are examined. In §2.5, we study the superconductivity mediated by spin-fluctuations, and in §2.6 we show the phase diagrams for various cases. In §2.7, we briefly examine the same mechanism for the extended Hubbard model. The last section is devoted to summary and discussion. This chapter contains the studies in our papers of ref.117 and 118 and unpublished results.

§2.2 Noninteracting Electrons on a Square Lattice

In this section, we examine the noninteracting electron system on a square lattice. The dispersion relation of the tight binding electron with n.n. and n.n.n. hopping is writen as

$$\varepsilon(\vec{k}) = - t (\cos(k_x) + \cos(k_y)) - \delta \cos(k_x)\cos(k_y) - \mu. \qquad (2.2.1)$$

Here $\varepsilon(\vec{k})$ has saddle points at $\vec{k}=\vec{k}_v=(0,\pm\pi),(\pm\pi,0)$ in energy-momentum space, which lead to logarithmic van Hove singularity of the density of states (DOS) at the energy $\varepsilon(\vec{k}_v)=\delta-\mu$, and if $\mu=\delta$, such singularity occurs at the Fermi-energy. In particular, if $\mu=\delta=0$, complete nesting of the Fermi-surface occurs simultaneously. (Fig.2.1.)

The dynamical susceptibility $\chi_0(\omega,\vec{q})$ is written in the form:

$$\chi_0(\omega,\vec{q}) = \frac{1}{N} \sum_{\vec{k}} \frac{f(\varepsilon(\vec{k})) - f(\varepsilon(\vec{k}+\vec{q}))}{\omega + (\varepsilon(\vec{k}+\vec{q}) - \varepsilon(\vec{k})) + i0+}, \qquad (2.2.2)$$

where $f(\varepsilon)=(e^{\beta\varepsilon}+1)^{-1}$. $\chi_0(\omega,\vec{q})$ has peaks at a nesting vector $\vec{q}=\vec{q}_m$. In particular, in the half filled case ($\mu=\delta=0$), the nesting is perfect and $\vec{q}_m=\vec{Q}=(\pm\pi,\pm\pi)$. In the case of $\mu\neq0$ and/or $\delta\neq0$, the total electron density deviates from 1 (the half filling) and then $\vec{q}_m$ shifts from $\vec{Q}$ (Fig.2.1 and 2.2).

In the case of $\delta=0$, the DOS is given by

$$\rho(\varepsilon) = \frac{1}{\pi^2 t} K((1 - (\varepsilon/2t)^2)^{1/2}), \qquad (2.2.3)$$

with the K function, i.e. a complete elliptic integral of the first kind, which shows the logarithmic behaviour near $\varepsilon=0$:

$$\rho(\varepsilon) \cong \frac{1}{\pi^2 t} \ln \frac{8t}{\varepsilon} . \qquad (2.2.4)$$

Using these expressions, the free susceptibility can be obtained for several cases. For $\mu=\delta=0$, logarithmic van Hove singularity at the Fermi-surface and the perfect nesting occur simultaneously, and then susceptibilities are obtained analytically as follows:

$$\chi_0(0,0+) = \frac{1}{\pi^2 t} \ln\left(\frac{16\, e^{\gamma}}{\pi} \frac{t}{T}\right) , \qquad (2.2.5)$$

$$\chi_0(0,\vec{Q}) = \frac{1}{2\pi^2 t} \ln^2\left(\frac{16\, e^{\gamma}}{\pi} \frac{t}{T}\right) + C_0 , \qquad (2.2.6)$$

with $C_0 = -0.0166$, which is obtained by a simple numerical integral (see §2.4). These expressions are very accurate as shown in Fig.2.3 and Fig.2.4. This logarithmic behaviour of $\chi_0(0,0+)$ and the square logarithmic behaviour of $\chi_0(0,\vec{Q})$ are due to the van Hove singularities in the two dimensional tight-binding electron systems. Furthermore for $2t>>\mu>>T$ in which the band fillingness deviate from half-filling, susceptibilities are obtained by low temperature expansion:

$$\chi_0(0,0+) = \frac{1}{\pi^2 t} \ln\left(\frac{8t}{\mu}\right) + \frac{1}{6t} \left(\frac{T}{\mu}\right)^2 + \cdots , \qquad (2.2.7)$$

$$\chi_0(0,\vec{Q}) = \frac{1}{2\pi^2 t} \ln^2\left(\frac{8t}{\mu}\right) - \frac{2}{\pi^2 t} \ln^2 2$$

$$+ \frac{1}{3t} \ln\left(\frac{8et}{\mu}\right) \left(\frac{T}{\mu}\right)^2 + \cdots . \qquad (2.2.8)$$

At the ground state, susceptibilities is related to the density of states as follows:

$$\chi_0(0,0+) = \rho(\mu) = \frac{1}{\pi^2 t} K\left((1 - (\mu/2t)^2)^{1/2} \right) , \qquad (2.2.9)$$

$$\chi_0(0,\vec{Q}) = \frac{1}{\pi^2 t} \int_{\mu}^{2t} d\varepsilon \, K\left((1 - (\varepsilon/2t)^2)^{1/2} \right) \frac{1}{\varepsilon} , \qquad (2.2.10)$$

The temperature dependences of $\chi_0(0,0+)$ and $\chi_0(0,\vec{Q})$ are obtained numerically for various μ and δ values and shown in Fig.2.3 and Fig.2.4, respectively. It is found that the logarithmic behaviour of $\chi_0(0,0+)$ and $\chi_0(0,\vec{Q})$ are rapidly suppressed with increasing or decreasing μ and δ, and the susceptibility $\chi_0(0,0+)$ becomes to have Pauli-paramagnetic form as expected.

In addition, we will briefly mention about the specific heat C_V in this system. At sufficiently low temperatures, the following expressions are obtained by the expansion in T/t for $\mu=\delta=0$,

$$C_V = \frac{2T}{3t} \ln \frac{3.999\ t}{T} , \qquad (2.2.11)$$

and by the expansion in T/μ for $\mu >> T$,

$$C_V = \frac{2T}{3t} \ln \frac{8\ t}{\mu} . \qquad (2.2.12)$$

The specific heat also shows the logarithmic behaviour as well as the susceptibility $\chi_0(0,0+)$.

As found in the results obtained above, even in the non-interacting system, the 2D tight binding model shows

characteristic behaviours of the susceptibilities and the specific heat which are enhanced due to the presence of van Hove singularities. Such properties of the present system may relate to the unusual behaviour of the susceptibility and the electrical resistivity, which changes from semiconductor like to metallic like, by slight doping in $(La_{1-X}Ba_X)_2CuO_4$.

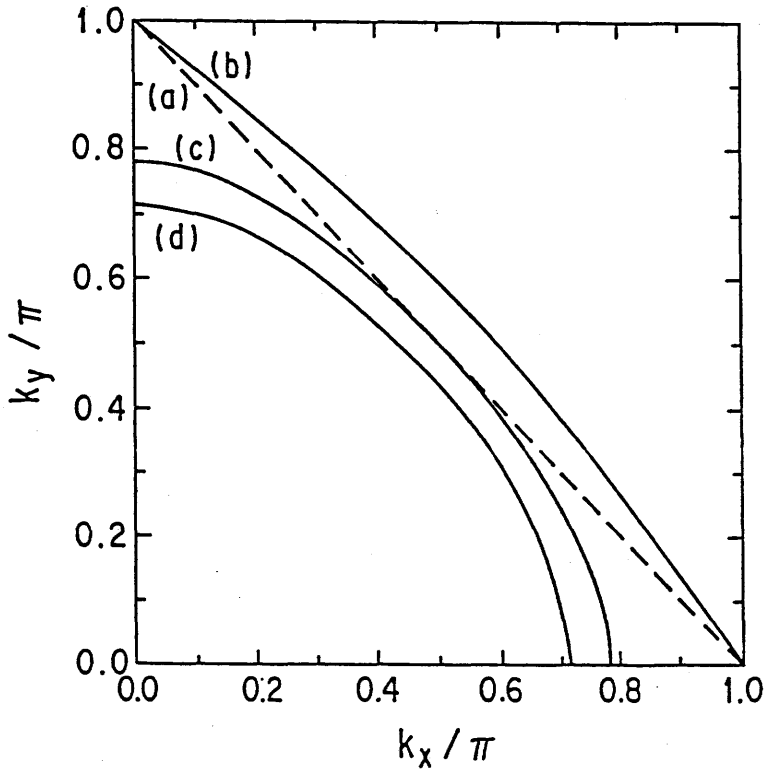

Fig.2.1.

Fermi-surfaces.

(a) $\delta=\mu=0$,

(b) $\delta/t=\mu/t=0.3$,

(c) $\delta/t=0.3$, $\mu/t=0$,

(d) $\delta/t=0.3$, $\mu/t=0.2$.

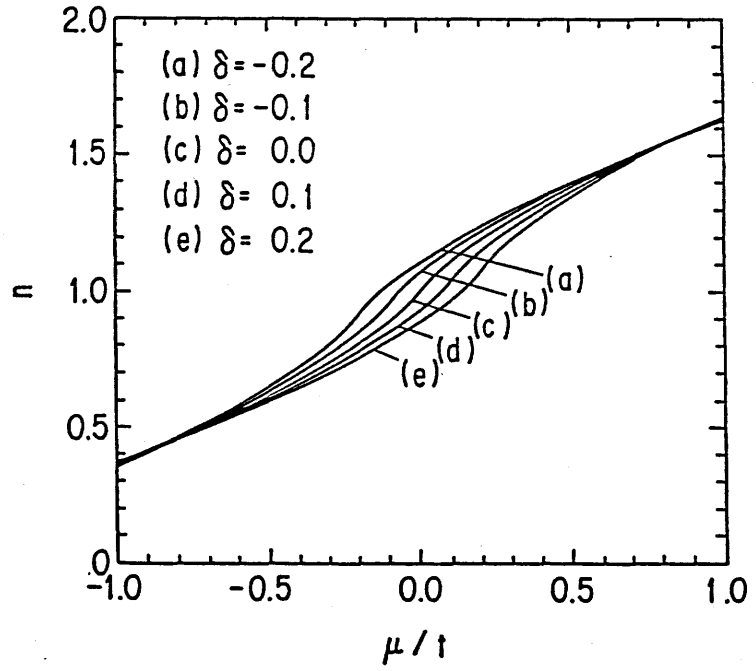

Fig.2.2. The electron numbers per site n.

(a) $\delta=-0.2t$,

(b) $\delta=-0.1t$,

(c) $\delta=0$,

(d) $\delta=0.1t$,

(e) $\delta=0.2t$.

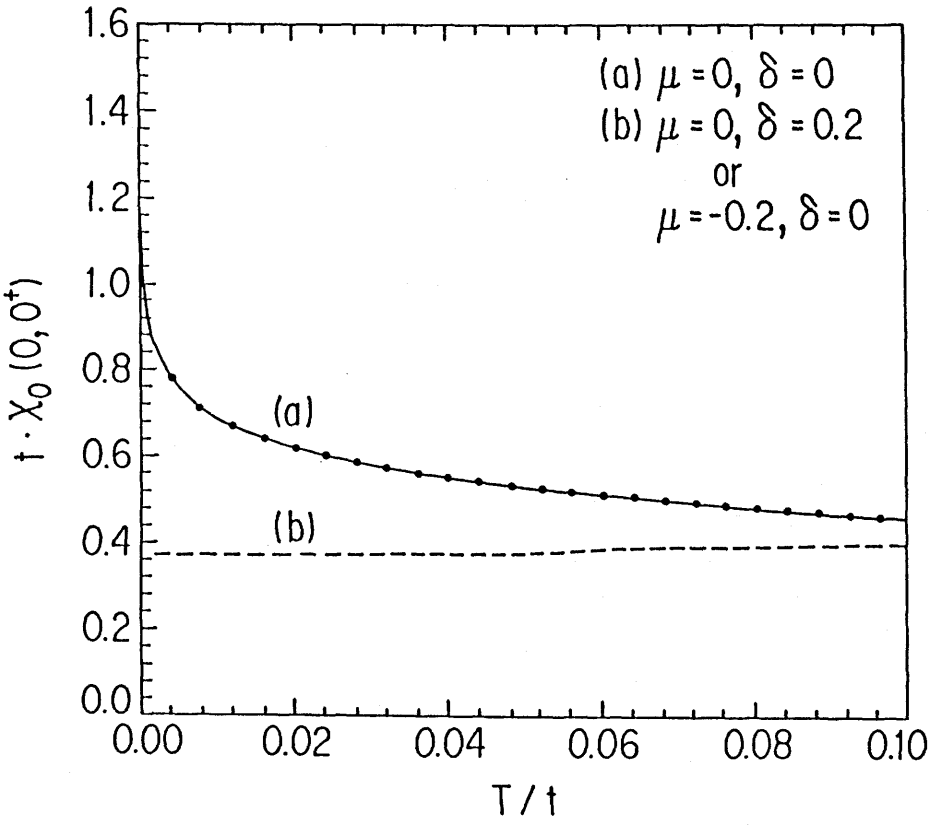

Fig.2.3. The susceptibility $\chi_0(0,0+)$. (a) $\mu=0$, $\delta=0$: The solid line is given by eq.(2.3.4) and the dots express the numerical results. (b) The broken line express the numerical results for $\mu=0$, $\delta=0.2t$ and for $\mu=-0.2t$, $\delta=0$. These two cases give almost same values of $\chi_0(0,0+)$.

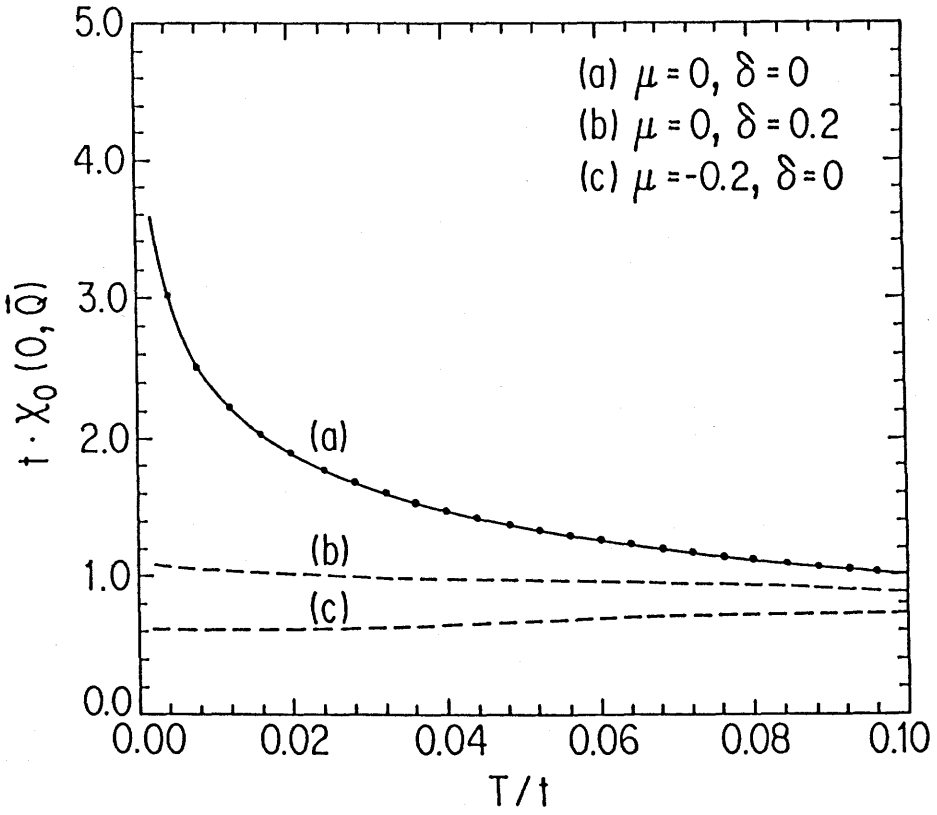

Fig.2.4. The susceptibility $\chi_0(0,\vec{Q})$. (a) μ=0, δ=0: The solid line is given by eq.(2.3.5) and the dots express the numerical results. (b) μ=0, δ=0.2t, (c) μ=-0.2t, δ=0.

§2.3 Spin-Density-Wave

In this section, we study the SDW transition. The antiferromagnetic susceptibility diverges at a temperature, that is, an SDW transition temperature T_{SDW}, if the repulsive interaction is sufficiently strong. Within an RPA, the SDW transition temperature is given by the equation:

$$1 = U \chi_0(0, \vec{q}_m) , \tag{2.3.1}$$

where $\vec{q}_m$ is the momentum at which $\chi_0(0,\vec{q}_m)$ takes maximum value. In particular, for $\mu=\delta=0$, where $\vec{q}_m=\vec{Q}=(\pm\pi,\pm\pi)$, we can easily obtain T_{SDW} as

$$T_{SDW} = \frac{16\, e^{\gamma}}{\pi} t \exp(- \sqrt{2}\, \pi \, (\frac{t}{U} - C_0)^{1/2}) , \tag{2.3.2}$$

from eqs.(2.2.6) and (2.3.1). This expression gives the maximum value of T_{SDW} for given U, since in this case ($\mu=\delta=0$) the Fermi surface is perfectly nesting. Moreover, as increasing or decreasing μ and δ, the T_{SDW} decreases rapidly as shown in Fig.2.5, while the peak of the T_{SDW} shifts at $\mu\cong\delta$ due to the van Hove singularities.

On the other hand, the T_{SDW} is slightly affected by the orthorhombic distortion, which changes the electron dispersion as

$$\varepsilon(\vec{k}) = -t_1(\cos(k_x)+\cos(k_y)) -t_2(\cos(k_x)-\cos(k_y)) -\mu. \tag{2.3.3}$$

We exhibit the SDW transition temperature for the orthorhombic lattice in Fig.2.6.

Next, we calculate an SDW gap M, which is given by

$$M = U \sum_{\vec{k}} \frac{\tanh \frac{E(\vec{k}) - D(\vec{k})}{2T} + \tanh \frac{E(\vec{k}) + D(\vec{k})}{2T}}{4E(\vec{k})} M , \qquad (2.3.4)$$

with $$E(\vec{k}) = \sqrt{t^2(\cos(k_x)+\cos(k_y))^2 + M^2} ,$$

and $$D(\vec{k}) = \delta \cos(k_x) \cos(k_y) + \mu ,$$

within the Hartree-Fock approximation. The interaction strength dependence of the gap M and the corresponding magnetic moment 2S for $\mu=\delta=0$ and T=0 are shown in Fig.2.7 and Fig.2.8, respectively. For example, it is found that if the band width 4t=20000K and T_{SDW}=250K, then $U \cong 0.73t$ and $2S \cong 0.24\ \mu_B$ at T=0, which is rather large value because of the van Hove singularity.

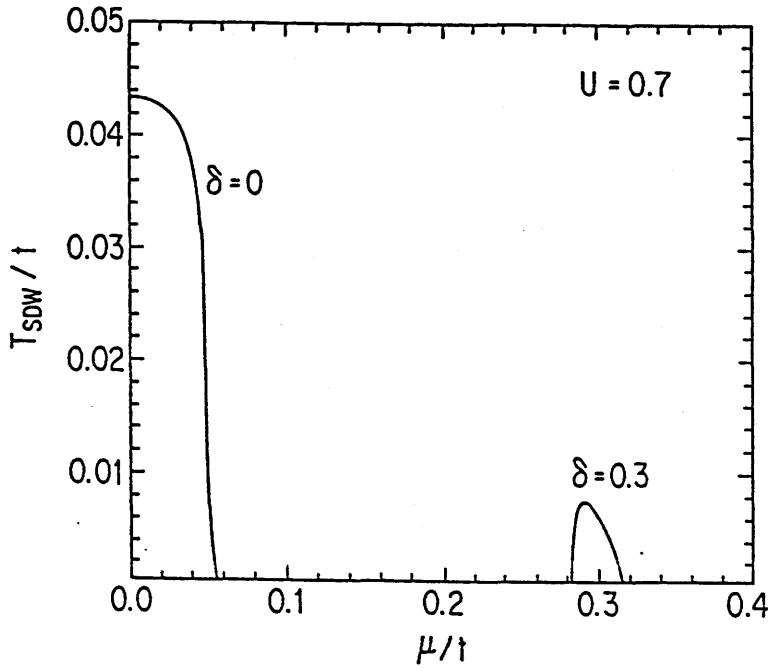

Fig.2.5. SDW transition temperature for U=0.7t.(a) δ=0, (b) δ=0.3t.

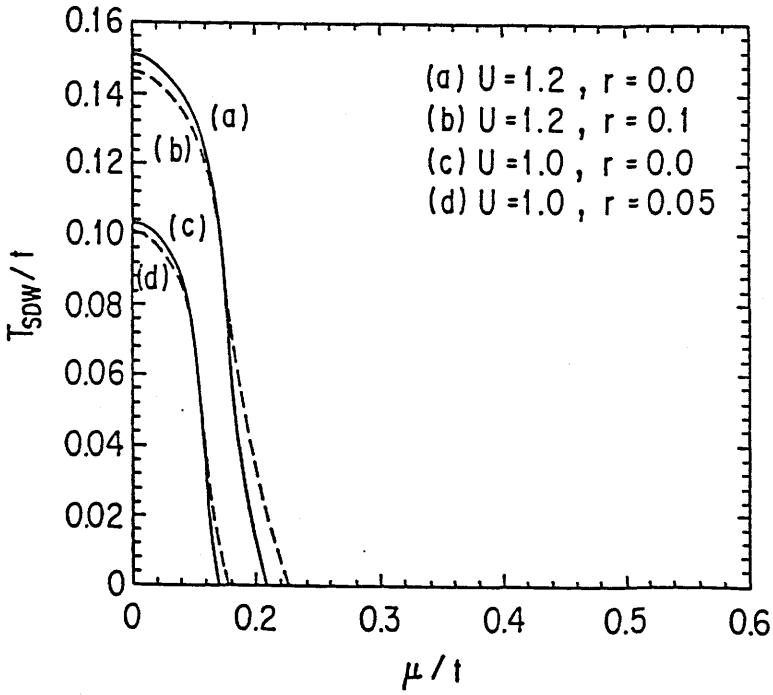

Fig.2.6. SDW transition temperature in orthorhombic case. (a) $U=1.2t_1$, $t_2=0$. (b) $U=1.2t_1$, $t_2=0.1t_1$. (c) $U=1.0t_1$, $t_2=0$. (d) $U=1.0t_1$, $t_2=0.05t_1$.

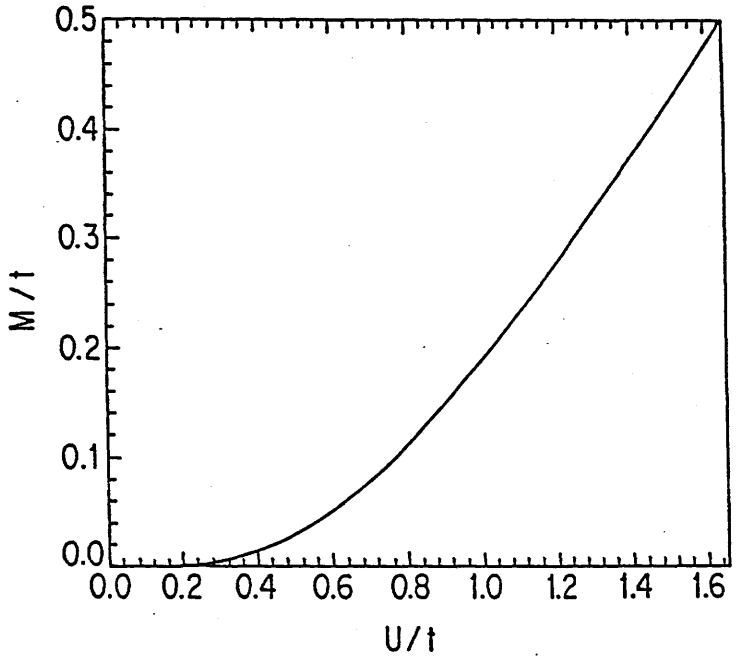

Fig.2.7. The SDW gap in a mean field theory.

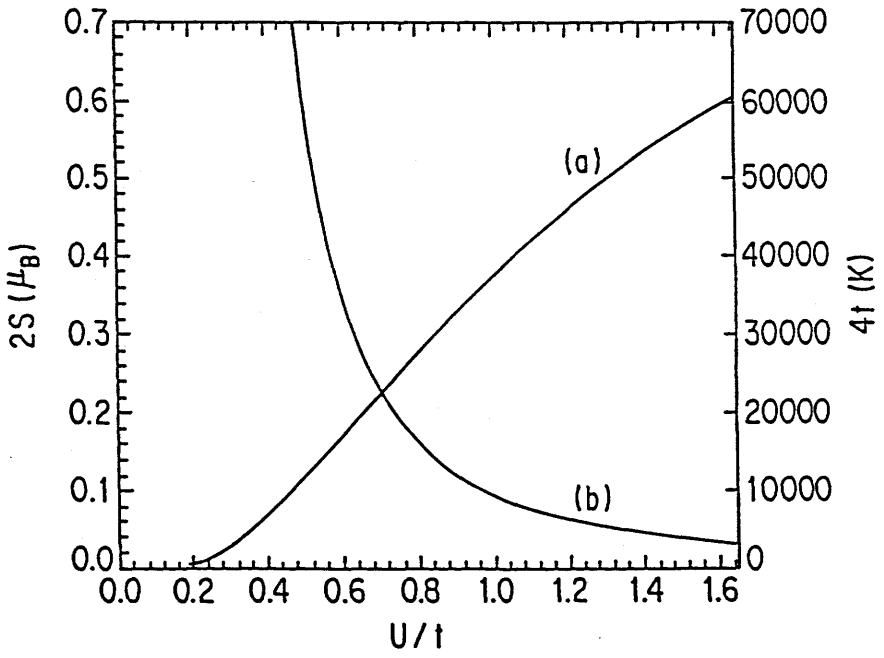

Fig.2.8. (a) The magnetic moment (2S) given by the SDW gap M. (b) The band width (4t) with fixed T_{SDW}=250K.

§2.4 Superconductivity Induced by Local Attractive Interaction

Before studying the spin-fluctuation exchange model we examine a simplified model for this mechanism in connection with the local nature of the interactions and the van Hove singularities in 2D systems. It has been often pointed out that the logarithmic enhancement of the DOS near the Fermi-level will enhance the superconductivity.[112~114] Here we demonstrate the specific features arising from such characteristics of the DOS in detail.

We study an effective Hamiltonian in this section, which describes tight-binding electron system with hopping and local interactions:

$$H = \sum_{i,j,\sigma} t_{ij} c_{i\sigma}^{\dagger} c_{j\sigma} - \mu \sum_{i} n_i + \frac{1}{2} \sum_{i,j} (\Gamma^{s}(\vec{r}_i - \vec{r}_j)\, \vec{\sigma}_i \cdot \vec{\sigma}_j + \Gamma^{n}(\vec{r}_i - \vec{r}_j)\, n_i \cdot n_j) , \qquad (2.4.1)$$

where i and j denote lattice sites, and $\sigma_i^{\alpha} = \sum_{\sigma,\sigma'} c_{i\sigma}^{\dagger} \sigma_{\sigma\sigma'}^{\alpha} c_{i\sigma'}$, and $n_i = \sum_{\sigma} c_{i\sigma}^{\dagger} c_{i\sigma}$ is an α (=x,y,z) component of the spin operator and the density operator at site i, respectively. Here Γ^{s} and Γ^{n} denotes the spin and charge interactions, respectively, and for example we can adopt the spin and charge fluctuations to them, which exchange interaction are studied in the next section in details. Apart from this, we can include the phonon mediated interaction in our effective Hamiltonian. In this section, we do not study nesting instabilities.

At first we consider the tetragonal case and assume the n.n. and n.n.n. transfers and rewrite the Hamiltonian (2.4.1) in a Bloch representation:

$$H = \sum_{k,\sigma} \varepsilon(\vec{k}) c^{\dagger}_{\vec{k}\sigma} c_{\vec{k}\sigma} + \frac{1}{2N} \sum_{q} \left(\Gamma^{s}(\vec{q})\ \vec{\sigma}(\vec{q})\cdot\vec{\sigma}(-\vec{q}) + \Gamma^{n}(\vec{q})\ n(\vec{q})\cdot n(-\vec{q}) \right) , \qquad (2.4.2)$$

$$\varepsilon(\vec{k}) = - t \left(\cos(k_x) + \cos(k_y)\right) - \delta \cos(k_x)\cos(k_y) - \mu , \qquad (2.4.3)$$

$$\Gamma^{a}(\vec{q}) = \sum_{n,m} \Gamma^{a}(n,m) \cos(nq_x) \cos(mq_y) \quad (a = s,n). \qquad (2.4.4)$$

Here we take the lattice constant as unity.

In the ladder approximation, the superconducting transition T_c is given by:

$$\Delta(\vec{k}) = \frac{1}{N} \sum_{k'} \Gamma(\vec{k},\vec{k}') \frac{\tanh \frac{\varepsilon(\vec{k}')}{2T_c}}{2\ \varepsilon(\vec{k}')} \Delta(\vec{k}') , \qquad (2.4.5)$$

where $\Gamma(\vec{k},\vec{k}') = 2\ \Gamma^{s}(\vec{k}+\vec{k}') + \Gamma^{s}(\vec{k}-\vec{k}') - \Gamma^{n}(\vec{k}-\vec{k}')$.

Here we neglect the interactions except the on-site and the n.n. interactions, and thus we obtain from eq.(2.4.4)

$$\begin{aligned}\Gamma(k,k') = &- \tilde{U} + \gamma^{s}(\cos(k_x)+\cos(k_y))\ (\cos(k'_x)+\cos(k'_y)) + \\ &+ \gamma^{d}(\cos(k_x)-\cos(k_y))\ (\cos(k'_x)-\cos(k'_y)) \\ &+ \gamma^{p}(\sin(k_x)\sin(k'_x) + \sin(k_y)\sin(k'_y)) , \qquad (2.4.6)\end{aligned}$$

where $\tilde{U}$ $(=\Gamma^{n}(0,0)+\Gamma^{s}(0,0))$ is the on-site Coulomb interaction renormalized by the fluctuations, and γ^{s}, γ^{p} and γ^{d}, are nearest neighbour interactions for s,p,and d-wave pairing:

$$\tau^s = \tau^d = 3\,\Gamma^s(1,0) - \Gamma^n(1,0),$$

$$\tau^p = -\,2\,\Gamma^s(1,0) - 2\,\Gamma^n(1,0).$$

The expressions for τ^s, τ^d, and τ^p tell us that the antiferromagnetic interaction ($\Gamma^s(1,0)>0$) leads to singlet pairings (s and d), while the ferromagnetic interaction ($\Gamma^s(1,0)<0$) yields p-wave pairings.

Corresponding these signs, we can assume the three types of pairing, that is

(1) d-wave pairing for $\tau_d<0$

$$\Delta(\vec{k}) = \Delta\,(\cos(k_x)-\cos(k_y)) \qquad (2.4.7)$$

(2) p-wave pairing for $\tau_p<0$

$$\Delta(\vec{k}) = \Delta\,\sin(k_x) \qquad (2.4.8)$$

(3) s-wave pairing for $U<0$

$$\Delta(\vec{k}) = \Delta \qquad (2.4.9)$$

This last case seems to be impossible at first glance, because generally the Coulomb repulsion will be strong enough to overcome other attractive interaction between two electrons on the same site. However, in the real material, the site means the lattice site which may extend in real space enough for electrons to shield the Coulomb interactions. In addition, strictly speaking, the n.n. s-wave is contribute to eq.(2.4.9), but such correction is very small since the n.n. s-wave vanishes on the Fermi-surface.

2.4.1 Behaviour of the transition temperatures

The equations for T_c are solved numerically for δ=0, 0.1, 0.2, 0.3 and various μ assuming d and s-wave pairing separately. (Fig.2.9 and 2.10.) For the d-wave pairing, the T_c shows a sharp maximum at $\mu=\delta$ where the van Hove singularities are on the Fermi-level. It is remarkable that T_c with different δ exhibit almost the same behaviour except the translation by $\mu-\delta$ and slight deviation of the maximum value. In fact, we have $T_c=0.0175t\pm0.0003t$ for $\mu=\delta=0$, and $T_c=0.0182t\pm0.0003t$ for $\mu=\delta=0.3t$, although the number of electrons per site n=1 for the former case, and n=1.2 for the later case. Hence we have the approximate relation $T_c(\mu,\delta)\cong T_c(\mu-\delta,0)$ as a function of μ and δ if δ is not too large ($\delta\lesssim0.3t$).

For negative $\tilde{U}$ and s-wave pairing, the T_c have the similar natures, although the widths of the peaks are more broad.

These behaviours are in contrast to that of SDW transition temperatures, for which the Fermi-surface nesting is essential.

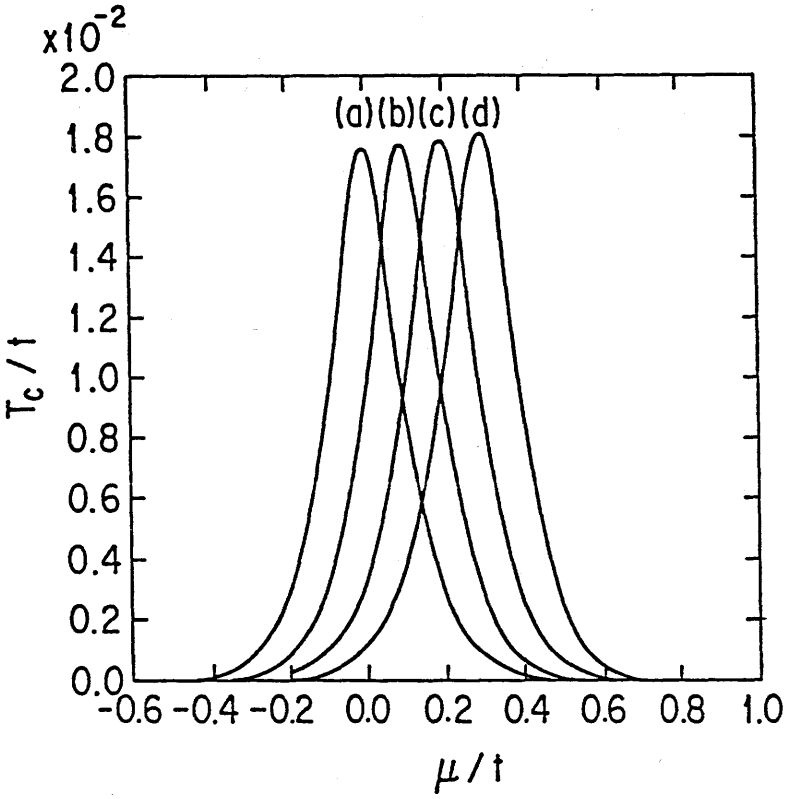

Fig.2.9. μ dependence of T_c in the d-wave pairing case for $\tau^d = t/4$: (a) $\delta/t=0$, (b) $\delta/t=0.1$, (c) $\delta/t=0.2$, (d) $\delta/t=0.3$. These graphs almost coincide with each other if one translates each graph by δ.

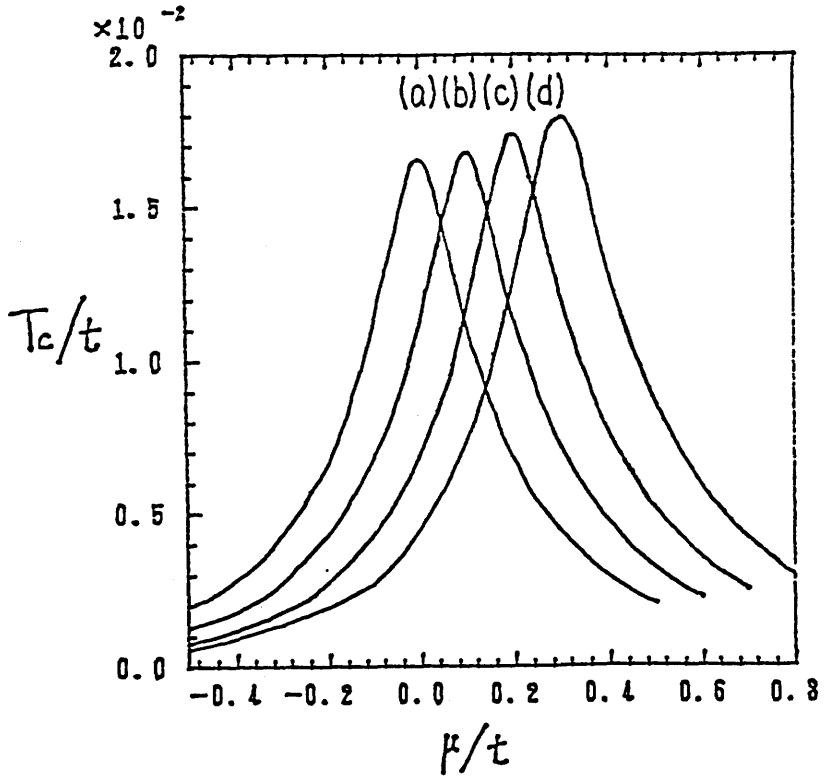

Fig.2.10. μ dependence of T_c of the s-wave pairing case for $\tilde{U}=t/2$: (a) $\delta/t=0$, (b) $\delta/t=0.1$, (c) $\delta/t=0.2$, (d) $\delta/t=0.3$.

2.4.2 Analytic expressions of the transition temperatures

Now we derivate the analytic expressions of T_c for $\mu=\delta=0$, which are approximately applicable for $\mu=\delta\neq 0$ from the relation mentioned above.

As an example of the derivations, we investigate the d-wave pairing case. Eq.(2.4.5) can be written in the form:

$$1 = \frac{\gamma^d}{\pi^2 t} \int_0^1 dx\ \rho(x)\ \frac{\tanh(\frac{t}{T_c}x)}{x}\ , \tag{2.4.9}$$

$$\rho(x) = \int_0^{2-2x} dy\ \frac{y^2}{\sqrt{(1-(y/2+x)^2)\ (1-(y/2-x)^2)}}\ , \tag{2.4.10}$$

where $y=\cos(k_x)-\cos(k_y)$ and $x=(\cos(k_x)+\cos(k_y))/2$. Now we divide the range of the integral of eq.(2.4.9) into two regions, that is, $0\leq x\leq x_c$ and $x_c\leq x\leq 1$, where we have introduced a cut x_c which satisfies $T_c/t<<x_c<<1$ and will be determined later. For the integration of $0\leq x\leq x_c<<1$, the DOS $\rho(x)$ can be approximated as

$$\rho(x) = 4\ \ln\ (\frac{1}{x}\ (\frac{2}{e})^2)\ , \tag{2.4.11}$$

neglecting the order of $x^2\ln(1/x)$, the contribution of which vanishes in the limit $T_c\to 0$. Thus eq.(2.4.9) is rewritten as:

$$1 = \frac{2\ \gamma^d}{\pi^2\ t}\ (\ \ln^2(\frac{t^*}{T_c}) + \pi^2 C\ )\ , \tag{2.4.12}$$

where $t^*=16e^{\gamma-2}t/\pi\cong 1.2276t$ with $\gamma\cong 0.57721$, and

$$\pi^2 C = [- \ln^2(4/e^2 x_c) - \ln^2(4e^{\gamma}/\pi) + \int_0^{\infty} dx \ln^2 x \frac{1}{ch^2 x} + \int_{x_c}^{1} dx \rho(x) \frac{\tanh \frac{t x}{T_c}}{2 x}]. \quad (2.4.13)$$

In the integral of the last term, we can set $\tanh(tx/T_c) \cong 1$ unless x_c is too small, and it is found that C is nearly constant for varying x_c. Therefore we set $x_c = 0.08$, which gives the numerical result $C \cong 0.169$, and finally we obtain the analytical expression:

$$T_c = t^* e^{- \pi \left(\frac{t}{2\gamma^d} - C \right)^{1/2}} . \quad (2.4.14)$$

In particular for weak coupling $2\gamma^d/t << 1/C \cong 5.917$, T_c is simply given by

$$T_c = t^* e^{- \pi \left(\frac{t}{2\gamma^d} \right)^{1/2}} . \quad (2.4.15)$$

The results eqs.(2.4.14) and (2.4.15) tell us that T_c is remarkably enhanced by the van Hove singularity and the usual BCS formula of T_c does not work in the case where the Fermi-level is at or in the vicinity of the van Hove singularity. In Fig.2.11, the numerical results of T_c are shown as well as those given by eqs.(2.4.14) and (2.4.15). It is found that the curve given by eq.(2.4.14) agrees very well with the numerical result over the whole region of γ^d while that given by eq.(2.4.15) could not be used except very small γ^d.

Along the similar way, we can obtain the formula for s-wave case:

$$T_c = t^* e^{-\pi(\frac{2t}{|U|} + C_s)^{1/2}}, \qquad (2.4.16)$$

with $t^*=16e^{\gamma}t/\pi\cong 9.0709t$ and $C_s\cong 0.0332$, which has an unusual form as well as that of d-wave case. On the other hand, for p-wave case, we obtain a BCS-like formula:

$$T_c = t\,\frac{4e^{\gamma}}{\pi}\exp(-\frac{\pi^2 t}{4\gamma^p} + C_p), \qquad (2.4.17)$$

with $C_p\cong -0.610$.

The accuracy of eq.(2.4.16) and eq.(2.4.17) is seen in Fig.2.12 and Fig.2.13 respectively.

2.4.3 Orthorhombic distortion

An orthorhombic distortion will change the electron dispersion as eq.(2.3.3). In this case two saddle points of the dispersion are on the Fermi-surface at $\mu=\pm 2t_2$. Thus, as shown in Fig.2.14, T_c has one maximum for $T_c >> t_2$ and as t_2 increases it becomes to take two maxima, the value of which decreases with increasing δ.

As was shown above, the behaviour of the superconductivity is quite different from ordinary one, because of the van Hove singularities, and our result also shows that the electrons near the saddle point of the electron dispersion is dominant in the superconductivity.

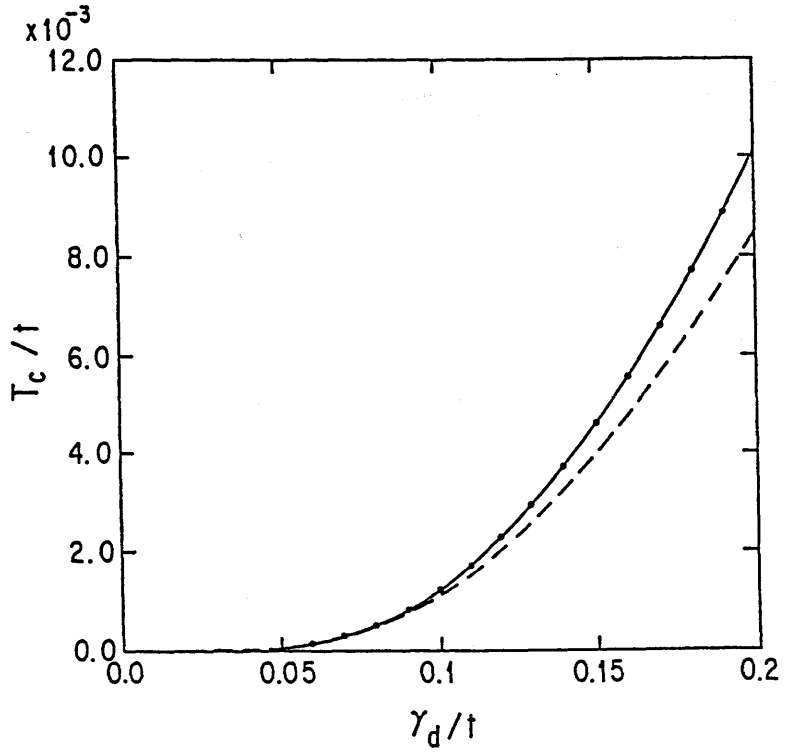

Fig.2.11. d-wave case; T_c versus τ^d. The points, line and broken line express, numerical result, those given by eq.(2.4.14) and (2.4.15) respectively.

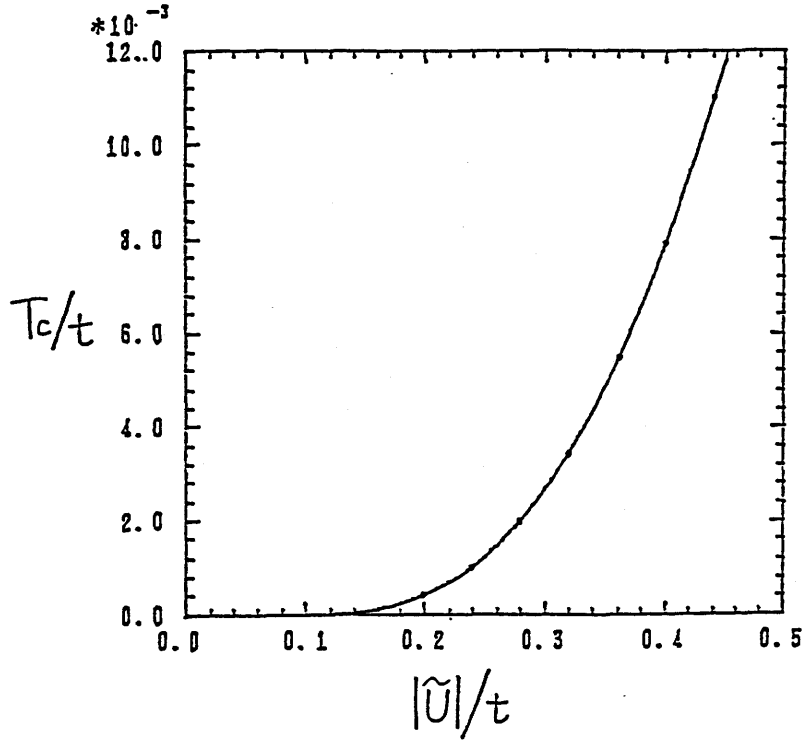

Fig.2.12.
s-wave case; T_c versus $|\tilde{U}|$. The points and line express, numerical result and that given by eq. (2.4.16) respectively.

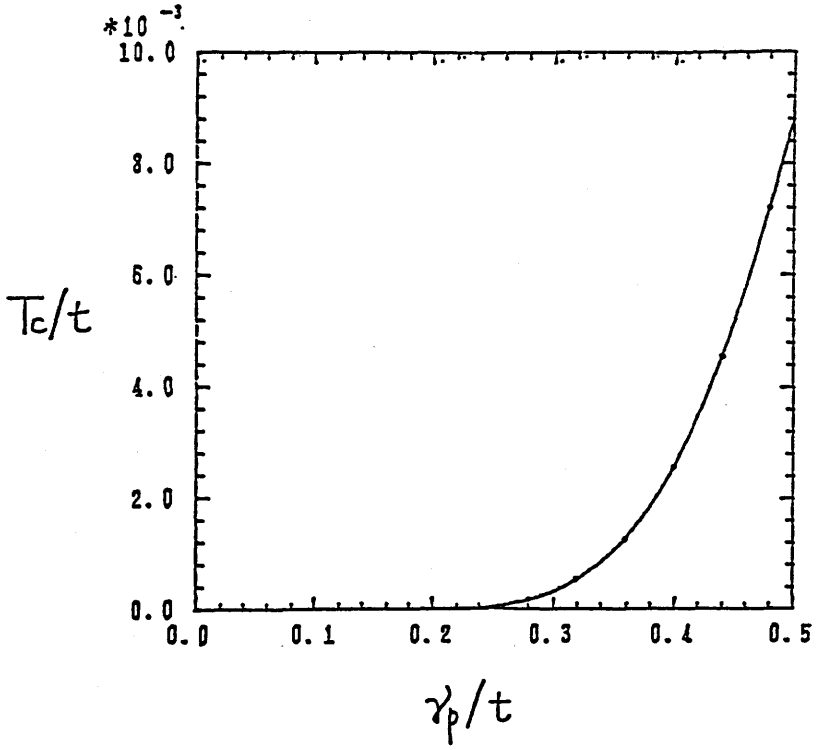

Fig.2.13.
p-wave case; T_c versus γ^p. The points and line express, numerical result and that given by eq. (2.4.17) respectively.

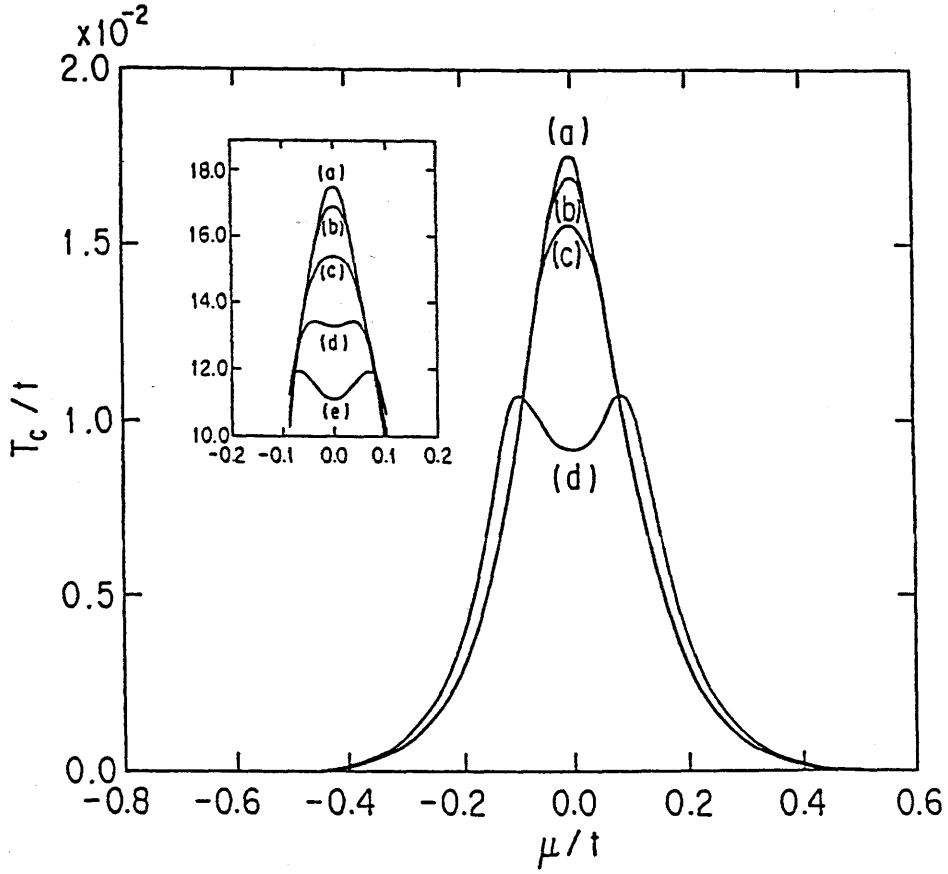

Fig.2.14. T_c of orthorhombic cases for τ^d=t/4: (a) r≡ t_2/t_1=0, (b) r=0.01, (c) r=0.02, (d) r=0.05. The insect shows fine peak structures: (a) r=0, (b) r=0.01, (c) r= 0.02, (d) r=0.03, (e) r=0.04.

§2.5 Superconductivity Mediated by Spin-Fluctuations

As was discussed in §2.1, the exchange of the spin-fluctuations gives attractive interactions between electrons and leads to the superconductivity. Here we study this mechanisms on the basis of 2D Hubbard model. Since this kind of electronic interaction has strong coupling nature and does not have a small cutoff in energy space such as a phonon exchange interaction, static approximation and averaging on the Fermi-surface is not appropriate especially for finite temperatures. Thus we do not approximate on the frequency dependence of the pairing and take into account the renormalization effect through the self energy.

Following Scalapino et al.[107] we treat the spin- and charge-fluctuations in RPA, whose diagrams are drawn in Fig.2.15. Thus the effective vertices for anti-parallel and parallel spins are given in the following:

$$\Gamma_{\alpha\beta}(k,k'q) = U + \frac{U^2 \chi_0(k+k'+q)}{1 - U \chi_0(k+k'+q)} + \\ + \frac{1}{2} \frac{U^2 \chi_0(k-k')}{1 - U \chi_0(k-k')} - \frac{1}{2} \frac{U^2 \chi_0(k-k')}{1 + U \chi_0(k-k')} , \tag{2.5.1}$$

$$\Gamma_{\sigma\sigma}(k,k'q) = \\ - \frac{1}{2} \frac{U^2 \chi_0(k-k')}{1 + U \chi_0(k-k')} - \frac{3}{2} \frac{U^2 \chi_0(k-k')}{1 - U \chi_0(k-k')} , \tag{2.5.2}$$

with $\sigma=\alpha$ or β, where k denotes $(\vec{k}, i\omega_n)$. The first term in eq. (2.5.1) is the on-site Coulomb repulsion, and the fourth term in

eq.(2.5.1) and the first term in eq.(2.5.2) describe the charge fluctuations, and the second and third terms in eq.(2.5.1) and the second term in eq.(2.5.2) describe the spin-fluctuations. We regard this set of diagrams as a boson propagator, and discuss the superconductivity mediated by these bosons.

The electron Green's functions are expressed as

$$G_k = (i\omega_n - \varepsilon(\vec{k}) - \Sigma(k))^{-1}, \qquad (2.5.3)$$

where $\Sigma(k)$ is the electron self-energy. We take the lowest diagram for the self-energy in this electron-boson system as shown in Fig.2.16. Then, resulting self-consistent equation is

$$\Sigma(k) = - \sum_{k'} \Gamma_{\alpha\alpha}(k,k') G_{k'} - \sum_{k'} U^2 \chi_0(k-k') G^0_{k'}, \qquad (2.5.4)$$

where $k=(\vec{k},i\omega)$ and $\sum_{k'} \equiv N^{-1} \sum_{\vec{k}'} T \sum_{n'}$, and G^0_k, is the bare electron Green's function. Here the second term is added to cancel the double counting contribution of the first term.

Now, we introduce the two-particle vertex Γ for singlet pairing in a ladder approximation which is shown in Fig.2.17:

$$\Gamma(k,k',q) = \Gamma_{\alpha\beta}(k,k',q) - \sum_{k''} \Gamma_{\alpha\beta}(k,k'',q) G_{k''+q} G_{-k''} \Gamma(k'',k',q) . \qquad (2.5.5)$$

The approximations for the two-particle vertex and the self-energies are consistent with each other in a diagramatic formulation of electron-boson systems. Then, the superconducting

transition temperature is given by the condition for the first appearance of the nontrivial solution of $\Delta(k)$, satisfying

$$\Delta(k) = - \sum_{k} \Gamma_{\alpha\beta}(k,k',0)\, G_{-k'}G_{k'}\Delta(k') \ , \tag{2.5.6}$$

$$\text{i.e.} \quad \det(\delta_{kk'} + \Gamma_{\alpha\beta}(k,k',0)\, G_{-k'}G_{k'}) = 0 \ . \tag{2.5.7}$$

The interaction given in eqs.(2.5.1) and (2.5.2) rapidly would decay in the real space, because the anti-parallel and parallel correlation alternately appear and cancel out by averaging over the direction in the present square lattice system. Hence, we expand eqs.(2.5.1) and (2.5.2) up to the n.n.n., as

$$\begin{aligned}
\Gamma_{\alpha\beta}(k,k',0) &= \tau_1^{(0)}(i\omega_n,i\omega_{n'}) \\
&+ \tau_1^{(1)}(i\omega_n,i\omega_{n'}) \left(\cos(k_x)\cos(k_x') + \cos(k_y)\cos(k_y')\right) \\
&+ \tau_2^{(1)}(i\omega_n,i\omega_{n'}) \left(\sin(k_x)\sin(k_x') + \sin(k_y)\sin(k_y')\right) \\
&+ \tau_1^{(2)}(i\omega_n,i\omega_{n'}) \left(\cos(k_x)\cos(k_y)\cos(k_x')\cos(k_y')\right. \\
&\qquad \left. + \sin(k_x)\sin(k_y)\sin(k_x')\sin(k_y')\right) \\
&+ \tau_2^{(2)}(i\omega_n,i\omega_{n'}) \left(\sin(k_x)\cos(k_y)\sin(k_x')\cos(k_y')\right. \\
&\qquad \left. + \cos(k_x)\sin(k_y)\cos(k_x')\sin(k_y')\right) \ .
\end{aligned} \tag{2.5.8}$$

$$\begin{aligned}
\Gamma_{\sigma\sigma}(k,0,q) &= \tau^{(0)}(i\omega_n) + \tau^{(1)}(i\omega_n)\left(\cos(k_x) + \cos(k_y)\right) \\
&\quad + \tau^{(2)}(i\omega_n)\cos(k_x)\cos(k_y) \ .
\end{aligned} \tag{2.5.9}$$

From eqs.(2.5.9) and (2.5.4), the self-energy can be similarly expanded in the momentum space:

$$\begin{aligned}
\Sigma(k) &= \Sigma^{(0)}(i\omega_n) + \Sigma^{(1)}(i\omega_n)\left(\cos(k_x) + \cos(k_y)\right) \\
&\quad + \Sigma^{(2)}(i\omega_n)\cos(k_x)\cos(k_y) \ ,
\end{aligned} \tag{2.5.10}$$

where $\Sigma^{(0)}(i\omega_n)$, $\Sigma^{(1)}(i\omega_n)$, and $\Sigma^{(2)}(i\omega_n)$ are given by eq.(2.5.4) being mixed with each other. Moreover we neglect the symmetric part of $\Sigma(k)$.

For two electrons with anti-parallel spins, $\gamma_1^{(0)}$, $\gamma_1^{(2)}$, $\gamma_2^{(2)}$, and $\gamma_2^{(1)}$ are repulsive, and $\gamma_1^{(1)}$ is attractive reflecting the antiferromagnetic correlation in the present system. This correlation leads to the n.n. singlet pairing, especially n.n. d-pairing, which is most enhanced by the van Hove singularity.[112~114] Strictly speaking, the n.n. d-pairing mode is necessarily mixed with the other pairing mode of the same symmetry, by the terms neglected in eq.(2.5.7). However, the numerical calculation shows that the next order corrections are negligibly small, as expected. Hence, we can rewrite eq.(2.5.7) into

$$\det(\delta_{nn'} + \gamma_1^{(1)}(i\omega_n, i\omega_{n'})\, W(i\omega_{n'})) = 0 \ , \tag{2.5.11}$$

where

$$\gamma_1^{(1)}(i\omega_n, i\omega_{n'}) \equiv \frac{1}{2N} \sum_{\vec{k}} \Gamma_{\alpha\beta}((\vec{k}, i\omega_n), (\vec{0}, i\omega_{n'}), 0) \cdot (\cos(k_x) + \cos(k_y)) \ , \tag{2.5.12}$$

$$W(i\omega_{n'}) \equiv \frac{1}{2N} \sum_{\vec{k}} G_{-k} G_k \cdot (\cos(k_x) - \cos(k_y))^2 \ . \tag{2.5.13}$$

Thus the problem reduces to eqs.(2.5.4) and (2.5.11) with eqs.(2.5.9), (2.5.10), (2.5.12), and (2.5.13).

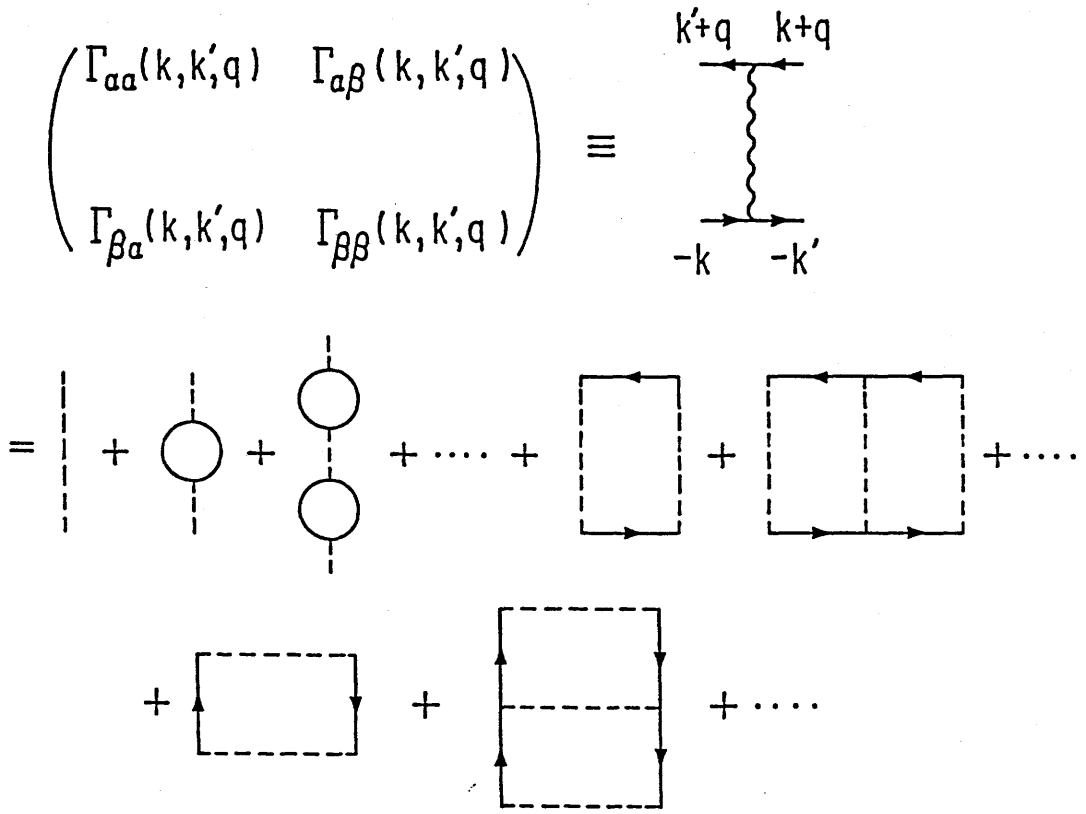

Fig.2.15. The effective vertices $\Gamma_{\sigma\sigma'}(k,k',q)$ in the RPA. The spin index σ and σ' denotes the spin of the electrons corresponding to the four momentum k'+q and -k, respectively, in this diagram. Other electron spins are automatically determined from the form of the Coulomb interaction in eq.(2.1.1). The solid and broken lines denote the bare Green's functions and the interaction U, respectively. These diagrams give eqs.(2.5.1) and (2.5.2).

Fig.2.16. The electron self-energy. The thick and thin line denote the renormalized and bare Green's functions, respectively. The wavy line is defined in Fig. 2.15. The momentum dependent contribution from the vertex $\Gamma_{\alpha\beta}$ is already included in these diagrams, from the definition of $\Gamma_{\sigma\sigma}$. This diagram gives eq.(2.5.4).

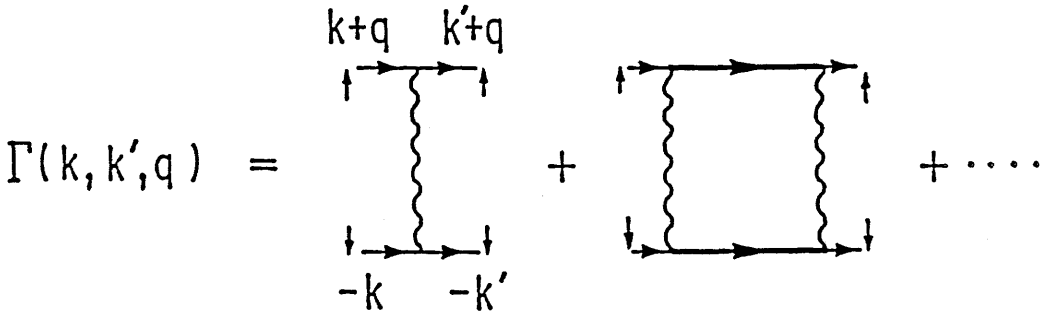

Fig.2.17. The two-particle vertex for a singlet pairing. The thick solid line express the renormalized Green's functions, and the wavy line is defined in Fig.2.15. This diagram gives eq.(2.5.5).

§2.6 Phase Diagrams

Eqs.(2.5.4), (2.5.9), and (2.5.10) are solved by self-consistent numerical calculation, which satisfactorily converges in four or five iterations. Using this result, eqs.(2.5.11), (2.5.12), and (2.5.13) are also solved numerically with results given in this section.

2.6.1 The case of δ=0

The numerical results are drawn in Fig.2.18(a)~(c) for δ=0. Here, we only study the case of μ>0 since the phase diagram only depends on the magnitude of μ due to the particle-hole symmetry. In those figures the solid, broken and dotted lines express T_{SDW}, T_c with and without the self-energy, respectively. As is seen in Fig.2.18(b) and (c), if one neglects the self-energy the superconducting transition temperature T_c is always higher than T_{SDW} and becomes higher as gets closer to T_{SDW}. The reason for this is the divergence of the effective interaction at T_{SDW}. However, if one takes into account the self-energy effect, T_c is remarkably suppressed due to the renormalization effect as is seen in Fig.2.18(a)~(c). Such strong suppression by the renormalization effect is a general feature of this kind of superconductivity, in which the attractive part of the interaction is taken out for pairing and the other strong repulsive part is avoided by symmetry in the gap equation. It should be noted, further, that the superconductivity is enhanced near the SDW boundary, although the resultant T_c is rather low. For examples, for δ=0 and U/t=0.8, 1.0, 1.2, we obtain the maximum value of T_{SDW}/t=0.0611, 0.1028,

0.1509 and that of $T_c/t=4.0\times10^{-4}$, 1.0×10^{-3}, 1.8×10^{-3}, respectively. ($T_c/T_{SDW}\lesssim0.0064$, 0.0096, 0.012.) If we takes the value of t which makes the maximum of T_{SDW} equal to 250K, then we have the maximum transition temperature T_c=1.6K, 2.4K, 3.0K and 4t=16400K, 9700K, 6600K, respectively. The region in which the superconductivity occurs increases with U as well as T_c. For U=0.6t the superconductivity does not appear except for extremely low temperatures.

The phase diagram in the U-μ plane at very low temperature $T=10^{-4}t$ is given in Fig.2.19. It is found that the superconductivity appears in the narrow region between the SDW and normal phase for $\mu\gtrsim0.05t$. For $\mu\lesssim0.05t$, the SDW is always more favourable than superconductivity at this temperature.

2.6.2 The case of δ=0.3t

Now we examine effects of the n.n.n. hopping. We set δ=0.3t as an example, and the numerical results are shown in Fig.2.20(a)~(c).

As is seen in Fig.2.20(a), T_{SDW} takes the maximum at $\mu\cong\delta$=0.3t where the van Hove singularity is at the Fermi-energy, and rapidly decreases with increasing $|\mu-\delta|$. The superconductivity appears in both sides of the SDW phases and the maximum values of it are $4\times10^{-4}t$, $1.2\times10^{-3}t$, and $1.8\times10^{-3}t$, for U=0.7t, 0.8t, and 0.9t, respectively. The important effects of the n.n.n. hopping are as follows: (1) T_{SDW} is remarkably suppressed because the nesting worsens; (2) T_c is enhanced because T_{SDW} is suppressed and thus the boundary of SDW approaches to the van Hove singularities; (3) T_c is higher for $\mu<\delta$ than that for $\mu>\delta$. The

remarkable enhancement of T_c can be found by comparing Figs.2.18(a) and Fig.2.20(b) for U=0.8t, which show that the $\max(T_c) \cong 4\times10^{-4}t$ for $\delta=0$ and $\max(T_c) \cong 1.2\times10^{-3}t$ for $\delta=0.3t$. The maximum SDW transition temperature is $T_{SDW}=0.0074t$ for U=0.7t, and 0.01985t for U=0.8t, and they give the ratio $T_c/T_{SDW} \lesssim 0.054$, 0.060. If we fit the values of $\max(T_{SDW})$ to 250K, then we obtain $T_c \lesssim 13.5K$ and 15.1K, and 4t=135000K and 4t=50000K, respectively. The phase diagram in the U-μ plane at $T=10^{-4}t$ is given in Fig.2.21. The superconductivity appears for $\mu \lesssim \delta=0.3t$ and $0.3t \lesssim \mu \lesssim 0.4t$, between the normal and SDW phases, and disappears rapidly for $\mu \gtrsim 0.4t$, because the most effective nesting vector moves far from $(\pm\pi,\pm\pi)$, and the antiferromagnetic correlation is suppressed.

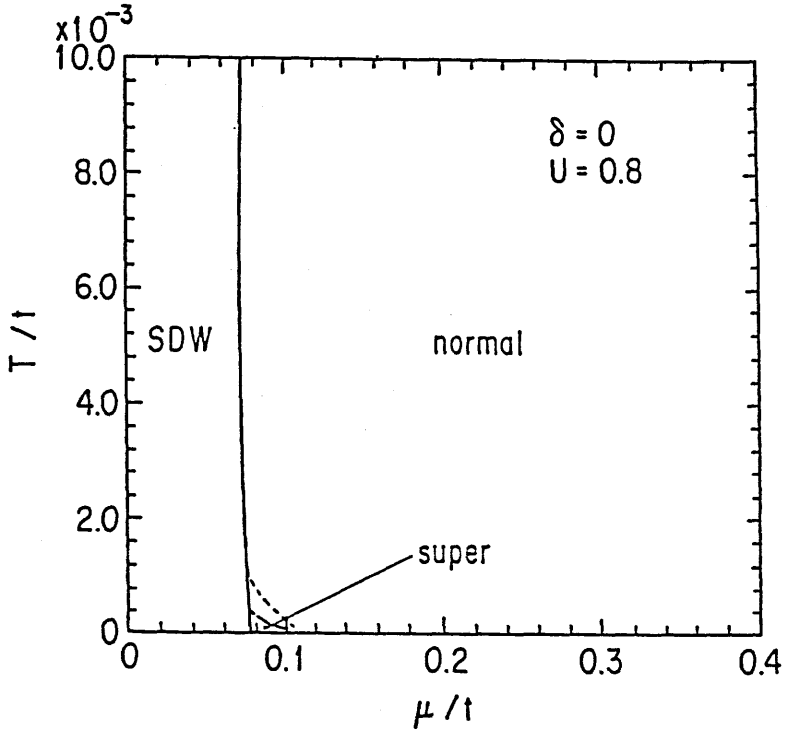

Fig.2.18(a). Phase diagram in T-μ space for δ=0 and U=0.8t. The solid, broken, and dotted lines express T_{SDW} and T_c with and without the self-energy, respectively.

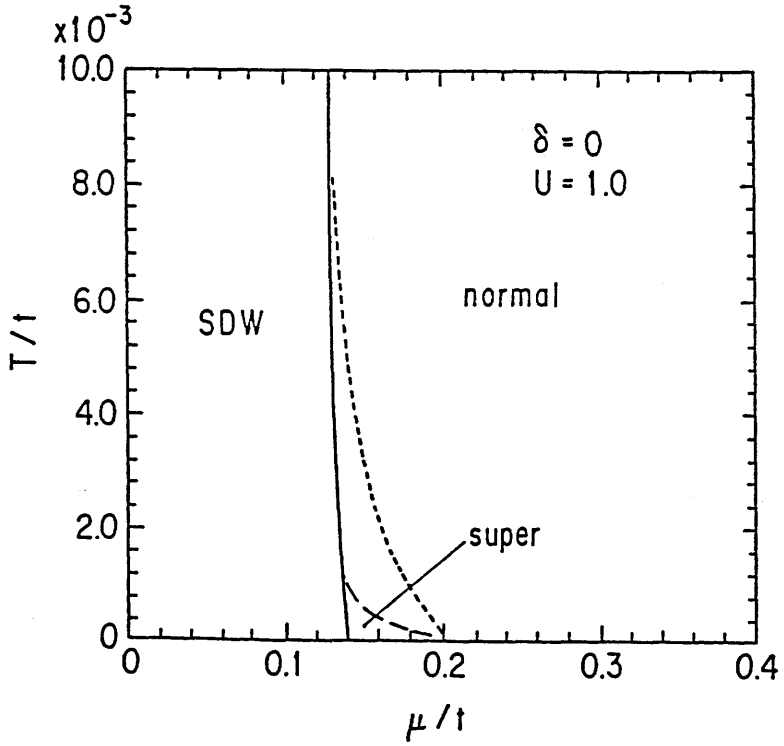

Fig.2.18(b). Phase diagram in T-μ space for δ=0 and U=1.0t. The solid, broken, and dotted lines express T_{SDW} and T_c with and without the self-energy, respectively.

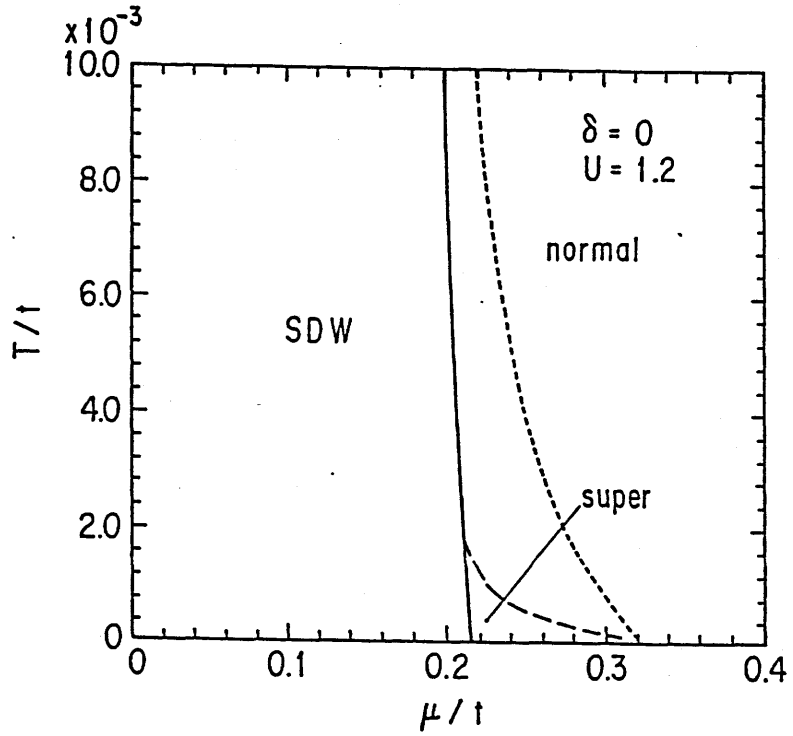

Fig.2.18(c). Phase diagram in T-μ space for δ=0 and U=1.2t. The solid, broken, and dotted lines express T_{SDW} and T_c with and without the self-energy, respectively.

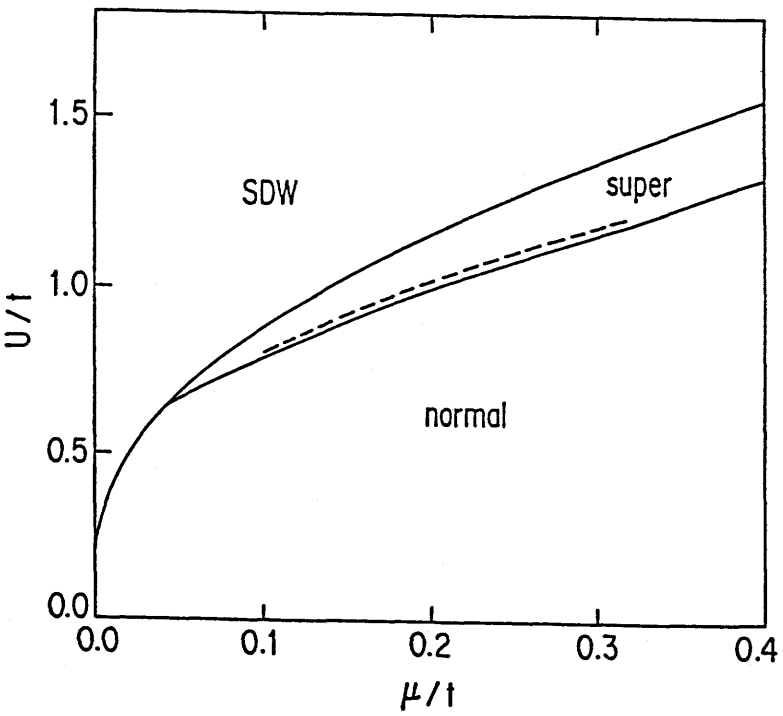

Fig.2.19. Phase diagram in U-μ space for δ=0. The self-energy is neglected for the solid line, and included for the broken line, which express the normal-superconducting phase boundaries.

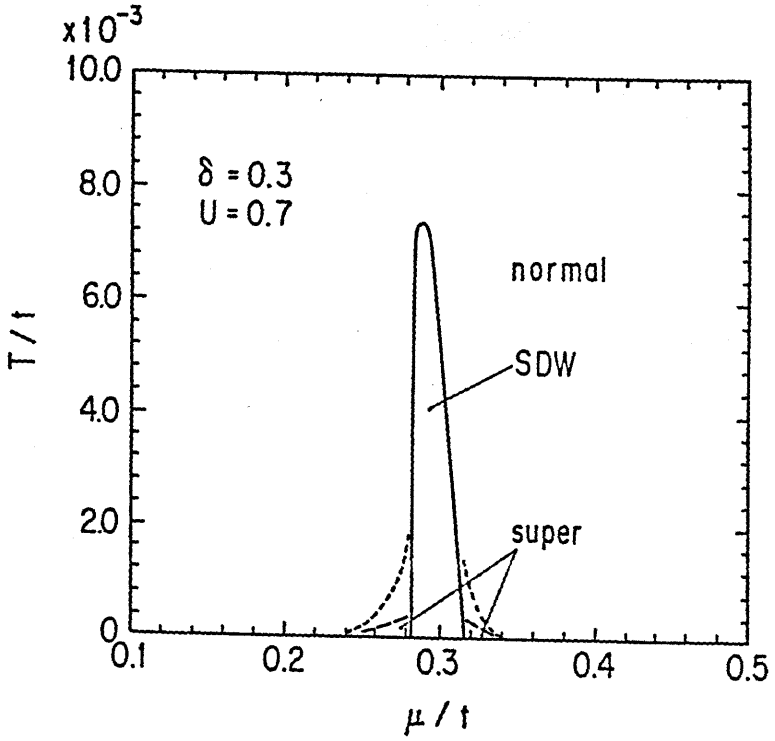

Fig.2.20(a). Phase diagram in T-μ space for δ=0.3t and U= 0.7t. The solid, broken and dotted line express T_{SDW} and T_c with and without the self-energy, respectively.

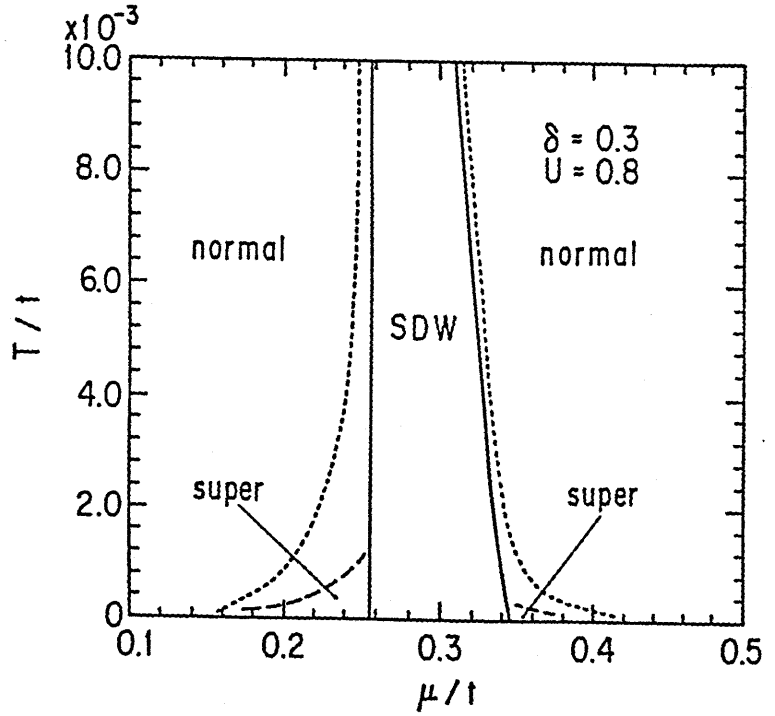

Fig.2.20(b). Phase diagram in T-μ space for δ=0.3t and U= 0.8t. The solid, broken and dotted line express T_{SDW} and T_c with and without the self-energy, respectively.

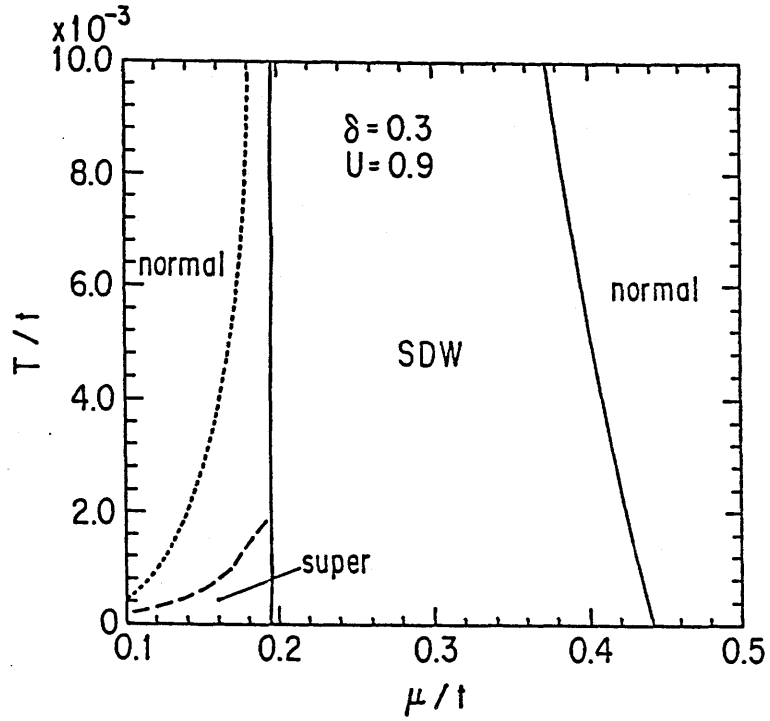

Fig.2.20(c). Phase diagram in T-μ space for δ=0.3t and U=0.9t. The solid, broken and dotted line express T_{SDW} and T_c with and without the self-energy, respectively.

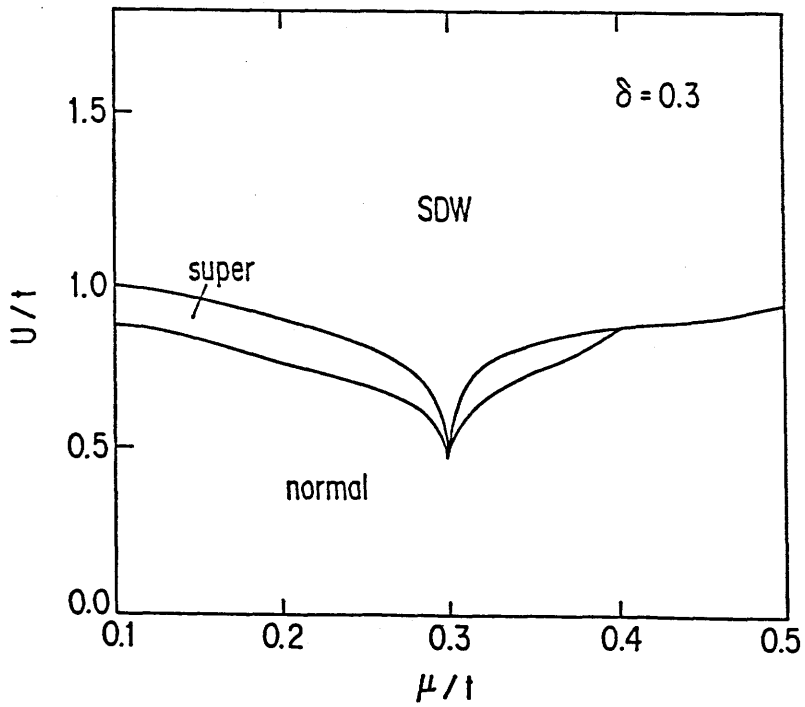

Fig.2.21. Phase diagram in U-μ space for δ=0.3t.The self-energy is neglected here.

§2.7 Superconductivity on the CuO_2 Plane

According to the prediction of the preceeding section, in the single-band Hubbard model, the superconducting transition temperatures would be too low to explain the high-T_c superconductivities, in agreement with quantum simulation.[109,110] However by the simulation, an extended Hubbard model

$$\begin{aligned} H = & \sum_{i,\sigma} [\, s_x\, d^{\dagger}_{i\sigma}\, p_{i+x\,\sigma} - s_x\, d^{\dagger}_{i\sigma}\, p_{i-x\,\sigma} + \text{h.c.} \,] \\ & + \sum_{i,\sigma} [\, s_y\, d^{\dagger}_{i\sigma}\, p_{i+y\,\sigma} - s_y\, d^{\dagger}_{i\sigma}\, p_{i-y\,\sigma} + \text{h.c.} \,] \\ & + \sum_{i,\sigma} \varepsilon_d\, d^{\dagger}_{i\sigma}\, d_{i\sigma} + \sum_{j,\sigma} \varepsilon_p\, p^{\dagger}_{j\sigma}\, p_{j\sigma} \\ & + U_d \sum_i n^d_{i\alpha}\, n^d_{i\beta} \,. \end{aligned} \tag{2.7.1}$$

may exhibit a remarkable enhancement of pairing susceptibility, and several theories have been proposed for this model.[115-116,119,120] In eq.(2.7.1), $d_{i\sigma}$ and $p_{j\sigma}$ denote an annihilation operator of electron with spin σ on the Cu-d-orbital at site i and that on the O-p-orbital at site j, respectively, and $n^d_{i\sigma}$ denotes the d-electron number. At first we neglect the O-O hopping and on-site Coulomb energy on O-site for simplicity. We briefly examine the present perturbation theory[119-120] based on this Hamiltonian.

In a band picture, we diagonalize the electron hopping terms and obtain the following dispersions:

$$\lambda^0 = \varepsilon_p$$

$$\lambda_k^{\pm} = \frac{1}{2} \{ \varepsilon_p \pm \sqrt{\varepsilon_p^2 + 16 (s_x^2 \sin^2(k_x/2) + s_y^2 \sin^2(k_y/2))} \} , \qquad (2.7.2)$$

which satisfy $\lambda_k^- < \lambda^0 < \lambda_k^+$. Here we set $\varepsilon_d = 0$. In the case of oxide superconductors, the upper band λ^+ will be nearly half-filled. The free (U=0) d-band-electron-Green's function is

$$G_k^d = [i\omega_n + \mu - \sum_{a=x,y} s_a^2 \frac{1}{i\omega_n - \varepsilon_p + \mu}]^{-1} , \qquad (2.7.3)$$

In our framework we have to calculate the spin and charge fluctuations in an RPA on the d-band electron motion and on-d-site Coulomb interaction. Thus the effective vertices are constructed by d-band free-susceptibility defined by

$$\chi_o^d(q) = - \sum_k G_{k+q}^d G_k^d . \qquad (2.7.4)$$

This can be rewritten in terms of upper and lower-band free (U=0) Green's function

$$G_k^{\pm} = [i\omega_n + \mu - \lambda_k^{\pm}]^{-1} , \qquad (2.7.5)$$

as

$$\chi_o^d(q) = - \sum_{a,b=\pm} \sum_k A_{k+q}^a A_k^b G_{k+q}^a G_k^b . \qquad (2.7.6)$$

with $A_k^{\pm} = \mp \lambda_k^{\mp} / \tilde{\lambda}_k$, $\qquad (2.7.7)$

$$\tilde{\lambda}_k = \sqrt{\varepsilon_p^2 + 16 (s_x^2 \sin^2(k_x/2) + s_y^2 \sin^2(k_y/2))} .$$

It costs little error to neglect the inter-band and intra-lower-band contributions, so we obtain

$$\chi_0^d(q) = -\sum_k A^+_{k+q}A^+_k \; G^+_{k+q}G^+_k \; . \qquad (2.7.8)$$

Furthermore, we shall note that for the nearly half-filled upper-band, the electron dispersion can be expanded near the Fermi-surface:

$$\lambda_k^{\pm} \cong \frac{1}{2}\{\varepsilon_p + \sqrt{\varepsilon_p^2 + 16s^2}\} - \frac{2s^2(\cos(k_x)+\cos(k_y))}{\sqrt{\varepsilon_p^2+16s^2}} \; , \qquad (2.7.9)$$

where we set $s_x=s_y=s$. From this the d-band free susceptibility χ_0^d can be scaled by the free susceptibility χ_0 on the square-lattice which appeared in before sections;

$$\chi_0^d \cong \left(\frac{\varepsilon_p - \sqrt{\varepsilon_p^2+16s^2}}{2\sqrt{\varepsilon_p^2+16s^2}}\right)^2 \cdot \chi_0\left(\text{of } t=\frac{2s^2}{\sqrt{\varepsilon_p^2+16s^2}}\right) \; . \qquad (2.7.10)$$

Numerical calculation of eq.(2.7.4) shows that the above approximations are very accurate.

SDW instability occurs in $U = U^d_{SDW}$ with

$$1 = U^d_{SDW}\left(\frac{\varepsilon_p - \sqrt{\varepsilon_p^2+16s^2}}{2\sqrt{\varepsilon_p^2+16s^2}}\right)^2 \cdot \chi_0(\vec{q}_m,0) \; , \qquad (2.7.11)$$

where $\vec{q}_m$ gives the maximum value to χ_o. Then the instability on the square-lattice occurs in $U = U^o_{SDW}$ with

$$U^o_{SDW} = U^d_{SDW} \left(\frac{\varepsilon_p - \sqrt{\varepsilon_p^2 + 16s^2}}{2\sqrt{\varepsilon_p^2 + 16s^2}}\right)^2 < U^d_{SDW} , \qquad (2.7.12)$$

for the same hopping energy near the Fermi-surface:

$$t/2 = \frac{s^2}{\sqrt{\varepsilon_p^2 + 16s^2}} . \qquad (2.7.13)$$

This means that the SDW transition will be suppressed by an effective weakening of the Coulomb repulsion.

Nevertheless, since the scaling low (2.7.10) holds for all momentum and Matsubara frequency, we conjecture that the superconductivity will not change qualitatively; the superconducting phases will be too poor for high-T_c even in the extended Hubbard model at least in the perturbation theory.

In a more realistic model, the O-O hopping terms

$$- \sum_{i,\sigma} u \left(p^\dagger_{i+x,\sigma} p_{i+y,\sigma} - p^\dagger_{i+x,\sigma} p_{i-y,\sigma} + \text{h.c.}\right)$$

$$- \sum_{i,\sigma} u \left(p^\dagger_{i-x,\sigma} p_{i-y,\sigma} - p^\dagger_{i-x,\sigma} p_{i+y,\sigma} + \text{h.c.}\right) . \qquad (2.7.14)$$

should be added to the Hamiltonian eq.(2.7.1). The free part of the Hamiltonian is similarly diagonalized with the eigen value (λ) equation

$$- (\lambda-\varepsilon_p)(\lambda-\lambda_k^+)(\lambda-\lambda_k^-) + 16\ u^2\ \lambda\ \sin^2(k_x/2)\ \sin^2(k_y/2)$$
$$- 32\ s_x\ s_y\ u\ \sin^2(k_x/2)\ \sin^2(k_y/2) = 0\ . \qquad (2.7.15)$$

The most important first order correction of u to the upper band dispersion is

$$- \delta\ \cos(k_x)\ \cos(k_y) =$$
$$- \frac{16\ u\ s^2\ \cos(k_x)\ \cos(k_y)}{\left(\sqrt{\varepsilon_p^2 + 16\ s^2} - \varepsilon_p\right)\sqrt{\varepsilon_p^2 + 16\ s^2}}\ , \qquad (2.7.16)$$

near the Fermi-surface of the nearly half-filled band. Thus an enhancement of T_c by O-O hopping is possible according to our results in §2.6.

§2.8 Summary and Discussion

We have studied 2D tight-binding electron systems in free and interacting cases and its superconductivity and SDW transition, in connection with high-T_c superconductors. The following is devoted to the summary and discussion.

Specific features of 2D systems were studied:
(1) Free electron system, (2) SDW transition, (3) Local pairing. Analytic and approximate expressions for several quantities were derived and a relation $T_c(\mu,\delta)\cong T_c(\mu-\delta,0)$ was found. Drastic effects of van Hove singularities were demonstrated.

The interplay and competition between the SDW and the superconductivity have been studied from the view-point of the perturbation theory based on the 2D Hubbard model. We found that superconductivity appears near the SDW boundary, and the transition temperatures are very sensitive to the chemical potential (i.e. to the number of the carriers) and the band parameter δ. These sensitivities result from the nesting of Fermi-surface and the van Hove singularity. In particular, increase of the n.n.n. hopping δ does not only suppress the SDW transition but also enhance the superconductivity remarkably. For example, for $U=0.8t$, the superconducting phase is very small with only n.n. hopping, but the n.n.n. hopping $\delta=0.3t$ increases the $\max(T_c)$ about three times higher, and does the ratio $\max(T_c)/\max(T_{SDW})$ about 10 times larger. While the superconducting phase appears in the region on the both sides of the SDW

phase, the remarkable enhancement is found the side near half-filling. Such tendency is found in the recent quantum simulation study by dos Santos.[122)]

We also found the strong suppression of T_c due to the electron renormalization. For example, $\max(T_c)/\max(T_{SDW}^{RPA})\sim 0.01$, for $\delta=0$ and $U=1.2t$, and $\max(T_c)/\max(T_{SDW}^{RPA})\sim 0.06$, for $\delta=0.3t$ and $U=0.8t$. If we fit the maximum value of T_{SDW}^{RPA} to ~250K, regarding it as a transition temperature of 3D long range order T_{SDW}^{3D} (although in general 2D T_{SDW}^{RPA} is larger than T_{SDW}^{3D}), we have 2.5K and 15K, respectively. These values are too low to explain the high-T_c superconductors, in spite of the over-estimation due to the RPA for the effective interaction. Even near the SDW boundary, since the strong fluctuations lead to the strong pairing interaction and the strong renormalization effect simultaneously, the resulting T_c can not be so enhanced, although a superconducting phase exists.

Here we shall comment on effects of orthorhombic distortion. T_{SDW} is slightly affected by the orthorhombic distortion, as was shown in Fig.2.5. On the other hand, van Hove singularities are at the Fermi-level in the case of $\mu=\pm 2t_2$, where t_2 is given in eq.(2.3.14). If the critical μ value at which the SDW phase vanishes is near $\mu=\pm 2t_2$, then the T_c may be enhanced by the van Hove singularity, since the superconducting phase is near the SDW boundary.

The same mechanism in the extended Hubbard model on the Cu-O plane was studied. The qualitatively same results were conjectured from the view-point of band-pictures.

Finally we shall mention about more improved estimation of T_c. We should be careful in the very vicinity of the SDW boundary, where the AF spin fluctuation significantly increases. There some improvements are needed for quantitative estimation of T_c. In particular, it would be most important to taking account of the renormalizaion effects and mode-mode coupling in estimating vertices given by eqs.(2.5.1) and (2.5.2). Such higher order effects will suppress the T_{SDW}, whereas it is still unknown whether T_c is enhanced or suppressed then. Moreover, we neglected the real parts of electron self-energies, which will lead to the quasi-gap near the Fermi-surface which may enhance T_c much more.[123] After our present theory many authors have improved these points.[124-126]

We should also note that our SDW state is 2D order obtained in RPA while the real AF ordering is 3D one and 2D AF fluctuation is observed with unusual behaviour. Taking into accounts the suppression of T_{SDW} due to the two-dimensionality, T_c may be more enhanced by the van Hove singularity and by strong fluctuations growing into of quasi-long range.

References 2.

1. J.G.Bednorz and K.A.Müller: Z.Phys. B **64**(1986)189.
2. S.Uchida, H.Takagi, S.Tanaka, and K.Kitazawa: Jpn.J.Appl. Phys. **26**(1987)L1.
3. K.Kishio, K.Kitazawa, S.Kanbe, I.Yasuda, H.Takagi, S.Uchida, K.Fueki, and S.Tanaka: Chem.Lett. **429**(1987).
4. C.W.Chu, P.H.Hor, R.L.Meng, L.Gao, Z.J.Huang, and Y.Q.Wang: Phys.Rev.Lett. **58**(1987)405.
5. S.Hikami, T.Hirai, and S.Kagoshima: Jpn.J.Appl.Phys.**26**(1987) 1314.
6. M.K.Wu, J.R.Ashburn, C.J.Torng, P.H.Hor, R.L.Meng, L.Gao, Z. J.Huang, Y.Q.Wang, and C.W.Chu: Phys.Rev.Lett. **58**(1987)908.
7. T.A.Faltens, W.K.Ham, S.W.Keller, K.J.Leary, J.N.Michaels, A.M.Stacy, H.-C. zur Loye, D.E.Morris, T.W.Barbee,III, L.C. Bourne, M.L.Cohen, S.Hoen, and A.Zettl: Phys.Rev.Lett. **59** (1987)915.
8. B. Batlogg, R. J. Cava, A. Jayaraman, R. B. van Dover, G.A. Kourouklis, S.Sunshine, D.W.Murphy, L.W.Rupp, H.S.Chen, A. White, K.T.Short, A.M.Mujsce, and E.A.Rietman: Phys.Rev. Lett. **58**(1987)2333.
9. L.C. Bourne, M.F. Crommie, A. Zettl, H. -C. zur Loye, S.W. Keller, K.L.Leary, A.M.Stacy, K.J.Chang, M.L.Cohen, and D. E.Morris: Phys.Rev.Lett. **58**(1987)2337.
10. K.J.Leary, H.-C. zur Loye, S.W.Keller, T.A.Faltens, W.K.Ham, J.N.Michaels, and A.M.Stacy: Phys.Rev.Lett. **59**(1987)1236.
11. L.F.Mattheiss: Phys.Rev.Lett. **58**(1987)1028.

12. K.Takegahara, H.Harima, and A.Yanase: Jpn.J.Appl.Phys. **26**, (1987)L352.
13. A.J.Freeman, J.Yu, and C.L.Fu: Phys.Rev.B **36**(1987)7111.
14. J.Yu, A.J.Freeman and S.-H.Xu: Phys.Rev.Lett. **58**(1987)1035
15. S.Massidda, J.Yu, A.J.Freeman, and D.D.Koelling: Phys.Rev. Lett. **A122**(1987)198.
16. J.Yu, S.Massidda, A.J.Freeman, and D.D.Koelling: Phys.Rev. Lett. **A122**(1987)203.
17. L.F.Mattheiss and D.R.Hamann: Solid State Commun. **63**(1987) 395.
18. T.Fujita, Y.Aoki, Y.Maeno, J.Sakurai, H.Fukuba, and H.Fujii: Jpn.J.Appl.Phys. **26**(1987)L368.
19. Y.Nishihara, M.Tokumoto, K.Murata, and H.Unoki: Jpn.J.Appl. Phys. **26**(1987)L1416.
20. D.Vaknin, S.K.Sinha, D.E.Moncton, D.C.Johnston, J.Newsam, C.R.Safinya, and H.King: Phys.Rev.Lett. **58**(1987)2802.
21. T.Freltoft, J.E.Fischer, G.Shirane, D.E.Moncton, S.K.Sinha, D.Vaknin, J.P.Remeika, A.S.Cooper, and D.Harshman: Phys.Rev. B **36**(1987)826.
22. B.X.Yang, S.Mitsuda, G.Shirane, Y.Yamaguchi, H.Yamauchi, and Y.Syono: J.Phys.Soc.Jpn. **56**(1987)2283.
23. S.Mitsuda, G.Shirane, S.K.Sinha, D.C.Johnston. M.S.Alvarez, D.Vaknin, and D.E.Moncton: Phys.Rev.B **36**(1987)822.
24. Y.Yamaguchi, H.Yamauchi, M.Ohashi, H.Yamamoto, N.Shimoda, M.Kikuchi, and Y.Syono: Jpn.J.Appl.Phys. **26**(1987)L447.
25. Y.J.Uemura, W.J.Kossler, X.H.Yu, J.R.Kempton, H.E.Schone, and D.Opie: Phys.Rev.Lett. **59**(1987)1045.

26. D.C.Johnston. J.P.Stokes, D.P.Goshorn, and J.T.Lewandouski: Phys.Rev.B **36**(1987)4007.

27. Y.Kitaoka, S.Hiramatsu, T.Kohara, K.Asayama, K.Ohishi, M. Kikuchi, and N.Kobayashi: Jpn.J.Appl.Phys. **26**,367(1987); Y. Kitaoka, S.Hiramatsu, K.Ishida, T.Kohara and K.Asayama: J. Phys.Soc.Jpn. **56**(1987)3026.

28. N.Nishida, H.Miyatake, D.Shimada, S.Okuma, M.Ishikawa, T. Takabatake, Y.Nakazawa, Y.Kuno, R.Keitel, J.H.Brewer, T.M. Riseman, D.L.Williams, Y.Watanabe, T.Yamazaki, K.Nishiyama, K.Nagamine, E.J.Ansaldo, E.Torikai: Jpn.J.Appl.Phys. **26** (1987)1856.

29. I.Furo, A.Janessy, L.Mihaly, P.Banki, I.Pocsik, I.Bakonyi, I.Heinmaa, E.Joon, and E.Lippmaa: Phys.Rev.B **36**(1987)5690.

30. N.P.Ong, Z.Z.Wang, J.Clayhold, J.M.Tarascon. L.H.Greene, and W.R.McKnnon: Phys.Rev.B **35**(1987)8807.

31. M.F.Hundley, A.Zettle, A.Stacy, M.L.Cohen: Phys. Rev. B **35**, (1987)8800.

32. S.Uchida, H.Takagi, H.Ishii, H.Eisaki, T.Yabe, S.Tajima, and S.Tanaka: Jpn.J.Appl.Phys. **26**(1987)L440.

33. C.Uher, A.B.Kaiser, E.Gmelin, and L.Walz: Phys.Rev.B**36**(1987) 5676.

34. B.W.Ricketts, R.B.Roberts, R.Driver, and H.K.Welsh: Solid State Commun. **64**(1987)1287.

35. C.Uher and A.B.Kaiser: Phys.Rev.B **35**(1987)5680.

36. S.W. Tozer, A.W. Kleinsasser, T. Penney. D. Kaiser, and F. Holtzberg: Phys.Rev.Lett. **59**(1987)1768.

37. T.Penney, M.W.Shafer, B.L.Olsen, and T.S.Plaskett: Adv. Ceramic Mater **2**(1987)577.

38. Z.Z.Wang, J.Clayhold, N.P.Ong, J.M.Tarascon, L.H.Greene, W.R.McKinnon, and G.W.Hull: Phys.Rev.B **36**(1987)7222.

39. P.Chandhri, R.J.Collis, P.Freitas, R.Gambino, J.Kirthley, R.Koch, R.Laibowitz, F.Legones, T.McGuire, T.Penney, A.Segmuler, and Z.Schesinger: to be published.

40. S.Uchida, H.Takagi, H.Yanagisawa, K.Kishio, K.Kitazawa, K.Fueki, and S.Tanaka: Jpn.J.Appl.Phys. **26**(1987)L445.

41. K.K.Singh, P.Ganguly and J.B.Goodenough: J.Solid State Chem. **52**(1984)254.

42. H.Takagi, S.Uchida, H.Obara, K.Kishio, K.Kitazawa, K.Fueki, and S.Tanaka: Jpn.J.Appl.Phys. **26**(1987)L434.

43. T.R.McGuire, T.R.Dinger, P.J.P.Freitas, W.J.Gallagher, T.S. Plaskett, R.L.Sandstrom, and T.M.Shaw: Phys.Rev.B **36**(1987) 4032.

44. A.Bezinge, J.L.Jorda, A.Junod, and J.Muller: Solid State Commun. **64**(1987)79.

45. H.Takagi, S.Uchida, H.Sato, H.Ishii, K.Kishio, T.Hasegawa, K.Kitazawa, K.Fueki, and S.Tanaka: to be published in Jpn. J.Appl.Phys. **26**(1987).

46. R.J.Cava, B.Batlogg, R.B.van Dover, D.W.Murphy, S.Sunshine, T.Siegrist, J.P.Remeika, E.A.Rietman. S.Zahurak, and G.P. Espinosa: Phys.Rev.Lett. **58**(1987)1676.

47. M.Gurvitch and A.T.Fiory: Phys.Rev.Lett. **59**(1987)1337.

48. Y.Nakazawa, M.Ishikawa, T.Takabatake, H.Takeya, T.Shibuya, K.Terakura, and F.Takei: Jpn.J.Appl.Phys. **26**(1987)L682.

49. T.Hatano, A.Matsushita, K.Nakamura, Y.Sakka, T.Matsumoto, and K.Ogawa: Jpn.J.Appl.Phys. **26**(1987)L721.

50. T.K.Chaki and M.Rubinstein: Phys.Rev.B **36**(1987)7259.

51. J.S.Tsai, Y.Kubo, and T.Tabuchi: Phys.Rev.Lett. **58**(1987) 1979.

52. T. Yamashita, A. Kawakami, T. Nishihara, Y. Hiratsu, and M. Takata: Jpn.J.Appl.Phys. **26**(1987)L635.

53. G.A.Held, P.M.Horn, C.C.Tsuei, S.J.Laplaca, J.G.Bednorz, and K.A. Muller: Solid State Commun. **64** (1987) 75; H. Takagi, S. Uchida, K.Kitazawa, and S.Tanaka: Jpn.J.Appl.Phys. **26**(1987) L123.

54. J.D.Jorgensen, H.B.Schuttler, D.G.Hinks, D.W.Capone II, K. Zhang, and M.B.Brodsky: Phys.Rev.Lett. **58**(1987)1024.

56. F.Izumi, H.Asano, T.Ishigaki, E.Takayama-Muromachi, Y. Uchida, and N.Watanabe: Jpn.J.Appl.Phys. **26**(1987)L1193, L1214.

57. L.Katano, S.Funahashi, T.Hatano, A.Matsushita, K.Nakamura, T.Matsumoto, and K.Ogawa: Jpn.J.Appl.Phys. **26**(1987)L1046, L1049.

58. Y. Nakazawa, M. Ishikawa, T. Takabatake, K. Koga, and K. Terakura: Jpn.J.Appl.Phys. **26**(1986)L796.

59. T.Takahashi, F.Maeda, S.Hosoya, and M.Sato: Jpn.J.Appl.Phys. **26**(1987)L349.

60. A. Fujimori, E. Takayama-Muromachi, Y. Uchida, and B. Okai: Phys.Rev.B **35**(1987)8814.

61. T.Takahashi, F.Maeda, S.Hosoya, and M.Sato: Jpn.J.Appl.Phys. **26**(1987)L349.

62. H.Ihara, M.Hirabayashi, N.Terada, Y.Kimura, K.Senzaki, and M.Takumoto: Jpn.J.Appl.Phys. **26**(1987)L460,L463.

63. B.Reihl, T.Riesterer, J.G.Bednorz, and K.A.Muller: Phys.Rev. B35(1987)8804; T.Riesterer, J.G.Bednorz, K.A.Muller, and B. Reihl: Appl.Phys.A **44**(1987)81.

64. A. Fujimori, E. Takayama-Muromachi, Y. Uchida, and B. Okai: Phys. Rev. B **35**(1987)8814; A.Fujimori, E.Takayama-Muromachi, and Y.Uchida: Solid State Commun. **63**(1987)857.

65. A. Bianconi, A. C. Costellano, M. De Santis, P. Delogn, A. Gargano, R.Giorgi: Solid State Commun. **63**(1987)1135.

66. G.Shirane, Y.Endoh, R.J.Birgeneau, M.A.Kastuer, Y.Hidaka, M.Oda, M.Suzuki, and T.Murakami: Phys.Rev.Lett. **59**(1987) 1613.

67. G.A. Kourouklis, A. Jayaraman, W. Weber, J.P. Remeika, G.P. Expinosa, A.S. Cooper, and R.G. Maines, Sr.: Phys. Rev. B **36** (1987)7218.

68. K.Kitazawa, T.Atake, M.Sakai, S.Uchida, H.Takagi, K.Kishio, T.Hasegawa, K.Fueki, Y.Saito, and S.Tanaka: Jpn.J.Appl.Phys. **26**(1987)L751.

69. Y.Maeno, Y.Aoke, H.Kamimura, J.Sakurai, and T.Fujita: Jpn.J. Appl.Phys. **26**(1987)L402.

70. W.K.Kwok, G.W.Crbtree, D.H.Hinks, D.W.Capone, J.D.Jorgensen, and K.Zhang: Phys.Rev.B **35**(1987)5343.

71. H.Takagi, S.Uchida, H.Obara, K.Kishino, K.Kitazawa, K.Fueki, and S.Tanaka: Jpn.J.Appl.Phys. **26**(1987)L434.

72. P.Gutsmiedl, G.Wolff, and K.Andres: Phys.Rev.B **36**(1987)4043.

73. K.Kitazawa, M.Sakai, S.Uchida, H.Takagi, K.Kishio, S.Kanbe, S.Tanaka, and K.Fueki: Jpn.J.Appl.Phys. **26**(1987)L342.

74. S.J.Collocott, G.K.White, S.X.Don, and R.K.Williams: Phys. Rev.B **36**(1987)5684.

75. H.Takagi, S.Uchida, Y.Saito, K.Fueki, and S.Tanaka: Jpn.J. Appl.Phys. **26**(1987)L748.

76. S.E.Inderhees, M.B.Salamon, T.A.Friedmann, and D.M.Ginsberg: Phys.Rev.B **36**(1987)2401.

77. N.V.Nevitt, G.W.Crabtree, and T.E.Klippert: Phys.Rev.B **36** (1987)2401.

78. M.B.Salamon and J.Bardeen: Phys.Rev.Lett. **59**(1987)2615.

79. P.M.Grant, S.S.P.Parkin, V.Y.Lee, E.M.Eugler, M.L.Ramirez, J.E.Vazquez, G.Lim, R.D.Jacowitz, and R.L.Greene: Phys.Rev. Lett. **58**(1987)2482.

80. R. J. Birgeveau, C. Y. Chen, D. R. Gabbe, H.P. Jenssen, M.A. Kastner, C.J.Peters, P.J.Picone, T.Thio, T.R.Thurston, H.L. Tuller, J.D.Axe, P.Boni and G.Shirane: Phys. Rev. Lett. **59** (1987)1329.

81. B. Fisher, E. Polturak, G. Koren, A. Kessel, R. Fisher, and L.Harel: Solid State Commun. **64**(1987)87.

82. J.R. Cooper, B.Alavi, L-W.Zhou, W.P.Beyermann, and G.Gruner: Phys.Rev.B **35**(1987)8794.

83. R.Yaozhong, H.Xuelong, Z.Yong, Q.Yitai, C.Zuyao, W.Ruiping, and Z.Qirui: Solid State Commun. **64**(1987)467.

84. S.Yan, P.Lu, H.Ma, Q.Jia, and X.Wang: Solid State Commun. **64**(1987)537.

85. M.W.Shafer, T.Penney, and B.L.Olson: Phys.Rev.B **36**(1987) 4047.

86. Z.Henkie, R.Horyi, Z.Bukowski, P.J.Markowski, and J.Klamut: Solid State Commun. **64**(1987)1285.

87. A.Masaki, H.Sato, S.Uchida, K.Kitazawa, S.Tanaka, and K. Inoue: Jpn.J.Appl.Phys. **26**(1987)L405.

88. L.Mihaly, L.Rosta, G.Coddens, F.Mezei, G.Hutiray, G.Kriza, and B.Keszei: Phys.Rev.B **36**(1987)7137.

89. J.B.Boyce, F.Bridges, T.Claeson, R.S.Howland, and T.H. Geballe: Phys.Rev.B **36**(1987)5251.

90. K. Ohbayashi, N. Ogita, M. Udagawa, Y. Aoki, Y. Maeno, and T.Fujita: Jpn.J.Appl.Phys. **26**(1987)L420.

91. S.Sugai, M.Sato, and S.Hosoya: Jpn. J. Appl. Phys. **26**(1987) 2495.

92. E.W.Feuton: Solid State Commun. **64**(1987)27.

93. M.Naito, D.P.E.Smith, M.D.Kirk, B.Oh, M.R.Hahn, K,Char, D.B. Mitze, J. Z. Sun, D. J. Webb, M. R. Beasley, O. Fisher, T.H. Geballe, R.H.Hammond, A.Kapitulnik, and C.P.Quate: Phys.Rev. B **35**(1987)7228.

94. Z. Schlesinger, R.T. Collins, D.L. Kaiser, and F. Holtzberg: Phys.Rev.Lett. **59**(1987)1958.

95. A. Barone, A. Di Chiara, G.Peluso, U.S.di Uccio, A.M.Cucolo, R.Vaglio, F.C.Matacotta, and E.Olzi: Phys. Rev. B **36** (1987) 7121.

96. R.T. Collins, Z. Schlesinger, R.H. Koch, R.B.Laibowitz, T.S. Plaskett, P.Freitas, W.J.Gallagher, R.L.Sandstorm, and T.R. Dinger: Phys.Rev.Lett. **59**(1987)704.

97. D.A.Bonn, J.E.Geedan, C.V.Stager, T.Timusk, M.G.Doss, S.L. Herr, K.Kamaras, C.D.Porter, D.B.Tanner, J.M.Tarascon, W.R. McKinnon, and L.H.Greene: Phys.Rev.B **35**(1897)8843.

98. J.Orunstein et al.: Phys.Rev.B **36**(1987)729.

99. R.T.Collins et al.: Phys.Rev.Lett. **59**(1987)704; P.E.Sulewski et al., Phys.Rev.B **35**(1987)5330.

100. P.M.Horn, D.T.Keane, G.A.Held, J.L.Jordan-Sweet, D.L.Kaiser, F.Holtzbery, and T.M.Rice: Phys.Rev.Lett. **59**(1987)2772.

101. T.M.Rice: Z.Phys. B **67**(1987)141 and references therein.

102. P.W.Anderson: Science **235**(1987)1196.

103. P.W.Anderson: Phys.Rev.Lett. **59**(1987)2497.

104. G.Baskaran, Z.Zou, and P.W.Anderson: Solid State Commun. **63** (1987)973.

105. P.W.Anderson, G.Baskaran, Z.Zou, and T.Hsu: Phys. Rev. Lett. **58**(1987)2790.

106. P.W.Anderson: Mater Res.Bull. **8**(1973)153.

107. D.J.Scalapino, E.Loh,Jr., and J.E.Hirsch: Phys.Rev.B**34**(1986) 8190.

108. K.Miyake, S.Schmitt-Rink, and C.M.Varma: Phys.Rev.B **34**(1986) 6554.

109. M.Imada: J.Phys.Soc.Jpn. **56**(1987)3793.

110. M.Imada and Y.Hatsugai: J.Phys.Soc.Jpn. **58**(1989)3752

111. H.Q.Lin, J.E.Hirsch, and D.J.Scalapino: Phys.Rev.B **37**(1988) 7359.

112. J.E.Hirsch and D.J.Scalapino: Phys.Rev.Lett. **56**(1986)2732.

113. F.J.Ohkawa: Jpn.J.Appl.Phys. **26**(1987)L652.

114. F.J.Ohkawa: J.Phys.Soc.Jpn. **56**(1987)2267.

115. V.J.Emery: Phys.Rev.Lett. **58**(1987)2794.

116. J.E.Hirsch: Phys.Rev.Lett. **59**(1987)228.

117. H.Shimahara and S.Takada: Jpn.J.Appl.Phys. **26**(1987)L1674.

118. H.Shimahara and S.Tadada: J.Phys.Soc.Jpn. **57**(1988)1044.

119. K. Miyake, T. Matuura, K. Sano, and Y. Nagaoka: Physica **148B** (1987)381; J.Phys.Soc.Jpn. **57**(1988)722.

120. K.Yonemitsu: preprint.

121. H.Shimahara: Thesis for degree of master of science, (1988).

122. R.R. dos Santos: Phys.Rev. B **39**(1989)7259; See also K.Saito and S.Takada: J.Phys.Soc.Jpn. **58**(1989)783.

123. K.Machida and M.Kato: Jpn.J.Appl.Phys. **26**(1987)L660.

124. N.E.Bickers, D.J.Scalapino, and S.R.White: Phys.Rev.Lett. **62** (1989)961.

125. K.Yonemitsu: submitted to J.Phys.Soc.Jpn.

126. H.Shimahara: J.Phys.Soc.Jpn. **58**(1989)1735.

Chapter 3.

Long-Range Spin-Fluctuations and Superconductivity in Quasi-One-Dimensional Organic Compounds

In this chapter, we study a weak coupling theory again. We examine the theory of the superconductivity mediated by antiferromagnetic spin-fluctuations (AFSF) in the quasi-one-dimensional (quasi-1D) Hubbard model, and apply it to the quasi-1D organic superconductors $(TMTSF)_2X$ and $(DMET)_2X$, which have been suggested to be itinerant electron systems. The superconducting transition temperature and the momentum dependence of gap function are calculated numerically. Long-range (>>lattice constant) nature of the AFSF is found to play an important role in the superconductivity. The obtained phase diagram is compared with that of the organics, and some qualitative agreements between the theory and experiments are obtained.

§3.1 Introduction

It is one of important problems in solid state physics to clarify the roles of electron correlations in exotic superconductivities which have been observed in heavy fermion systems, organic superconductors, and oxide high-T_c superconductors, as we have discussed in chapter 1. On this problem it has been argued

within the Fermi-liquid theory that antiferromagnetic spin-fluctuations (AFSF) assisted by Fermi-surface nesting may enhance the pairing interaction[1-4] and also renormalize the properties of normal electrons strongly.[5] The applicability of this mechanism to heavy fermion compounds and Bechgaard salts has been discussed by Emery,[1] Scalapino et al.[2] and Miyake et al.[3] Moreover the relation to the high-T_c superconductors has been also discussed by Miyake et al.[6] We have also studied this mechanism on the basis of a square lattice Hubbard model in connection with the two-dimensional specific features.[5]

Among these the organic superconductors $(TMTSF)_2X$ ($X=PF_6$, AsF_6, SbF_6, TaF_6, ···)[7,8] and $(DMET)_2X$ ($X=Au(CN)_2$, AuI_2, $AuCl_2$, I_3, ···)[9-11] seem to be a typical example, since the AFSF dominate the system rather than CDW fluctuations, as seen in the experimental phase diagrams[7,8] where normal, spin-density-wave (SDW), and superconducting phase exist on the border of each other. There the superconducting transition temperatures T_c are sensitively enhanced as one approaches SDW boundary by decreasing the pressure in spite of the reduction of density of states (DOS) around the Fermi-surface due to SDW fluctuations, and in some compounds they become constant in the vicinity of the boundary. Such enhancements seem to be explained within the above theory straightforwardly, although the phonon mediated pairing remains as one of the possible mechanisms.[12] We would discuss this phase diagram in detail later. Moreover we must note that the similar phase diagrams have been found in oxide high-T_c superconductors[13,14] in which an electron correlation would play

some essential role in the superconductivity,[15-17] although these are different from the organics in many respects.[18]

Another characteristic of these organic superconductors is the anisotropy of the order-parameter, as pointed out by Takigawa et al.[19] and Hasegawa et al.[20] from the behaviour of NMR relaxation rate in $(TMTSF)_2ClO_4$ below T_c, which is similar to those of the heavy fermion compounds (UPt_3, UBe_{13}, $CeCu_2Si_2$).[21-23]

In general the anisotropic superconductivity is expected to occur when a local pairing interaction is strong. The spatial range of the pairing interaction is given roughly by v_F/ω_c, where v_F is the absolute value of the Fermi-velocity and ω_c is the characteristic energy of the exchange boson. For example an ordinary phonon mediated pairing interaction is of long range (>> lattice constant (a)) since the Fermi-energy ε_F is much larger than ω_c, and then the local lattice structure would be smeared out and the isotropic pairing would occur, if the Coulomb repulsion is sufficiently screened by electrons. However, when the ω_c is as large as ε_F, the range of the pairing interaction is very short (~a). Then we should be careful about the Coulomb repulsion, since the larger ω_c means the less retardation effect. Nevertheless when the electron screening restrict the Coulomb repulsion to on-site, the superconductivity would occur even by such a short-range pairing interaction. Then the anisotropic superconductivity is possible to occur according to the band structure and other properties of the pairing interaction. However such a large ω_c seems to be difficult for phonon mediated pairing interactions, so the anisotropy of the pairing gives the

most important basis for the applicability of the non-phonon theory.

In addition to such a large characteristic energy scale comparable to the Fermi-energy, the AFSF exchange pairing interaction has another smaller energy scale which reflects the critical behaviour near the SDW transition point. The AFSF shows a critical slowing down as one approaches to the SDW transition and leads to the retarded and long range pairing interaction. As a result of such a long range interaction the superconductivity would be remarkably enhanced near the SDW boundary. On the other hand this long range AFSF reduce the DOS around the Fermi-surface and make what is called a pseudo gap which works against the superconductivity. In the present case two opposite effects would be particularly remarkable because of the quasi-one-dimensionality. Thus even the qualitative behaviour of T_c on the phase diagram is not trivial and whether the experimental phase diagram could be obtained or not within the theory should be examined by a detailed calculation in which this smaller characteristic energy is sufficiently taken into account. This would be fulfilled by an accurate treatment of the momentum and/or frequency dependence of the interaction.

In this chapter we study the superconductivity induced by the exchange of the AFSF in the absence of the phonon. We take the long range AFSF in the theory from above reasons through the momentum dependence of the interaction. Most of our purpose lies in demonstrating its importance.

Our treatment in this chapter is based on the quasi-one dimensional (quasi-1D) Hubbard Hamiltonian;

$$H = \sum_{i,j,\sigma} t_{ij}\, c^{\dagger}_{i\sigma}\, c_{j\sigma} + U \sum_{i} n_{i\alpha}\, n_{i\beta} \,, \tag{3.1}$$

$$\text{with} \quad t_{ij} = N^{-1} \sum_{\vec{k}} e^{i\,\vec{k}\cdot\vec{R}_{ij}}\, \varepsilon_{\vec{k}} \,, \tag{3.2}$$

$$\text{and} \quad \varepsilon_{\vec{k}} = -2t\cos(k_x) - 2t'\cos(k_y) - 2t''\cos(k_z) - \mu \,, \tag{3.3}$$

where i and j denote lattice sites and $\vec{k}$ is a crystal momentum, and the lattice constants are taken as unity. The summation $\sum_{\vec{k}}$ is taken over the first Brillouin zone and $\sum_{i}$ is taken over all N sites. $c^{\dagger}_{i\sigma}$ and $c_{i\sigma}$ are creation and annihilation operator of an electron (or a hole) with spin σ at site i, respectively, and $n_{i\sigma}$ are its number operators. We take the x-axis along the stacks i.e. in the most conductive direction. Bearing $(TMTSF)_2X$ in mind we take t as 0.25eV.[24] Now we suppose the simplified model in which the inter-chain-hopping integral t' increases with the pressure from $t' \cong 0.02t \sim 0.2t$ (the value at ambient pressure[7,25]) and t'' is negligibly small compared with t'.[25-27] The SDW transition is easily reproduced within this model.[26,27]

More realistically there are phonons which contribute largely. Furthermore it is not settled whether the superconductivity does exist or not in the pure single band Hubbard model as the true ground states.[28-30] However, because our purpose is to examine the roles of the AFSF in quasi-1D electron systems, which dominate near the SDW boundary, we concentrate our study on the simplest model in which the strong AFSF occurs.

In §3.2, we examine the AFSF itself and its exchange vertices. In §3.3, we study the renormalizations for the normal state electrons and estimate the reduction of the DOS. In §3.4 the superconductivity is examined. The anisotropy of the order-parameter and the theoretical phase diagram are obtained. Lastly §3.5 is devoted to discussion. The validity of the employed approximations is discussed there. The study in this chapter has been presented in our papers of ref.31.

§3.2 Spin-Fluctuations

(i) Fluctuations and effective vertices

We adopt an RPA for spin- and charge-fluctuation following Scalapino et al. As a result, the spin-susceptibility $\chi(q)$ at temperature T is easily obtained as

$$\chi(q) = \frac{\chi_0(q)}{1 - U\,\chi_0(q)} , \tag{3.4}$$

$$\text{with} \quad \chi_0(q) = N^{-1} \sum_{\vec{k}} \frac{f(\varepsilon_{\vec{k}+\vec{q}}) - f(\varepsilon_{\vec{k}})}{i\,\nu_m - \varepsilon_{\vec{k}+\vec{q}} + \varepsilon_{\vec{k}}} , \tag{3.5}$$

and $f(\varepsilon) = (e^{\varepsilon/T} + 1)^{-1}$. Here q denotes $(\vec{q}, i\nu_m)$ with crystal momentum $\vec{q}$ and Matsubara frequency $i\nu_m = 2m\pi iT$. Within the same approximation[2,5] the effective vertices for two electrons with antiparallel spins are

$$\Gamma_{\alpha\beta}(k,k',q) = \tau_1(k-k') + \tau_2(k+k'+q) \tag{3.6}$$

$$\text{with} \quad \tau_1(q) = U + \left(- \frac{1}{2} \frac{U^2\,\chi_0(q)}{1 + U\,\chi_0(q)} + \frac{1}{2} \frac{U^2\,\chi_0(q)}{1 - U\,\chi_0(q)} \right) , \tag{3.7}$$

$$\tau_2(q) = \frac{U^2\,\chi_0(q)}{1 - U\,\chi_0(q)} , \tag{3.8}$$

and those for electron self-energies,

$$\Gamma_{\sigma\sigma}(k,k',q) =$$

$$-\frac{1}{2}\frac{U^2\,\chi_0(k-k')}{1+U\,\chi_0(k-k')}-\frac{3}{2}\frac{U^2\,\chi_0(k-k')}{1-U\,\chi_0(k-k')}\ ; \qquad (3.9)$$

they are defined in Fig.2.15, where k denotes $(\vec{k},i\omega_n)$ with $i\omega_n=(2n+1)\pi iT$, and α, β denotes the up and down spins, respectively. The vertex (3.9) is used only for electron self-energy, and is different from a triplet pairing interaction. In eq.(3.9), the minus sign due to the closed loops which appear in diagrams for the self-energy are considered beforehand.

(ii) Spin-density-wave instability

The SDW transition temperature (T_{SDW}^{RPA}) is given by the equation: $1 = U\,\chi_0(\vec{q}_m,0)$, within the RPA, the validity of which has been discussed by Yamaji.[26] Here $\vec{q}_m$ gives the maximum value of χ_0.

At t'=0, the T_{SDW}^{RPA} is expressed as

$$T_{SDW}^{RPA}(t'=0) = \frac{8e^{\gamma}\sin^2 k_F}{\pi\,|\cos k_F|}\,t\,\exp\left(-\frac{4\pi t\,\sin k_F}{U}\right) \qquad (3.10)$$

with Euler constant $\gamma=0.57721\cdots$. In particular, if we set $k_F=\pi/4$ for 1/4-filled band, then we have

$$T_{SDW}^{RPA}(t'=0) = \frac{4\sqrt{2}\,e^{\gamma}}{\pi}\,t\,\exp\left(-\frac{2\sqrt{2}\,\pi\,t}{U}\right). \qquad (3.11)$$

We fix this 20K for t=2500K which gives the value of U as 1.48253t. Then we have T_{SDW}^{RPA} = 12K for $t'\cong 0.136t$ for example, and

the critical value of t' at which the SDW vanishes is $t'_c \cong 0.142t \sim 0.145t$ for sufficiently low temperatures, as shown in the phase diagram of Fig.3.1. (For T=0, we obtain $t'_c \cong 0.145t$.) Our choise of the parameters is reasonable for $(TMTSF)_2X$ with $X=PF_6$, SbF_6, $\cdots$, which have $T_{SDW}=12K$ and $t'=0.02t \sim 0.2t$[7,25] at ambient pressure. It should be also noted that t' acts as an effective parameter which is introduced to distort the Fermi-surface, in our simplified model.

In this chapter we take U=1.48253t and investigate the normal state properties and superconductivity for $t' \gtrsim t'_c$. The chemical potential μ is adjusted for every value of t' so that the hole number is fixed at N/2. For example, $\mu \cong -\sqrt{2}t$ for t'=0, and
$\mu \cong -1.398t$ for t'=0.15t.

(iii) Critical behaviour of spin-fluctuations

For t'=0, the nesting of the Fermi-surfaces is perfect. Then the AF free susceptibility χ_0 is easily obtained analytically for m>>1, as

$$\chi_0(i\nu_m, 2k_F) = \frac{1}{4\pi t \sin(k_F) D_m} \ln\left(\frac{D_m + 1}{D_m - 1} \frac{D_m - \cos(2k_F)}{D_m + \cos(2k_F)}\right) , \quad (3.12)$$

with $D_m = \left(1 + \left(\frac{\nu_m}{4t \sin(k_F)}\right)^2\right)^{1/2}$. This formula actually holds for $m \gtrsim 1$ with only a little error ($\lesssim 1\%$).

As t' increases from zero the nesting worsens and the expression of $\chi_0(i\nu_m, 2k_F=\pi/2)$ deviates from eq.(3.12). However the deviation is small for $|\nu_m| \gtrsim \Delta\varepsilon_F$, where $\Delta\varepsilon_F$ is of the order of the

energy difference of electrons between the state on the Fermi-surface and that translated by the nesting vector. The logarithmic enhancement of the free susceptibility as T→0 is suppressed by $\Delta\varepsilon_F$ which acts as a lower energy cutoff. Unfortunately an accurate estimation of $\Delta\varepsilon_F$ is difficult, so we roughly estimate as $\Delta\varepsilon_F \sim 2t'^2/t \sin(k_F)$, which is obtained for the Fermi-surface at $k_y=\pi$.

From the above arguments we obtain a rough estimation of characteristic energy scale of AFSF which reflects the critical behaviour in the imperfect nesting case in the RPA by replacing T by $\Delta\varepsilon_F$ in the well-known Orstein-Zernike form in a perfect nesting case:

$$\kappa u = \frac{\Delta\varepsilon_F}{(N(0)U)^{1/2}} \left(\frac{U_{SDW} - U}{U_{SDW}} \right)^{1/2}, \qquad (3.13)$$

where $U_{SDW} \equiv \chi_0(\vec{q}_m,0)^{-1} \cong \chi_0(\vec{Q},0)^{-1}$, $\vec{Q}\equiv(\pi/2,\pi)$, and N(0) is the DOS at the Fermi-level. The value of κu is estimated as $0.9\times10^{-2}t$ for $t'=0.144t$ and $T=0.4\times10^{-4}t$, and as $0.015t$ for $t'=0.15t$ and $T=0.4\times10^{-4}t$.

The spatial range (r_x in x-direction and r_y in y-direction) of the spin-fluctuation and its exchange interaction is obtained by using the relation $r_x \sim 2t \sin(k_F)/\kappa u \times a$ and $r_y \sim 2t'/\kappa u \times b$ where a and b is the lattice constant for each direction. This gives that $r_x \sim 50\times a$ and $r_y \sim 10\times b$ for $t'=0.15t$ and $T=0.4\times10^{-4}t$, and $r_x \sim 80\times a$ and $r_y \sim 16\times b$ for $t'=0.144t$ and $T=0.4\times10^{-4}t$.

The characteristic energy κu sensitively changes on the phase diagrams, and thus our theory needs to take account of this

energy scale, in order to obtain the qualitatiive behaviour of the T_c on the phase diagrams.

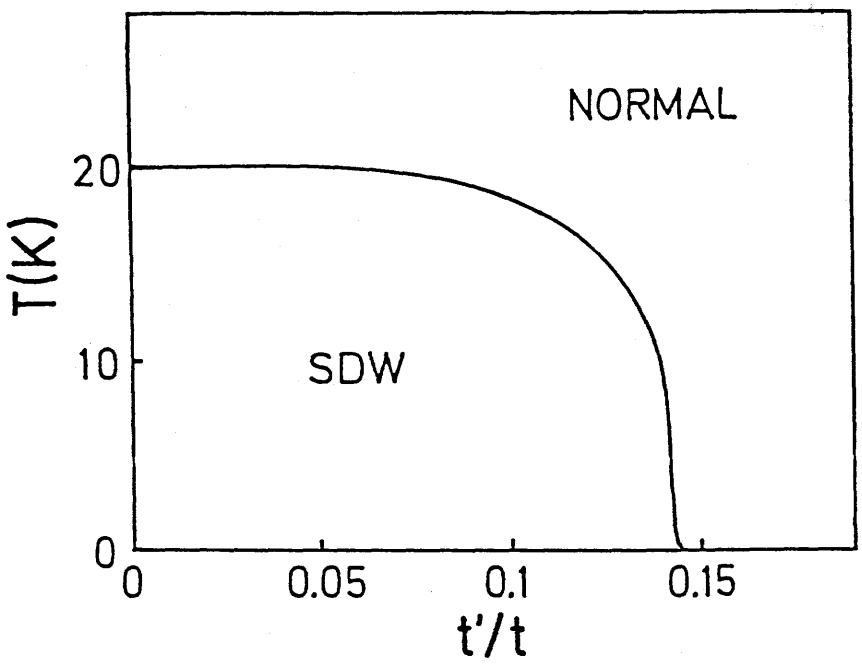

Fig.3.1. The SDW transition temperature as a function of the transverse hopping integrals. We take t=2500K and U=1.48253t.

§3.3 Normal State Electrons

(i) Electron Green's function

Our basic approximations are the same as those in the previous chapter,[5] that is the Hartree-Fock approximation for electron self-energies (Fig.2.16) and a ladder approximation for two-particle vertices (Fig.2.17). These two approximations are consistent with each other in a diagramatic formulation of an electron-boson system regarding the diagrams of spin and charge fluctuations as boson propagators.

The resulting electron Green's function is

$$G_k = (i\omega_n - \varepsilon(\vec{k}) - \Sigma(k))^{-1}, \tag{3.14}$$

$$\text{with} \quad \Sigma(k) = -\sum_{k'} \Gamma_{\alpha\alpha}(k,k',0)\, G_{k'} - \sum_{k'} U^2\, \chi_0(k-k')\, G^0_{k'}, \tag{3.15}$$

$$\text{and} \quad G^0_{k'} = (i\omega_n - \varepsilon(\vec{k}))^{-1}. \tag{3.16}$$

Here $\sum_k \equiv N^{-1} \sum_{\vec{k}} T \sum_n$, and the second term of eq.(3.15) is added to cancel the double counting contribution in the first term. Further the two-particle vertex Γ for antiparallel-spin-pairing is

$$\Gamma(k,k',q) = \Gamma_{\alpha\beta}(k,k',q) - \sum_{k''} \Gamma_{\alpha\beta}(k,k',q) G_{k''+q} G_{k''} \Gamma(k'',k',q), \tag{3.17}$$

(ii) Approximations for the self-energy

The self-energy $\Sigma(k)$ can be generally written as

$$\Sigma(k) = \Sigma^s(k) + i\,\Sigma^a(k), \tag{3.18}$$

where $\Sigma^s(k)$ and $\Sigma^a(k)$ are real and satisfy $\Sigma^s(k)=\Sigma^s(-k)$ and $\Sigma^a(k)=-\Sigma^a(-k)$. We think that the most important effects of the self-energy are the mass renormalization[5] and the pseudo gap near the SDW transition. Thus our approximations should be those which retain these two effects. So we introduce the following simplifications: Noting that the essential effect of the frequency dependence of $\Gamma_{\sigma\sigma}$ mainly appears in the linear frequency dependence of Σ, i.e. that of Σ^a, in the case of $\kappa u>>T$, (1) we neglect the retardation of $\Gamma_{\sigma\sigma}$ in the equation of Σ^s, but will retain the momentum dependence of Σ^s, which leads to the reduction of the DOS. However, if the same approximation is taken in the equation for Σ^a, the Σ^a vanishes, and the mass enhancement effects are largely missed. Therefore we will retain the frequency dependence in the equation for Σ^a, but (2) ignore the momentum dependence there, for simplicity. The validity of the approximation (1) is discussed later. Hence we put

$$\Sigma(k) = \Sigma^s(\vec{k}) + i\,\Sigma^a(i\omega_n). \tag{3.19}$$

The resulting self-consistent equations are

$$\Sigma^a(i\omega_n) = -T\sum_{n'}\Gamma^{(0)}_{\alpha\alpha}(i\omega_n-i\omega_{n'})\,W^a(i\omega_{n'}) + \Sigma^a_0(i\omega_n), \tag{3.20}$$

and
$$\Sigma^s(\vec{k}) = -N^{-1}\sum_{\vec{k}'}\Gamma_{\alpha\alpha}(\vec{k}-\vec{k}';0)\,W^s(\vec{k}') + \Sigma^s_0(\vec{k}), \tag{3.21}$$

with
$$\Gamma^{(0)}_{\alpha\alpha}(i\nu_m) \equiv N^{-1}\sum_{\vec{q}}\Gamma_{\alpha\alpha}(\vec{q};i\nu_m), \tag{3.22}$$

$$\Gamma_{\alpha\alpha}(\vec{k}-\vec{k}';i\omega_n-i\omega_{n'}) \equiv \Gamma_{\alpha\alpha}(k,k',0), \tag{3.23}$$

$$W^a(i\omega_{n'}) = N^{-1}\sum_{\vec{k}'}\frac{-(\omega_{n'}-\Sigma^a(i\omega_{n'}))}{(\omega_{n'}-\Sigma^a(i\omega_{n'}))^2+(\varepsilon_{\vec{k}'}+\Sigma^s(\vec{k}'))^2}, \tag{3.24}$$

$$W^{s}(\vec{k}') = T \sum_{n'} \frac{-(\varepsilon_{\vec{k}'} + \Sigma^{s}(\vec{k}'))}{(\omega_{n'} - \Sigma^{a}(i\omega_{n'}))^2 + (\varepsilon_{\vec{k}'} + \Sigma^{s}(\vec{k}'))^2} , \tag{3.25}$$

$$\Sigma^{a}_{o}(i\omega_n) = i N^{-1} \sum_{\vec{k}} \sum_{k} U^2 \chi_o(k-k') G^{o}_{k'} , \tag{3.26}$$

$$\Sigma^{s}_{o}(\vec{k}) = - \sum_{k'} U^2 \chi_o(\vec{k}-\vec{k}', i\nu_m=0) G^{o}_{k'} , \tag{3.27}$$

Furthermore, we introduce the following extra approximation for numerical calculation around t'~0.1t and not in the vicinity of the SDW transition points. It is expressed as

$$\Sigma^S(\vec{k}) = \begin{cases} \Sigma^S(k_x - k_x^0(k_y) + k_x^0(k_y^0), k_y^0) , & \text{if } 0 \leq k_x - k_x^0(k_y) + k_x^0(k_y^0) \leq \pi , \\ \Sigma^S(\pi, k_y^0) , & \text{if } \pi \leq k_x - k_x^0(k_y) + k_x^0(k_y^0) , \\ \Sigma^S(0, k_y^0) , & \text{if } k_x - k_x^0(k_y) + k_x^0(k_y^0) \leq 0 , \end{cases} \tag{3.28}$$

where $k_x^0(k_y)$ is a function

$$k_x^0(k_y) = \cos^{-1}\left(\frac{2t'\cos k_y + \mu}{-2t}\right) , \tag{3.29}$$

and k_y^0 is a constant parameter taken as $\pi/2$ in this chapter. Equations (3.28) and (3.29) mean that we regard that the behaviour of $\Sigma^S(\vec{k})$ around the Fermi-surface is almost independent of k_y.

If the nesting is almost perfect, this approximation would be reasonable in quasi-1D systems. In particular eq.(3.28) holds exactly in 1D systems. However as the nesting worsens this causes the overestimation of the reduction of the DOS around the Fermi-surface near $k_y \sim \pi$ or $k_y \sim 0$ owing to the choice of $k_y^0 = \pi/2$. Nevertheless this overestimation would be small within our parameter region; there the difference between the state on the Fermi-surface and that translated by the nesting vector $\sim \vec{Q}$ is estimated as less than $\pi/100$ in the momentum space, which is smaller than the width of the peak of the effective vertices around the nesting vector. Moreover such a small difference of the Fermi-surface nesting would almost disappear when the pseudo gap is formed, since the pseudo gap adjusts the Fermi-surface so that the total energy is lowered. It is true, however, that our approximation becomes invalid in the vicinity and inside of the SDW boundary where the region around the Fermi-surface in which the self-energy varies critically is smaller than the mismatching

of the nesting in the momentum space. However we do not investigate such a parameter region in this chapter, because other approximations we employed such as RPA would also become invalid there.

(iii) Numerical results

Using the above approximations, we solve the self-consistent equations (3.20)~(3.27) numerically. The results are shown in Fig.3.2 ~ 3.5.

The value of $\Sigma^a(i\omega_n)$ is found to be almost t'-independent. As seen from Fig.3.2, it increases with ω_n almost linearly for $\omega_n \lesssim t$ with the coefficient 0.16, and after reaching the maximum around $\omega_n \cong 4t$ they decrease as ω_n^{-1}.

If we could set the effective cutoff energy of the interaction (ω_c) like the Debye frequency in the phonon system, the expected behaviour of Σ^a would be as

$$\Sigma^a(i\omega_n) \begin{cases} \sim N(0)\ \omega_n & (\omega_n << \omega_c) \\ \sim N(0)\ \omega_c \ \text{sign}\ \omega_n & (\omega_c << \omega_n << N(0)^{-1}) \\ \sim \omega_c\ /\ \omega_n & (N(0)^{-1} << \omega_n) \end{cases}$$

The present result of the numerical calculation is seen to be consistent with this behaviour if we take $\omega_c \sim N(0)$.

The behaviour of $\Sigma^s(\vec{k})$ is shown in Fig.3.3. It is found that the overall behaviour of $\Sigma^s(\vec{k})$ is almost the same for t'=0.144t and t'=0.15t except near the Fermi-surface. The slope of $\Sigma^s(\vec{k})$ near the Fermi-surface becomes steeper as one approaches the SDW boundary (Fig.3.4). Thus the reduction of the DOS around the

Fermi-level ($\varepsilon \sim -1.2t$) becomes remarkable near the SDW boundary as shown in Fig.3.5. Contrarily the band narrowing is found to be almost independent of t'.

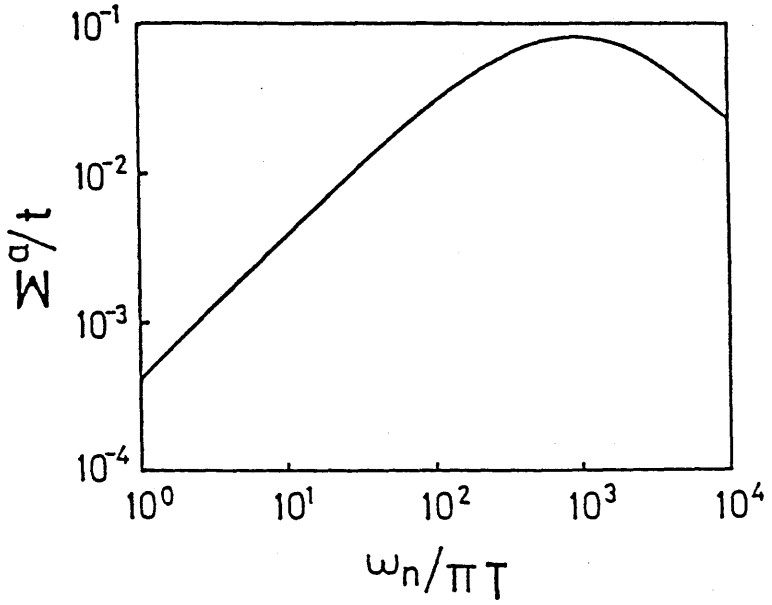

Fig.3.2. The antisymmetric part of the self-energy Σ^a as a function of the Matsubara frequency ω_n. T=0.0008t, U=1.48253t. The lines of t'=0.144t and t'=0.15t are almost the same.

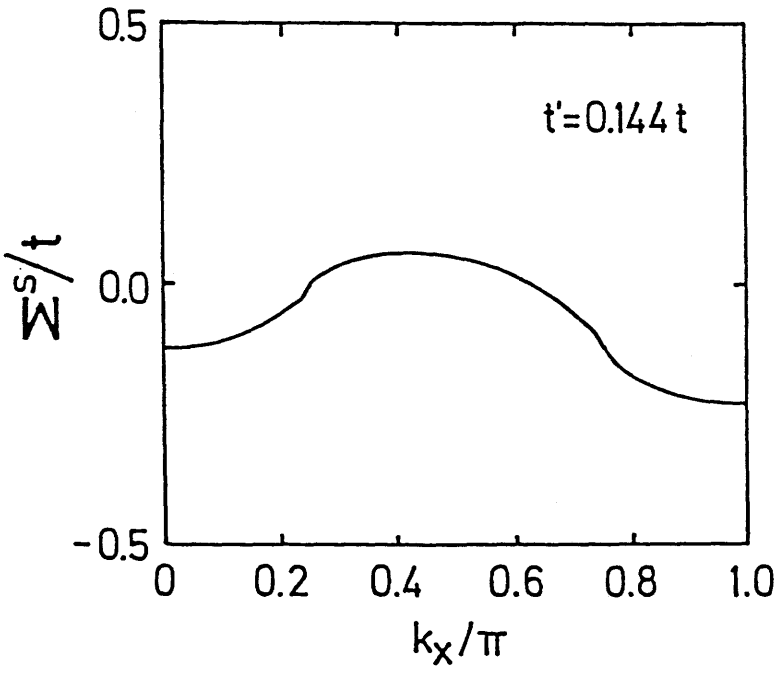

Fig.3.3(a). The symmetric part of the electron self-energy $\Sigma^s(k_x,k_y=\pi/2)$, for t'=0.144t.

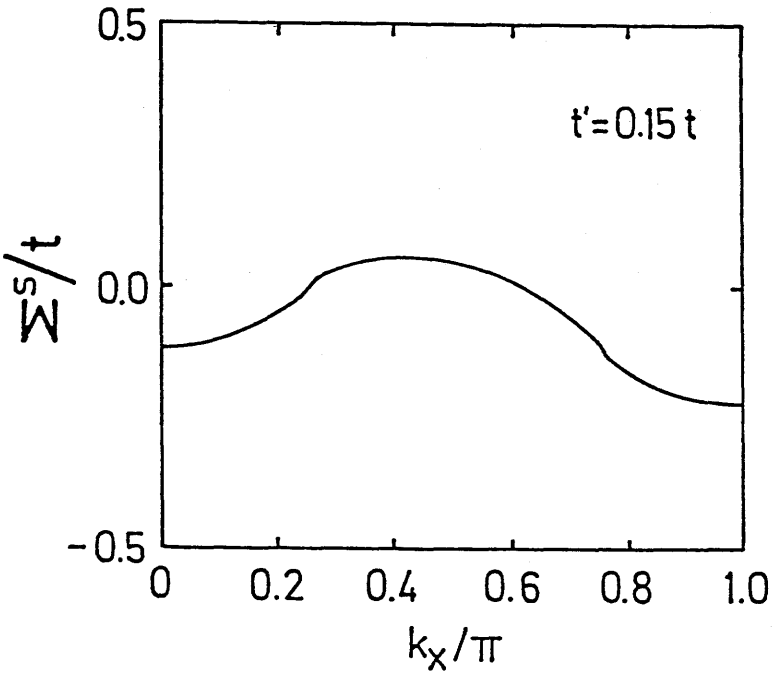

Fig.3.3(b).
The symmetric part of the electron self-energy $\Sigma^s(k_x, k_y=\pi/2)$, for t'=0.15t.

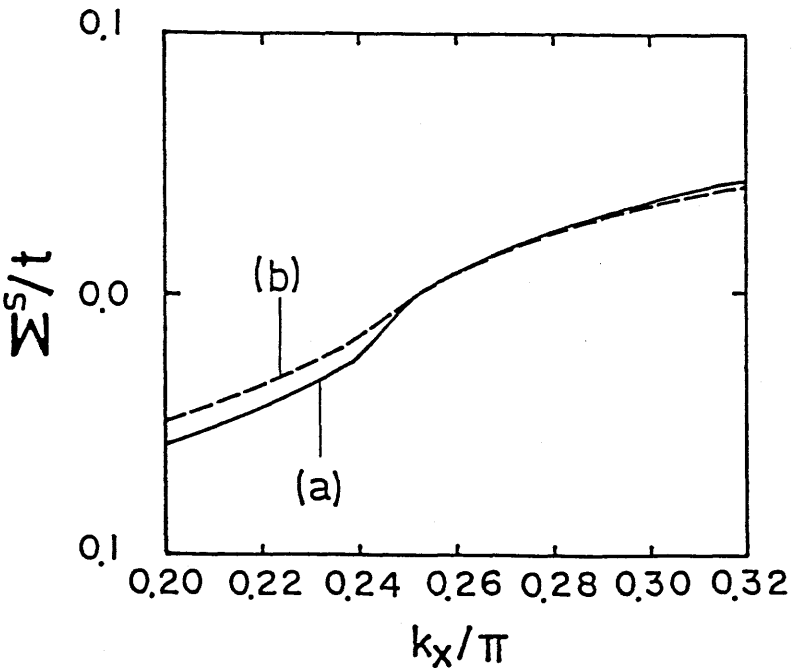

Fig.3.4.
The symmetric part of the self-energy Σ^s near the Fermi-surface of $k_y=\pi/2$.
(a) t'=0.144t, and
(b) t'=0.15t.

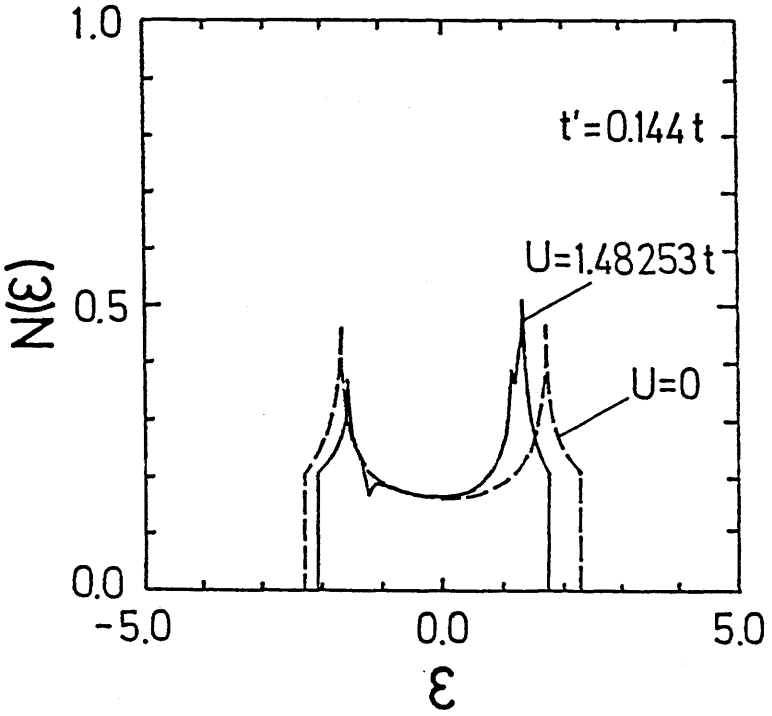

Fig.3.5(a). Density of states N(ε) as a function of the electron energy ε, for t'=0.144t. The solid and broken line show the cases for U=1.48253t and U=0, respectively.

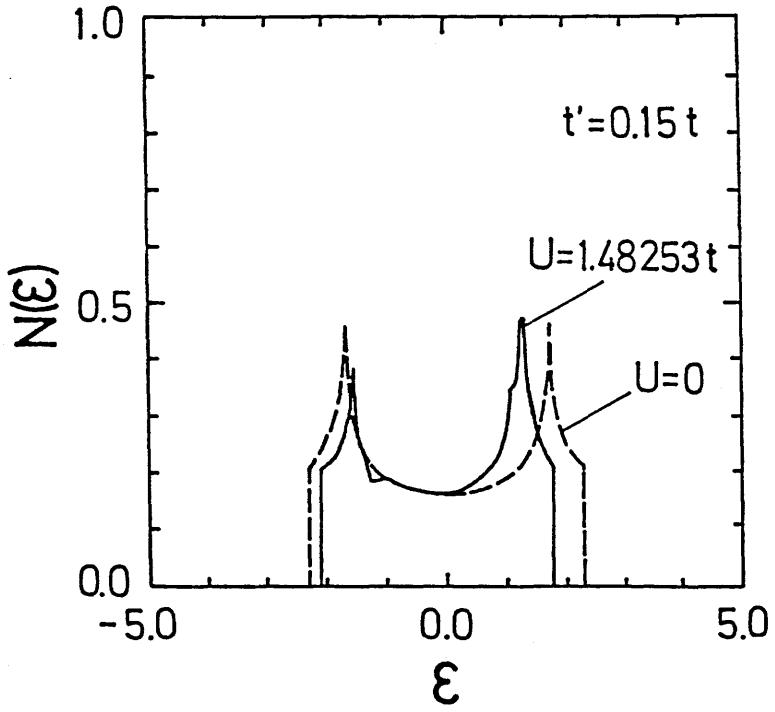

Fig.3.5(b). Density of states N(ε) as a function of the electron energy ε, for t'=0.15t. The solid and broken line show the cases for U=1.48253t and U=0, respectively.

§3.4 Superconductivity

The superconducting instability is signalled by the divergence of multiple scattering vertex for two electrons, i.e. by the first appearance of the nontrivial solution of $\Delta(k)$ which satisfies

$$\Delta(k) = - \sum_{k'} \Gamma_{\alpha\beta}(k,k',0)\, G_{-k'}G_{k'}\, \Delta(k') \ , \tag{3.30}$$

in our approximation (eq.(3.17)). We introduce an eigen value ε which goes to zero as $T \to T_c$ and rewrite eq.(3.30) in a matrix form as

$$(1 - A)\, \Delta = \varepsilon\, \Delta \ , \tag{3.31}$$

with a matrix $A \equiv (A_{kk'}) \equiv (-\Gamma_{\alpha\beta}(k,k',0)\, G_{-k'}G_{k'})$. Here $\Delta = (\Delta(k))$ is an eigen vector belonging to ε, and at $T=T_c$ it becomes the gap anisotropy.

Now we employ the approximation consistent with that of the previous section. We neglect the ω_n dependence of $\Gamma_{\alpha\beta}$ and also of $\Delta(k)$. Then, the Matsubara frequencies in $\Gamma_{\alpha\beta}$ are replaced by 0, and the summation $T\sum_{n'}$ is taken only on $G_{-k'}G_{k'}$ in eq.(3.30). The validity of this approximation will be discussed in the final section. Moreover we expand $\Delta(\vec{k})$ as

$$\Delta_{mni} = N^{-1} \sum_{\vec{k}} h_{mni}(\vec{k})\, \Delta(\vec{k}) \ ,$$

in terms of the ortho-normal set of functions $h_{mni}(\vec{k})$ defined by

$$
\begin{aligned}
h_{mn1}(\vec{k}) &= w_{mn1}\ \cos(mk_x)\ \cos(nk_y)\ , \\
h_{mn2}(\vec{k}) &= w_{mn2}\ \cos(mk_x)\ \sin(nk_y)\ , \\
h_{mn3}(\vec{k}) &= w_{mn3}\ \sin(mk_x)\ \cos(nk_y)\ , \\
h_{mn4}(\vec{k}) &= w_{mn4}\ \sin(mk_x)\ \sin(nk_y)\ ,
\end{aligned}
$$

where w_{mni} being the normalization factor, s.t. $N^{-1} \sum_{\vec{k}} h_{mni}^{2}(\vec{k}) = 1$.

Then eq.(3.31) can be written explicitly as

$$
\sum_{m'n'i'} (\delta_{mni}{}^{m'n'i'} - A_{mni}{}^{m'n'i'})\ \Delta_{m'n'i'} = \varepsilon\ \Delta_{mni}\ , \qquad (3.32)
$$

where the matrix A is defined by summing up G_k, G_{-k}, in the frequency space;

$$
\begin{aligned}
A_{mni}{}^{m'n'i'} &= N^{-2} \sum_{\vec{k}} \sum_{\vec{k}'} h_{mni}(\vec{k})\ \Gamma_{\alpha\beta}(\vec{k},\vec{k}')\ W(\vec{k}')\ h^{m'n'i'}(\vec{k}')\ , \\
\Gamma_{\alpha\beta}(\vec{k},\vec{k}') &= \Gamma_{\alpha\beta}((\vec{k},0),(\vec{k}',0),0)\ , \qquad (3.33) \\
W(\vec{k}') &= T \sum_{n'} G_{k'}, G_{-k'}\ .
\end{aligned}
$$

Since the matrix A does not have off-diagonal elements with respect to the suffix i (=1,2,3,4) from the spatial inversion symmetry, we can decouple the eigen equation by this suffix. From numerical calculation we find that the i=1 order parameter is most favourable in comparison with the others. Thus we will retain the i=1 eigen equation only and suppress the suffix i after this.

The values of the Fourier transform of the singlet pairing interaction

$$N^{-1} \sum_{\vec{q}} \left(\gamma_1(\vec{q},0) + \gamma_2(\vec{q},0) \right) e^{imq_x+inq_y} , \qquad (3.34)$$

and that of the triplet pairing interaction

$$N^{-1} \sum_{\vec{q}} \left(\gamma_1(\vec{q},0) - \gamma_2(\vec{q},0) \right) e^{imq_x+inq_y} , \qquad (3.35)$$

are shown in Table 3.1. These are defined by

$$N^{-2} \sum_{\vec{k}} \sum_{\vec{k}'} h_{mni}(\vec{k}) \left(\gamma_1(\vec{k}-\vec{k}') + \gamma_2(\vec{k}+\vec{k}') \right) h_{mni}(\vec{k}') ,$$

with i=1,4, for the singlet pairings and i=2,3, for the triplet pairings, and eq.(3.35) is easily derived by changing variable as $\vec{k}' \rightarrow -\vec{k}'$ in the term of γ_2. Numerical calculation shows that the latter is much weaker than the former.

From Table 3.1, the Fourier transform of $\Gamma_{\alpha\beta}$ is seen to decrease rather rapidly, so we introduce the upper cutoff m_c and n_c in the summation of eq.(3.32). Then the eigen value ε must be replaced by a function of m_c and n_c ($\varepsilon(m_c,n_c)$) which is expected to converge to the true ε for sufficiently large values of m_c and n_c.

In Fig.3.6, the m_c dependence of $\varepsilon(m_c,n_c)$ is shown for n_c=2, and it is seen that $\varepsilon(m_c,n_c)$ increases monotonically with increasing m_c (i.e. including the long-range components of AFSF), and becomes almost constant for $m_c \gtrsim 30$. The value of $\varepsilon(m_c,n_c)$ is found to be almost the same for $n_c \geq 2$, and n_c=2 is always sufficient for any values of parameters used here. It should be also noted that the saturation occurs at larger m_c as the temperature decreases.

Now we bliefly mention about the pairing susceptibility χ_{super} for electron pair $A^{\dagger}\equiv N^{-1}\sum_{\vec{k}}\delta(\vec{k})c^{\dagger}_{\vec{k}\alpha}c^{\dagger}_{-\vec{k}\beta}$, which is defined by $\chi_{super}\equiv\int_0^{\beta}d\tau\langle A(\tau)A^{\dagger}\rangle$, where $\delta(\vec{k})$ is an arbitrary normalized function and $A(\tau)\equiv e^{\tau H}Ae^{-\tau H}$. In particular if $\delta(\vec{k})\propto\Delta(k)$, then within our approximations,

$$\chi_{super} = \sum_{k} \delta(\vec{k})\ W(k)\ \delta(\vec{k})\ \frac{1}{\varepsilon}\ , \qquad (3.36)$$

with $W(k)=G_kG_{-k}$. Thus for any $\delta(\vec{k})$ which is not orthogonal to $\Delta(k)$ in four-momentum space, the χ_{super} diverges as $T\to T_c$ as expected. The temperature dependence of pairing susceptibility for the most enhanced electron pair (eq.(3.36)) is plotted in Fig.3.7. There the χ_{super} for $m_c=31$ and $n_c=2$, and that for $m_c=8$ and $n_c=2$ are compared and it is found that the χ_{super} is remarkably enhanced at low-temperatures owing to the long range (large m) components of the pairing interaction. We obtain $T_c\cong 0.4K$ for $t'=0.15t$ although this would be only rough estimation because of our approximations.

From now on we will show the other numerical results obtained from eq.(3.32).

The amplitudes of the most enhanced electron pairs (Δ_{mn}) at $T=0.5K\cong T_c$ and $t'=0.15t$ are shown in Table 3.2(a). They may be regarded as the gap anisotropy at superconducting instability point. The amplitude of the intra-chain next nearest neighbour (n.n.n.) component ($\sqrt{2}\ \Delta_{2,0}\cos(2k_x)$) is seen to be largest. This is because of the strong on-chain fluctuations due to the quasi-1D motion of electrons.

The momentum dependence of the order-parameter $\Delta(\vec{k})$ is plotted in Fig.3.8. From this figure it is found that; (1) $\Delta(\vec{k})$ has a line of node on the Fermi-surface; (2) the peak is found on the Fermi-surface consistently with the itinerant electron picture. Such a sharp peak structure is not appear in the absence of the long range fluctuation, and then the superconductivity is very weak as found in Fig.3.6 and 3.7. Therefore this second point shows that the contribution of the electrons near the Fermi-surface is enhanced by the long-range components of the pairing interaction in the gap equation and thus the superconductivity is enhanced by them.

The theoretical phase diagram is shown in Fig.3.9. When the renormalization effects for normal electrons are ignored the T_c is seen to increase remarkably near the SDW boundary owing to the long range AFSF. (The T_c by the short range AFSF exchange only are found to be extremely low from the numerical estimation.) However, if one takes into account the electron self-energy mentioned in §3.2, then the superconductivity is significantly suppressed because of the strong renormalization effect. In particular such a suppression becomes remarkable near the SDW boundary because of the pseudo gap. As a result of these competitions, we can see the qualitative agreement with the experimental phase diagrams.[7,8] (1) The T_c sensitively decreases from ~1K to ~0K with increasing t' from ~0.144t (in the vicinity of SDW boundary) to ~0.153t. (2) The increase of the T_c as approaching the SDW boundary is not so remarkable. (3) Moreover the superconducting phase seems to continue to exist on the border of the SDW phase.

The gap anisotropy varies as a function of t' (Fig.3.10 and Table 3.2). The amplitudes of the short range components in the chain direction (n=0) $\sqrt{2}\ \Delta_{2,0}\cos(2k_x)$ ··· decrease and those of the long range components $\sqrt{2}\ \Delta_{10,0}\cos(10k_x)$ ··· increase as approaching the SDW boundary.

Table 3.1. The values of the Fourier components of the pairing interaction of eq.(34) with t'=0.15t and U=1.48253t.

(a) singlet pairing

t'/t		0.150	
T/t		0.00080	
m \ n	0	1	2
0	2.769	−0.067	0.020
1	0.181	0.006	−0.002
2	−0.465	0.087	−0.031
3	−0.084	−0.004	0.004
4	0.252	−0.102	0.036
5	0.056	−0.002	−0.005
6	−0.150	0.107	−0.044
7	−0.033	0.009	0.005
8	0.084	−0.099	0.052
9	0.025	−0.014	−0.003
10	−0.058	0.083	−0.057
11	−0.010	0.016	0.000
12	0.041	−0.066	0.057
13	0.007	−0.015	0.004
14	−0.049	0.050	−0.052
15	−0.004	0.012	−0.006
16	0.041	−0.039	0.045
17	0.013	−0.009	0.006
18	−0.042	0.033	−0.037
19	−0.006	0.007	−0.004
20	0.034	−0.030	0.031
21	0.010	−0.005	0.003
22	−0.038	0.028	−0.028
23	−0.007	0.004	−0.002
24	0.026	−0.027	0.025
25	0.011	−0.004	0.001
26	−0.025	0.025	−0.024
27	0.000	0.004	−0.001
28	0.020	−0.024	0.024
29	0.003	−0.003	0.001
30	−0.026	0.023	−0.024
31	−0.001	0.002	−0.001

(b) triplet pairing

t'/t		0.150	
T/t		0.00080	
m \ n	0	1	2
0	0.768	0.024	−0.013
1	−0.078	−0.002	0.001
2	0.187	−0.031	0.010
3	0.032	0.002	−0.001
4	−0.100	0.036	−0.012
5	−0.020	0.001	0.002
6	0.051	−0.038	0.015
7	0.014	−0.003	−0.002
8	−0.029	0.036	−0.018
9	−0.004	0.005	0.001
10	0.018	−0.029	0.020
11	0.005	−0.005	0.000
12	−0.008	0.023	−0.020
13	−0.002	0.005	−0.002
14	0.012	−0.017	0.018
15	0.003	−0.004	0.002
16	−0.015	0.013	−0.015
17	0.000	0.003	−0.002
18	0.014	−0.011	0.013
19	0.005	−0.002	0.001
20	−0.015	0.010	−0.011
21	−0.003	0.002	−0.001
22	0.008	−0.009	0.009
23	0.004	−0.001	0.001
24	−0.011	0.009	−0.008
25	0.000	0.002	0.000
26	0.008	−0.009	0.008
27	0.004	−0.001	0.000
28	−0.009	0.008	−0.008
29	0.000	0.001	0.000
30	0.004	−0.008	0.008
31	0.001	−0.001	−0.000

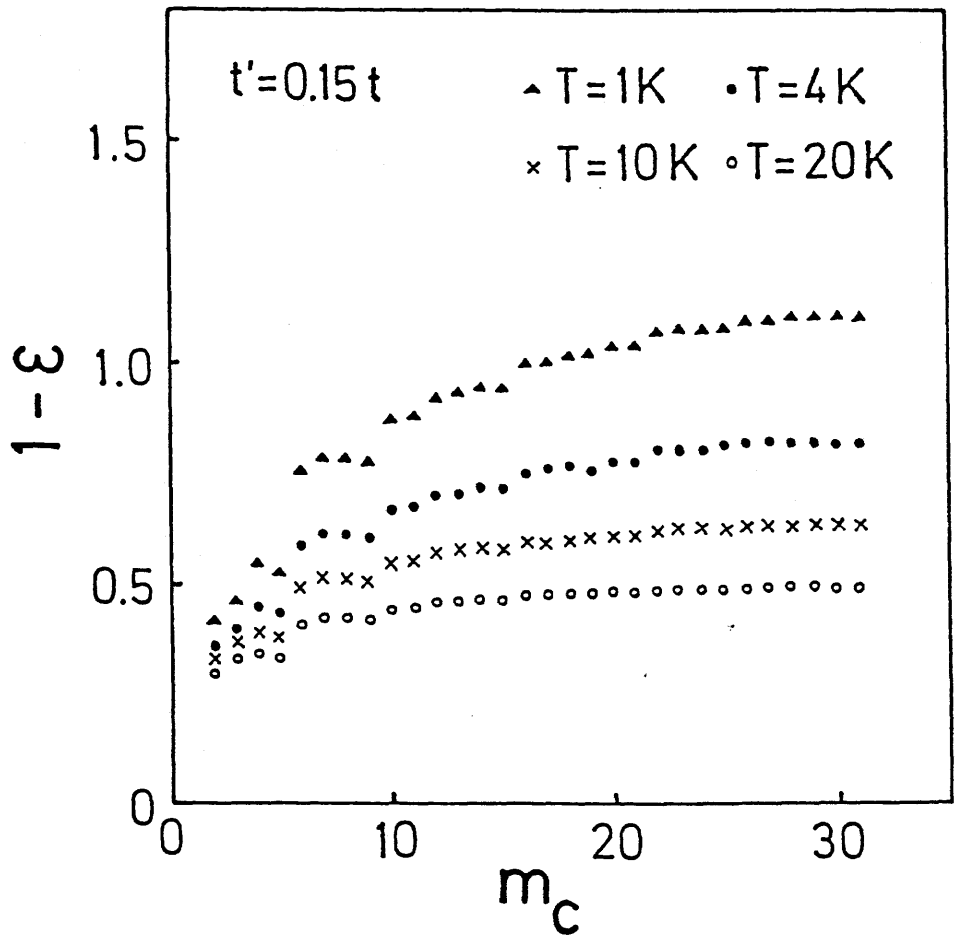

Fig.3.6. The m_c dependence of the eigen value of the matrix A (i.e. $1-\varepsilon(m_c,n_c=2)$) for t'=0.15t. The closed triangles, closed circles, crosses, and open circles denote those for T=0.0004t (1K), 0.0016t (2K), 0.0020t (10K) and 0.0040t (20K), respectively.

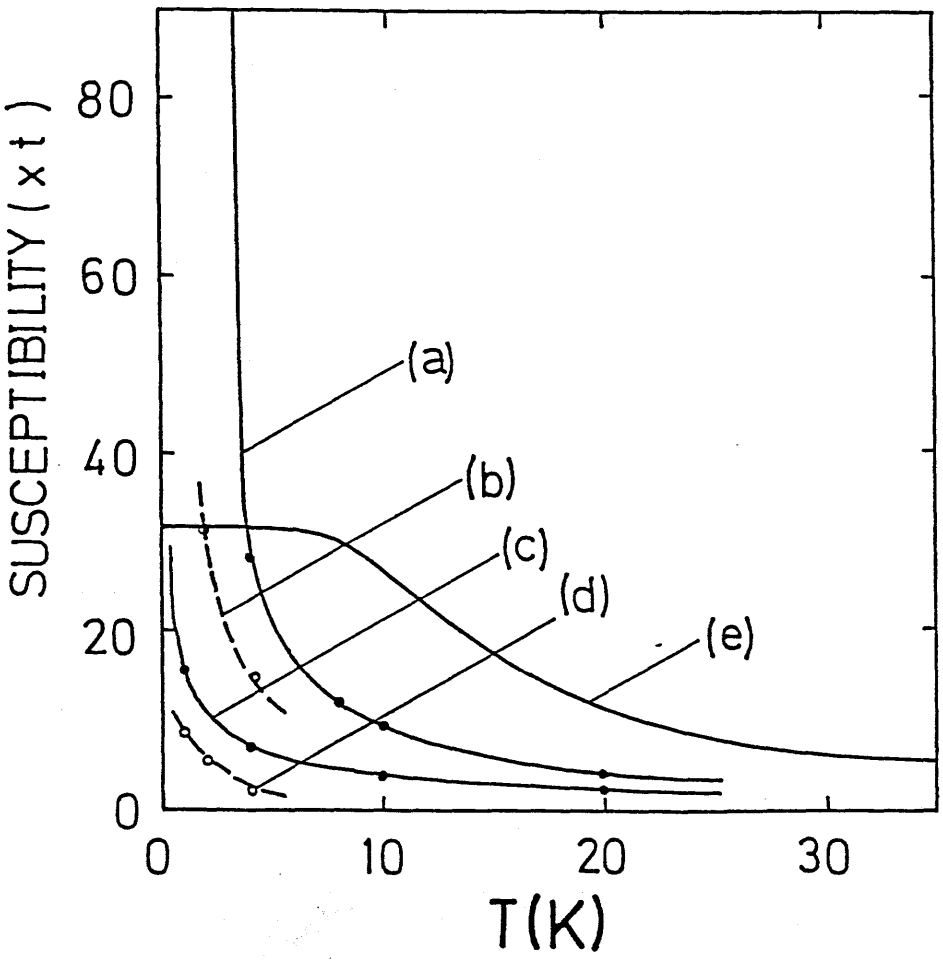

Fig.3.7. The pairing susceptibilities and spin-susceptibility for U=1.48253t and t'=0.15t. (a) The pairing susceptibility χ_{super} for m_c=31, n_c=2 (neglecting the self-energy). (b) m_c=31, n_c=2 (including the self-energy). (c) m_c=8, n_c=2 (neglecting the self-energy). (d) m_c=8, n_c=2 (including the self-energy). (e) The staggered spin-susceptivility $\chi(\vec{Q},0)$. The lines of (a)~(d) are to guide for eyes.

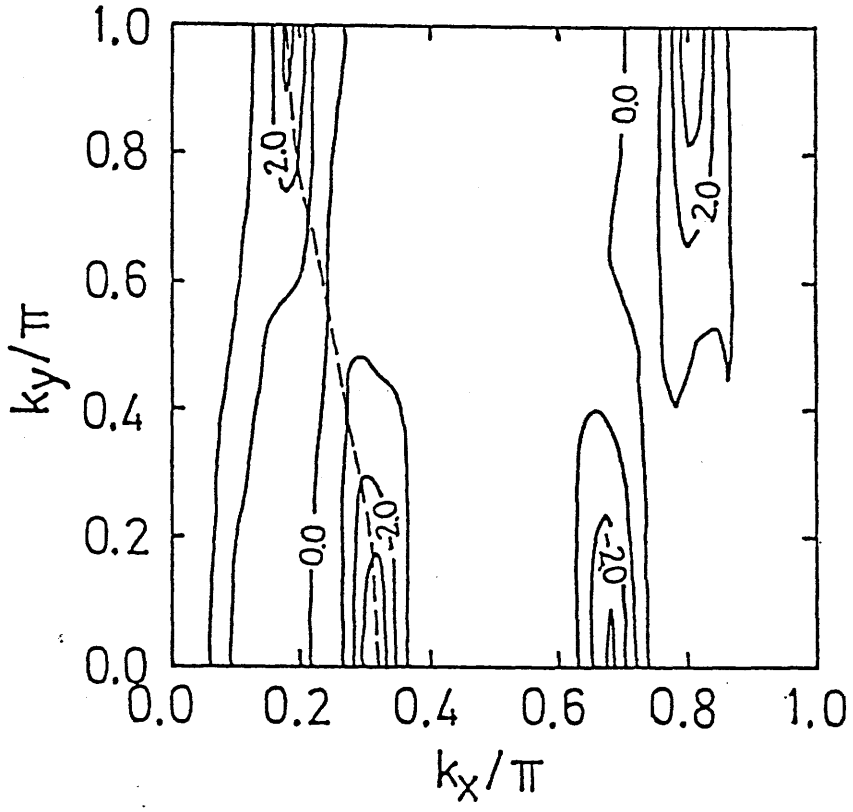

Fig.3.8(a). Momentum dependence shown by the contour lines of the order-parameter $\Delta(\vec{k})/\Delta$ in the momentum space for t'=0.15t, T=0.0002t(~T_c), and U=1.48253t. The renormalization effects for the electron Green's functions are included. Here Δ is the normalization factor s.t. $N^{-1}\sum_{\vec{k}} \Delta(\vec{k})^2/\Delta^2=1$. The broken line shows the unperturbed Fermi-surface.

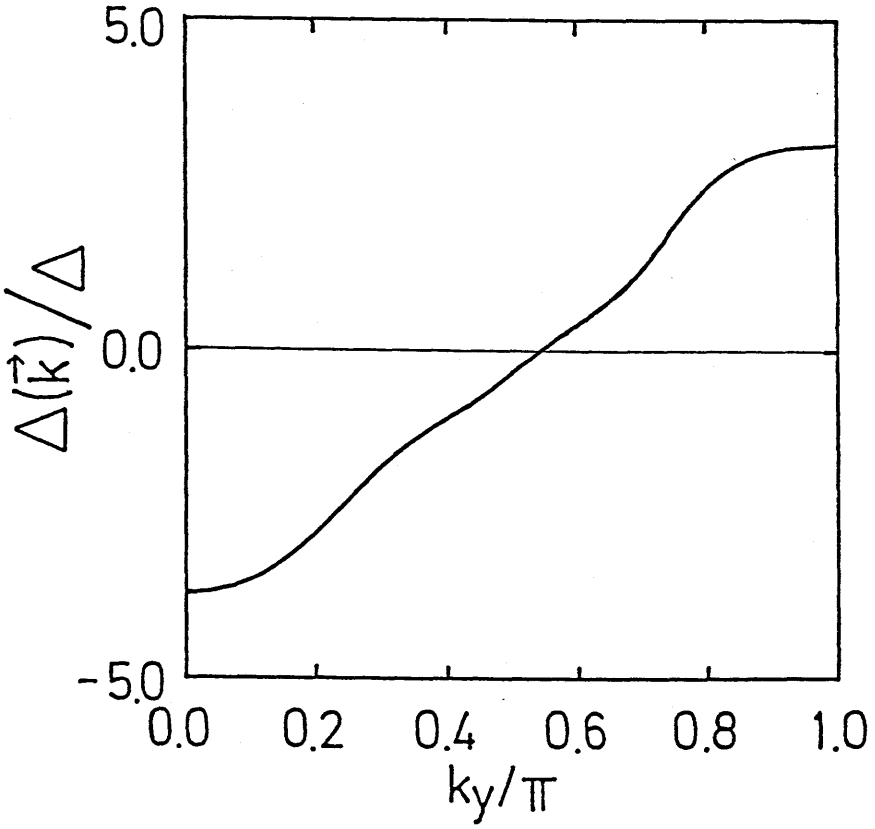

Fig.3.8(b). Momentum dependence of the order-parameter (Fig.3.8(a)) along the Fermi-surface.

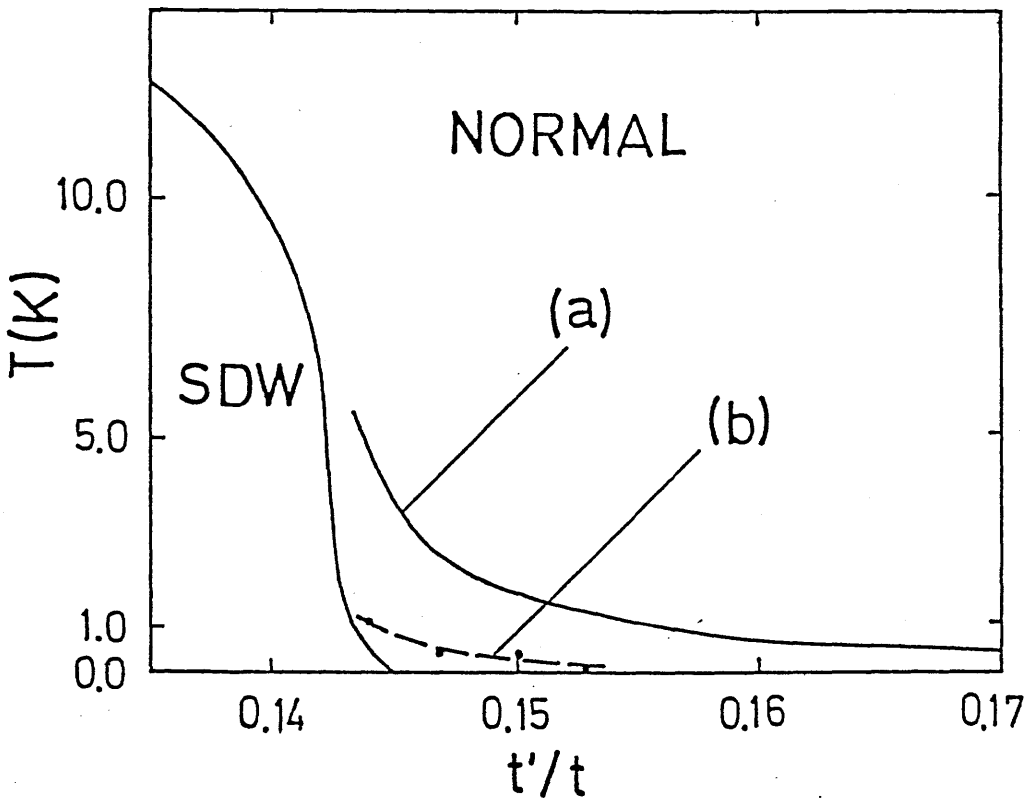

Fig.3.9. The phase diagram on T-t' plane (U=1.48253t). The unlavelled solid line shows the SDW transition temperatures. The solid line (a) and the closed circles show the T_c without and with the renormalization effects, respectively. The broken line (b) is to guide for eyes.

Table 3.2. The amplitudes of the order-parameters $\Delta_{m,n}$ (normalized as unity) for $T=0.00020t\equiv T_c$ (with the re-normalization effects).

(a) t'=0.15t

t'/t		0.150	
T/t		0.00020	
m \ n	0	1	2
0	0.074	−0.220	−0.008
1	−0.081	0.017	0.001
2	0.696	0.010	0.034
3	0.129	0.009	−0.002
4	−0.051	0.297	0.009
5	0.097	0.004	−0.007
6	−0.451	−0.017	−0.100
7	−0.088	0.005	0.007
8	0.030	−0.013	0.001
9	−0.038	0.006	0.003
10	0.169	−0.005	0.106
11	0.025	0.019	0.001
12	−0.015	−0.156	−0.007
13	0.008	−0.032	0.002
14	−0.066	0.019	−0.010
15	−0.006	−0.024	0.001
16	0.004	0.126	−0.002
17	0.000	0.024	0.005
18	−0.017	−0.016	−0.063
19	−0.007	0.010	−0.007
20	0.009	−0.065	0.010
21	−0.008	−0.008	−0.004
22	0.053	0.007	0.072
23	0.014	−0.002	0.004
24	−0.012	0.003	−0.012
25	0.006	−0.002	0.002
26	−0.040	0.006	−0.049
27	−0.006	−0.003	−0.001
28	0.007	0.039	0.006
29	−0.001	0.006	0.000
30	0.014	−0.014	0.008
31	0.001	0.002	0.000

(b) t'=0.144t

t'/t		0.144	
T/t		0.00040	
m \ n	0	1	2
0	0.051	−0.249	−0.009
1	−0.068	0.011	0.000
2	0.609	0.008	0.042
3	0.101	0.004	−0.002
4	−0.038	0.316	0.009
5	0.080	0.006	−0.004
6	−0.475	−0.014	−0.113
7	−0.074	0.006	0.004
8	0.027	−0.044	−0.001
9	−0.039	0.002	0.002
10	0.231	−0.002	0.120
11	0.031	0.012	0.001
12	−0.017	−0.161	−0.004
13	0.013	−0.022	0.002
14	−0.102	0.017	−0.030
15	−0.010	−0.019	0.000
16	0.006	0.176	−0.002
17	−0.002	0.021	0.002
18	−0.001	−0.018	−0.065
19	−0.003	0.012	−0.005
20	0.006	−0.113	0.011
21	−0.006	−0.010	−0.004
22	0.066	0.010	0.102
23	0.011	−0.004	0.004
24	−0.013	0.030	−0.014
25	0.007	0.001	0.002
26	−0.071	0.004	−0.085
27	−0.007	−0.001	−0.002
28	0.011	0.042	0.009
29	−0.003	0.004	−0.001
30	0.039	−0.016	0.035
31	0.002	0.002	0.000

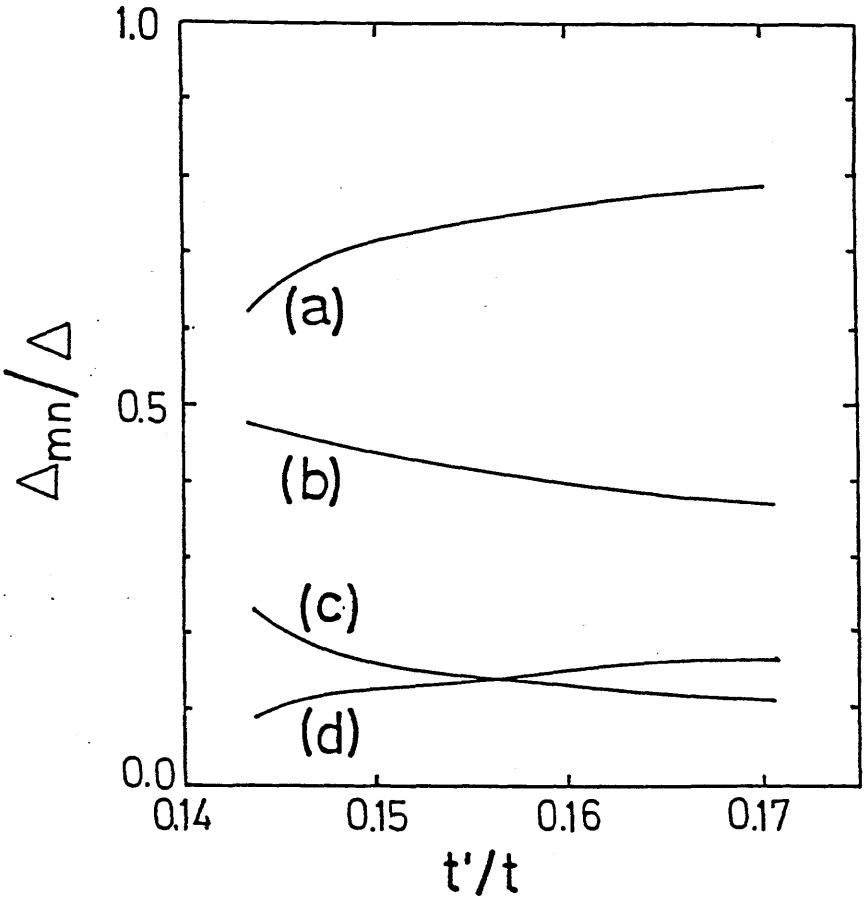

Fig.3.10. The amplitudes of the order-parameters as functions of t', in the case of no renormalization effects, U=1.48253t and $T \equiv T_c$(for each t'). (a) $\Delta_{2,0}/\Delta$, (b) $\Delta_{6,0}/\Delta$, (c) $\Delta_{10,0}/\Delta$, (d) $\Delta_{3,0}/\Delta$. Here Δ is the normalization factor s.t. $\sum_{m,n} \Delta_{m,n}^2/\Delta^2 = 1$.

§3.5 Discussion

We have obtained the momentum dependence of the order parameters and the phase diagram which agrees qualitatively with experiments. We found the importance of the long range spin-fluctuations on each chain, by more accurate treatements in the momentum space than previous works,[2,3,5] for the application to the quasi-1D systems.

Now we discuss the validity of our approximations. First, the retardation of the interaction was ignored. It leads to the overestimation of the interaction, although that is roughly valid because the characteristic energies $N(0)^{-1}$ and κu of the spin-fluctuations are much larger than the temperatures. However, because we take account of any characteristic energy scales of the vertices through the momentum dependence and such energy scales act as an effective energy cutoff in eqs.(3.21) and (3.30), the overestimated high energy processes are not considered to contribute largely to these equations. Thus, in spite of the absence of the energy cutoff like the Debye frequency in the BCS theory, such an overestimation is not so serious as changing the physical characteristics. On the other hand, within an approximation employed by Scalapino et al.,[2] the effective vertices are averaged on the Fermi-surface in the momentum space, and the frequency dependence is also neglected. Such an approximation would not be appropriate for our purpose of examining the long-range AFSF and obtaining the T_c and its behaviour, because there is not a definite energy cutoff much smaller than the Fermi-energy.

Further we have regarded the AFSF exchange vertices as boson propagators. This would be roughly valid for the system dominated by the AFSF at least semi-phenomenologically. Furthermore we have implicitly assumed the appropriate hopping of electron in z-direction which is small compared to t' but large enough to suppress the thermal fluctuations on each conductive plane justifying the mean field approximation. From these reasons a realistic estimation of the AFSF contribution in $(TMTSF)_2X$ and $(DMET)_2X$ needs more accurate calculation beyond the RPA and the ladder approximation. Moreover the maximum value of T_c depends on the choice of U, which is not accurately known experimentally. Nevertheless we think that our treatment would clarify an essential aspect of these compound from the qualitative agreement with the experiments, and from the agreement in the order of T_c. For example, $T_c \lesssim 0.4\sim1.4$K and $T_{SDW} \lesssim 12$K for $(TMTSF)_2X$,[7,8] and $T_c \lesssim 0.5\sim1.9$K and $T_{SDW} \lesssim 2.8\sim25$K for $(DMET)_2X$,[9~11] experimentally. On the other hand, the theoretical result is $T_c \lesssim 4.4\times10^{-4}t$ (i.e. 1.1K if t=2500K) for U=1.48253t. Then $T_{SDW}=8.0\times10^{-3}t$ (=20K) for t'=0, and $T_{SDW}=4.8\times10^{-3}t$ (=12K) for t'=0.136t, and the SDW phase vanishes at t'~0.145t.

In addition in the present case the 2D van Hove singularities of the DOS does not cause any peculiarity as seen in the square lattice case. However if the transverse hopping t' increases as $2t' \sim 2t+\mu$ ($\mu \cong -1.3t$, $t' \cong 0.35t$ for 1/4-filled band) and the Fermi-surface is near the saddle point of the dispersion, then the superconductivity may be enhanced by the large DOS according to the value of U, although the AFSF would be hardly assisted by the Fermi-surface nesting. It must be also noted that

a some kind of frustrations which suppress the AF ordering may enhance the superconductivity cooperatively with the van Hove singularities.[5)]

Rererences 3.

1. V.J.Emery: Synth.Met. **13**(1986)21.
2. D.J.Scalapino, E.Loh,Jr, and J.E.Hirsch: Phys.Rev.B **34**(1986) 8190; **35**(1987)6694.
3. K.Miyake, S.Schmitt-Rink, and C.M.Varma: Phys.Rev. B **34**(1986) 6554.
4. J.E.Hirsch: Phys.Rev.Lett. **54**(1985)1317.
5. H. Shimahara and S. Takada: J. Phys. Soc. Jpn. **57** (1988)1044.
6. K.Miyake, T.Matsuura, K.Sano, and Y.Nagaoka: Physica **148B** (1987)381; J.Phys.Soc.Jpn. **57**(1988)722.
7. D. Jerome and H.J. Schulz: Adv. Phys. **31**(1982)299; and references therein.
8. R.Brusetti, M. Ribault, D. Jerome, and K. Bechgaard: J. Phys. (Paris) **43**(1982)801.
9. K.Kikuchi, K.Murata, Y.Honda, T.Namiki, K.Saito, K.Kobayashi, T. Ishiguro, and I. Ikemoto: J. Phys. Soc. Jpn. **56**(1987)2627.
10. K.Kikuchi, K.Murata, Y.Honda, T.Namiki, K.Saito, T.Ishiguro, K.Kobayashi, and I. Ikemoto: J. Phys. Soc. Jpn. **56**(1987)3436; K.Kikuchi et al.:Solid State Commun. **66**(1988)405.
11. K.Kikuchi, M.Kikuchi, T.Namiki, K.Saito, I.Ikemoto, K.Murata, T.Ishiguro, and K.Kobayashi: Chem.Lett.(Tokyo) **1987**(1987)931.
12. K.Yamaji: Solid State Commun. **61**(1987)413.
13. T.Fujita, Y.Aoki, Y.Maeno, J.Sakurai, H.Fukuba, and T.Fujii: Jpn.J.Appl.Phys. **26**(1987)L368.
14. N. Nishida, H. Miyatake, D. Shimada, S. Okuma, M.Ishikawa, T. Takabatake, Y.Nakazawa, Y. Kuno, R. Keitel, J.H. Brewer, T.M. Riseman, D.L. Williams, Y. Watanabe, T.Yamazaki, K.Nishiyama,

K.Nagamine, E.J.Ansaldo, and E.Torikai: J. Phys. Soc. Jpn. **57** (1988)597.

15. T.A.Faltens, W.K.Ham, S.W.Keller, K.J.Leary, J.N.Michaels, A. M. Stacy, H.-C. zur Loye, D. E. Morris, T.W. Barbee,III, L.C. Bourne, M.L.Cohen, S. Hoen, and A. Zettl: Phys. Rev. Lett. **59** (1987)915.
16. L.C.Bourne, M.F.Crommie, A.Zettl, H.-C.zur Loye, S.W. Keller, K.L.Leary, A.M.Stacy, K.J.Chang, M.L. Cohen, and D.E. Morris: Phys.Rev.Lett. **58**(1987)2337.
17. B. Batlogg, R. J. Cava, A. Jayaraman, R. B. van Dover, G. A. Kourouklis, S.Sunshine, D.W. Murphy, L.W. Rupp. H.S. Chen, A. White, K.T.Short, A.M.Mujsce, and E.A.Rietman: Phys.Rev.Lett. **58**(1987)2333.
18. H.Fukuyama and Y.Hasegawa: Physica **B148**(1987)204.
19. M.Takigawa, H.Yasuoka, and G.Saito: J.Phys.Soc. Jpn. **56**(1987) 873.
20. Y. Hasegawa and H. Fukuyama: J. Phys. Soc. Jpn. **56** (1987)877.
21. D.E. MacLaughlin, C. Tien, W.G. Clark, M.D. Lan, Z.Fisk, J.L. Smith, and H.R.Ott: Phys.Rev.Lett. **53**(1984)1833.
22. Y. Kitaoka, K. Ueda, T. Kohara, K. Asayama, Y. Onuki, and T. Komatsubara: J.Magn.Magn. **52**(1985)341.
23. D.J. Bishop, C.M.Varma, B.Batlogg, E.Bucher, Z.Fisk, and J.L. Smith: Phys.Rev.Lett. **53**(1984)1009.
24. C.S.Jacobsen, D.B.Tanner, and K.Bechgaard: Phys.Rev. Lett. **46** (1981)1142.
25. P.M.Grant: J.Phys.Colloq. 44(1983)C3-847; Phys.Rev.B **26**(1982) 6888.
26. K.Yamaji: J.Phys.Soc.Jpn. **51**(1982)2787.

27. Y.Hasegawa and H.Fukuyama: J.Phys.Soc.Jpn. **55**(1986)3978.

28. M.Imada: Jpn.J.Appl.Phys. **26**(1987)985.

29. S.R.White, R.L.Sugar, and R.T.Scalettar: preprint.

30. H.Q.Lin, J.E.Hirsch, and D.J.Scalapino: Phys. Rev. B **37**(1988) 7359.

31. H.Shimahara: J.Phys. Soc. Jpn. **58**(1989)1735; in Proceeding of the Physics and Chemistry of Organic Superconductors, edited by G. Saito and S. Kagashima (Springer-Verlag, Berlin, Heidelberg, New York, to be published).

Chapter 4.

Magnetic Properties and Superconductivity of Strongly Correlated Electron Systems

In this chapter, we study the t-J model, which describs the strong repulsive interaction between electrons on each site, and reduces to the antiferromagnetic Heisenberg model in the half-filled band limit. The t-J model can be derived from the strong coupling Hubbard model in the case of $J<<t$.

The method used in this chapter is a Green's function decoupling scheme in real space, so called Hubbard III approximation improved by Kawabata, which is appropriate to the strong correlation regime. Applying this method to the t-J model of any hole concentrations, we find that the magnetic property changes rapidly from that of localized spin systems to that of itinerant electron systems as hole concentration increased from half-filling. In the half-filled band limit, the susceptibility is shown to reduce to the Curie-Weiss form in the mean field approximation on the exchange term of the Hamiltonian. It is also found that the antiferromagnetic transition temperature takes its maximum at half-filling and decreases very rapidly with slight hole-doping. Superconductivity is also examined within a similar approximation. It is found that superconductivity is difficult to occur in the strong coupling Hubbard model but it occurs in the t-J model for large J far from the half-filling. It is also found

that the d-wave pairing is more favourable than the s-wave pairing. The relation to the oxide high T_c superconductors is discussed.

§4.1 Introduction

The strongly correlated electron system is a longstanding subject of interest, which has been studied from various aspects such as the Mott-Hubbard transition,[1] the magnetic properties[2-6] and the superconductivity.[7-10] The oxide high-T_c superconductors[11,12] have attracted current interest from this view-point, since the strong on-site correlation was experimentally revealed from the facts that Cu atoms on CuO_2 planes exist almost as Cu^{++} with spin 1/2,[13] and also they exhibit (1) a gradual change from the insulating phase to the metallic phase with decreasing electron number from the half-filled state,[14-16] (2) a localized antiferromagnetic (AF) phase in the nearly half-filled case,[14,17] and (3) the high-T_c superconductivity.[11,12] Thus numerous works have been devoted so far to clarify physical properties of the strong coupling Hubbard model. In the strong coupling limit the Hubbard model is transformed into the t-J model:

$$H = \sum_{i,j,\sigma} t_{ij}\, \tilde{c}^{\dagger}_{i\sigma}\, \tilde{c}_{j\sigma} + \sum_{i,j} 2J_{ij}(S_i \cdot S_j - \frac{1}{4} n_i n_j) + \sum_{i,\sigma} \varepsilon_{i\sigma}\, n_{i,\sigma} \,, \tag{4.1.1}$$

where we defined $\tilde{c}_{i\sigma} = n^{-}_{i-\sigma} c_{i\sigma}$, $n^{-}_{i-\sigma} = 1 - n_{i-\sigma}$, $n_{i\sigma} = c^{\dagger}_{i\sigma} c_{i\sigma}$, and $S_i = 1/2 \cdot c^{\dagger}_{i\alpha} \sigma_{\alpha\beta} c_{i\beta}$. Here $J_{ij} = J = t^2/U$ and $t_{ij} = -t$ for the nearest

neighbour (n.n.) sites (i,j) and otherwise $J_{ij}=0$ and $t_{ij}=0$. Moreover we ignore the terms of the order of t^2/U in the hopping terms of eq.(4.1.1) in comparison to t.

The t-J model can be derived in a strong coupling limit of the d-p model which is a realistic model of the high-T_c superconductors.[18,19] It should be noted that in the half-filled limit, the t-J model reduces to the AF Heisenberg model, since the hopping term of eq.(4.1.1) does not work actually due to the prohibition of the double occupancy.

In the original Hubbard model, doubly occupied sites appear, except for infinite U. This effect is, however, small enough compared to that of the second term of eq.(4.1.1), since the expectation value $\langle n_{i\sigma}n_{i-\sigma}\rangle$ is estimated less than order of $e^{-(-W+U)/T}$ with temperature T, where W is the band width of U=0 system and we have used the fact that the energy gain due to the electron hopping through the occupied sites is less than order of W. Therefore the description by the t-J model would be valid for sufficiently strong correlations and low temperature satisfying $-W+U>>T$.

In the strong coupling Hubbard model or the t-J model, the short range correlations of electrons are considered to dominate physical properties, especially for the nearly half-filled case in which the electrons exhibit a localized character. As one of the approximations which is appropriate for this kind of problem, a Green's function decoupling scheme was proposed by Hubbard with successful results in the study of the Mott-Hubbard transition,[1] (Hubbard III). However, later, Kawabata pointed out that in the half-filled case the Hubbard III approximation does not reproduce

the Curie law for the magnetic susceptibility, in the Hubbard model with infinite U. He resolved this difficulty by proposing the improved Hubbard III approximation, and showed that the susceptibility obeys the Curie-Weiss law, although he made some assumptions to show it.[2)]

In this chapter, we apply the improved Hubbard III approximation to the t-J model, and investigate the magnetic properties and the superconductivity.

For the magnetic properties, we examine the behaviour of the susceptibility, AF transition temperature T_{AF}, and sublattice magnetization at any hole concentrations. We expect that our approximation is adequate unless the hole concentration is large.

For the superconductivity, we attribute the attractive interaction for the pairing to the nearest neighbour interaction J_{ij}, and assume the picture of local pairing.[20)] This picture is rather different from the BCS superconductivity. In BCS superconductivity, the **k**-space condensation around the Fermi surface occurs, and thus the long-range nature of interactions[24)] such as that mediated by phonons and para-magnon are essential in the BCS superconductivity. On the other hand, for the superconductivity of the local pairing, it is essential to take into account local correlations. Hence we apply the improved Hubbard III approximation to the superconductivity of the local pairing, similarly to the case of the magnetic properties.

Moreover, in the t-J model including cases of rather large J, the favourable symmetry of the superconductivity is also unknown theoretically. In the weak coupling Hubbard model d-symmetry pairing is shown to be favourable because of the nature

of the attractive interaction induced by spin-fluctuations[21-25] and also because of the van Hove singularities in the square lattice.[20,23,25] However, in the t-J model, it is uncertain, although a numerical work supports the d-wave superconductivity.[9]

In §4.2, we investigate the normal state Green's function and the momentum distribution of the quasi-particles. In §4.3, the magnetic susceptibility is calculated in the non-half-filled case, and the Curie-Weiss law is proven to hold in the half-filled limit. In §4.4, the improved Hubbard III approximation is extended to the antiferromagnetic case and the antiferromagnetic transition temperatures are obtained. In §4.5, the superconductivity is studied and the d-symmetry of the order parameter is shown to be favourable. In §4.6, we examine the Green's function for various band structures in connection with the ferromagnetic instability. The last section is devoted to summary and discussion. The main part of this chapter has been published in our three papers of ref.26.

§4.2 Normal Electron Green's Function in J=0

We introduce a retarded Green's function $G_{AB}(t)$ for Fermion operator A and B defined by

$$G_{AB}(t) \equiv \langle A|B\rangle_t \equiv -i\theta(t)\ \langle [A(t),B]_+\rangle_t \ , \tag{4.2.1}$$

with $A(t)\equiv e^{iHt}A\ e^{-iHt}$. It's Fourier transform is denoted by

$$G_{AB}(\omega) \equiv \langle A|B\rangle_\omega \equiv \int_{-\infty}^{\infty} dt\ e^{i\omega t}\ \langle A|B\rangle_t \ . \tag{4.2.2}$$

First, we investigate the single particle Green's function $G_{ij\sigma}(\omega)\equiv\langle\tilde{c}_{i\sigma}|\tilde{c}_{j\sigma}^{\dagger}\rangle_\omega$ in the case of J=0. Then $G_{ij\sigma}(\omega)$ satisfies the following equation of motion;

$$\begin{aligned}
&(\omega-\varepsilon_{i\sigma})\ \langle\tilde{c}_{i\sigma}|\tilde{c}_{j\sigma}^{\dagger}\rangle_\omega \\
&= \langle n_{i-\sigma}^{-}\rangle\ (\delta_{ij} + \sum_k t_{ik}\ \langle\tilde{c}_{k\sigma}|\tilde{c}_{j\sigma}^{\dagger}\rangle_\omega) \\
&+ \sum_k t_{ik}\ \langle\ \delta n_{i-\sigma}^{-}\tilde{c}_{k\sigma}\ |\tilde{c}_{j\sigma}^{\dagger}\rangle_\omega + \sum_k t_{ik}\ \langle\ \tilde{c}_{k-\sigma}\tilde{c}_{i-\sigma}^{\dagger}\tilde{c}_{i\sigma}|\tilde{c}_{j\sigma}^{\dagger}\rangle_\omega \ ,
\end{aligned} \tag{4.2.3}$$

where $\delta n_{i-\sigma}^{-}\equiv n_{i-\sigma}^{-}-\langle n_{i-\sigma}^{-}\rangle$. The second and third terms in the right hand side are termed the scattering correction and the resonance broadening correction, respectively, following Hubbard.[1)]

In the following, we calculate these correction terms in the paramagnetic phase adopting the Hubbard III approximation improved by Kawabata.[2)]

The Green's function $\langle \delta n_{i-\sigma}^{-} \tilde{c}_{k\sigma} | \tilde{c}_{j\sigma}^{\dagger} \rangle_{\omega}$ $(i \neq k)$ which appears in the scattering correction approximately satisfies the following equation of motion;

$$(\omega-\varepsilon_{k\sigma}) \langle \delta n_{i-\sigma}^{-} \tilde{c}_{k\sigma} | \tilde{c}_{j\sigma}^{\dagger} \rangle_{\omega} = \langle n_{k-\sigma}^{-} \rangle \sum_{l} t_{kl} \langle \delta n_{i-\sigma}^{-} \tilde{c}_{l\sigma} | \tilde{c}_{j\sigma}^{\dagger} \rangle_{\omega} , \tag{4.2.4}$$

where we neglect the higher order contribution of the transfer integral and correlation functions similarly to the Hubbard III. By noting that $\langle \delta n_{i-\sigma}^{-} \tilde{c}_{i\sigma} | \tilde{c}_{j\sigma}^{\dagger} \rangle_{\omega} = \langle n_{i-\sigma} \rangle \langle \tilde{c}_{i\sigma} | \tilde{c}_{j\sigma}^{\dagger} \rangle_{\omega}$, eq.(4.2.4) is easily solved as in Appendix 4.A and gives an expression of the scattering correction:

$$\sum_{k} t_{ik} \langle \delta n_{i-\sigma}^{-} \tilde{c}_{k\sigma} | \tilde{c}_{j\sigma}^{\dagger} \rangle_{\omega} = n_{-\sigma} \Omega_{\sigma}(\omega) \langle \tilde{c}_{i\sigma} | \tilde{c}_{j\sigma}^{\dagger} \rangle_{\omega} , \tag{4.2.5}$$

with

$$\Omega_{\sigma}(\omega) \equiv l_{\sigma}(\omega) - g_{\sigma}(\omega)^{-1} , \tag{4.2.6}$$

$$l_{\sigma}(\omega) \equiv (\omega-\varepsilon_{\sigma})/n_{-\sigma}^{-} , \tag{4.2.7}$$

and $$g_{\sigma}(\omega) \equiv N^{-1} \sum_{k} (l_{\sigma}(\omega) - \varepsilon_{k})^{-1} , \tag{4.2.8}$$

where $\varepsilon_{\sigma} \equiv \varepsilon_{i\sigma}$, $n_{-\sigma} \equiv \langle n_{i-\sigma} \rangle$, and $n_{-\sigma}^{-} \equiv 1-n_{-\sigma}$. Here $l_{\sigma}(\omega)$ and $g_{\sigma}(\omega)$ are a locator and a Green's function, respectively, without both the scattering and resonance broadening corrections.

The resonance broadening correction is similarly calculated from the following approximate equation of motion for $i \neq k$:

$$\begin{aligned} &(\omega-\varepsilon_{i\sigma}+\varepsilon_{i-\sigma}-\varepsilon_{k-\sigma}) \langle \tilde{c}_{k-\sigma} \tilde{c}_{i-\sigma}^{\dagger} \tilde{c}_{i\sigma} | \tilde{c}_{j\sigma}^{\dagger} \rangle_{\omega} \\ &\equiv \sum_{l} t_{kl} \langle n_{k\sigma}^{-} \tilde{c}_{l-\sigma} \tilde{c}_{i-\sigma}^{\dagger} \tilde{c}_{i\sigma} | \tilde{c}_{j\sigma}^{\dagger} \rangle_{\omega} - \sum_{k'} t_{ik'} \langle \tilde{c}_{k-\sigma} \tilde{c}_{k'-\sigma}^{\dagger} \tilde{c}_{i\sigma} | \tilde{c}_{j\sigma}^{\dagger} \rangle_{\omega} \end{aligned}$$

$$\equiv n_{\sigma}^{-} \sum_{l} t_{kl} \langle \tilde{c}_{l-\sigma}\tilde{c}_{i-\sigma}^{\dagger}\tilde{c}_{i\sigma} | \tilde{c}_{j\sigma}^{\dagger} \rangle_{\omega} - t_{ik} \langle \tilde{c}_{k-\sigma}\tilde{c}_{k-\sigma}^{\dagger} \rangle \langle \tilde{c}_{i\sigma} | \tilde{c}_{j\sigma}^{\dagger} \rangle_{\omega} \ . \tag{4.2.9}$$

This approximation is the same with that in the Hubbard III except the last term. In the Hubbard III $\langle \tilde{c}_{k-\sigma}\tilde{c}_{k-\sigma}^{\dagger} \rangle = \langle n_{k-\sigma}^{-} n_{k\sigma}^{-} \rangle$ is decoupled as $\langle n_{k-\sigma}^{-} \rangle \langle n_{k\sigma}^{-} \rangle$. Later Kawabata pointed out that in the half-filled and strong-coupling limit, this approximation does not result the Curie law for the susceptibility which is expected in this limit, and showed that the Curie law is obtained by using that $\langle n_{k-\sigma}^{-} n_{k\sigma}^{-} \rangle = 0$ in the above limit, with some assumptions. On the other hand in the t-J model, since the double occupancy is excluded, we can exactly put $\langle \tilde{c}_{k-\sigma}\tilde{c}_{k-\sigma}^{\dagger} \rangle = 1-n \equiv n_h$, with $n = n_{\alpha} + n_{\beta}$, and easily extend Kawabata's treatment to the non-half-filled case. Thus we obtain an expression of resonance broadening correction from eq.(4.2.9):

$$\sum_{k} t_{ik} \langle \tilde{c}_{k-\sigma}\tilde{c}_{i-\sigma}^{\dagger}\tilde{c}_{i\sigma} | \tilde{c}_{j\sigma}^{\dagger} \rangle_{\omega} = \frac{n_{-\sigma}}{n_{\sigma}^{-}} \Omega_{-\sigma}(\omega - \varepsilon_{\sigma} + \varepsilon_{-\sigma}) \langle \tilde{c}_{i\sigma} | \tilde{c}_{j\sigma}^{\dagger} \rangle_{\omega} \ . \tag{4.2.10}$$

Substituting eqs.(4.2.5) and (4.2.16) to the equation of motion (4.2.3), and using the Fourier transform $G_{k\sigma}(\omega) \equiv \sum_{i} e^{-ik \cdot R_{ij}} \cdot G_{ij\sigma}(\omega)$, we obtain

$$G_{k\sigma}(\omega) = (L_{\sigma}(\omega) - \varepsilon_{k})^{-1}, \tag{4.2.11}$$

$$G_{\sigma}(\omega) \equiv G_{ii\sigma}(\omega) = N^{-1} \sum_{k} G_{k\sigma}(\omega) \ , \tag{4.2.12}$$

with

$$L_\sigma(\omega) \equiv \frac{1}{n_{-\sigma}} \left[\omega - \varepsilon_\sigma - n_{-\sigma}\Omega_\sigma(\omega) - \frac{n_{-\sigma}}{n_\sigma} \Omega_{-\sigma}(\omega-\varepsilon_\sigma+\varepsilon_{-\sigma})\right] . \quad (4.2.13)$$

Now we introduce a self-consistency by replacing uncorrected locator $l_\sigma(\omega)$ and Green's function $g_\sigma(\omega)$ in eq.(4.2.6) with corrected ones, that is, $L_\sigma(\omega)$ and $G_\sigma(\omega)$, respectively, following Hubbard. This is performed without any arguments on its validity, but it would be convincing from the successful results of Hubbard[1] on the metal-insulator transition and from those of Kawabata[2] on the magnetic properties mentioned above. Thus the self-consistent equations are composed of eqs.(4.2.11)~(4.2.13), and

$$\Omega_\sigma(\omega) = L_\sigma(\omega) - G_\sigma(\omega)^{-1}, \quad (4.2.14)$$

$$\text{with} \quad n_\sigma = -\frac{1}{\pi} \int d\omega \, f(\omega) \, \mathrm{Im} \, G_\sigma(\omega) . \quad (4.2.15)$$

and $f(\omega) \equiv (e^{\omega/T}+1)^{-1}$.

It is worthwhile noting that in this self-consistent scheme if we neglect the resonance broadening correction given by the last term in the bracket of eq.(4.2.13), this scheme reduces to the CPA.[3] The CPA has been used by Fukuyama and Yoshida for the study of the high T_c superconductivity in the t-J model.[10] However, it is known that the CPA does not lead to the correct localized limit of the magnetic properties in the half-filled band limit similarly to the Hubbard I approximation, in which both the scattering and the resonance broadening correction are neglected.[1,27-29]

In the case of $\varepsilon_\sigma=-\mu$ and particular choice of the density of states (DOS),[1,2]

$$\rho(\varepsilon) = \begin{cases} \frac{4}{\pi W}\left[1-\left(\frac{2\varepsilon}{W}\right)^2\right]^{1/2}, \\ 0\ , \end{cases} \tag{4.2.16}$$

with the band width W, the self-consistent equations can be analytically solved as

$$G_\sigma(\omega) = \frac{4(2-n)}{W^2}\left(\omega+\mu \pm \sqrt{(\omega+\mu)^2-(W/2)^2}\ \right), \tag{4.2.17}$$

where $n=2n_\sigma$. Here the sign before the square root is determined so that $G_\sigma(\omega)$ satisfies the required analyticity ($\mathrm{Im}\, G_\sigma(\omega)<0$ and $G_\sigma(\omega)\propto 1/(\omega+\mu)$ for $|\omega+\mu|>>W/2$).

The momentum distribution $n_p\equiv n(\varepsilon_p)$ is given by

$$n_p = -\frac{1}{\pi}\int d\omega\, f(\omega)\, \mathrm{Im}\, G_{p\sigma}(\omega)\ . \tag{4.2.18}$$

We calculate the n_p for the DOS (4.2.16) and plot them in Fig.4.1. It is found that Fermi-surface does not exist for all n_h due to the presence of the quasi-particle damping although the damping decreases with n_h and vanishes as $n_h\to 1$. This means that the quasi-particle loses the phase coherence of the motion in a mean-free path. It should be noted that the strong on-site correlation would make the quasi-particle heavy and tend to be localized especially near the half-filled band case. This circumstance is expressed by the presence of the damping in our

treatment. It seems, however, that some global features such as the existence of Fermi-surface might be lost in the present approximation, especially in the case far from $n_h=0$. This is in contrast to the idea that the Fermi-liquid theory would work even in this strong coupling case except the half-filled band case, although it is not still clear that the Fermi-liquid theory holds in this case. Nevertheless, even if a small Fermi-jump exists near the half-filled band case, since the local correlation would be most important concerning the localized AF phase and the superconductivity of the local pairing in a nearly half-filled band case, our treatment would be reasonable for these problems.

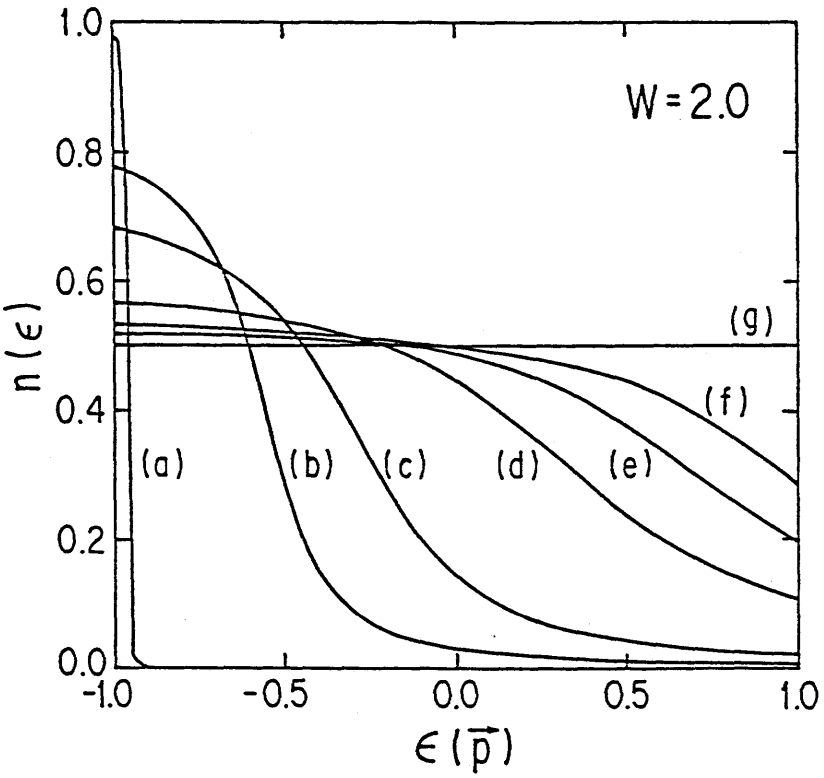

Fig.4.1. The crystal momentum distribution of the quasi-particle at T=0. ε_p is bare electron dispersion. (a) n_h=0.99, (b) n_h=0.7, (c) n_h=0.5, (d) n_h=0.2, (e) n_h=0.1, (f) n_h=0.05, (g) n_h=0.0. The unit is taken as W=2.

§4.3 Magnetic Susceptibility

In this section we examine the magnetic susceptibility for J=0 and that for J≠0. In order to calculate the susceptibility we add the term of $-g\mu_B H \sum_i S_i^z$ to the Hamiltonian, where H, g, and μ_B are the uniform magnetic field, Lande g-factor, and Bohr magneton, respectively. We take g=2 for simplicity, and also put $h=\mu_B H$.

When J=0, Green's function is obtained by replacing $\varepsilon_\sigma=-\mu$ with $\varepsilon_\sigma=-\mu-h\sigma$, in eq.(4.2.14):

$$L_\sigma(\omega) = \frac{1}{n_{-\sigma}^-}\left[\omega + \mu + h\sigma - n_{-\sigma}\Omega_\sigma(\omega) - \frac{n_{-\sigma}}{n_\sigma^-}\Omega_{-\sigma}(\omega+2h\sigma)\right], \quad (4.3.1)$$

where $n_\sigma=n/2+\sigma m$.

Now we define $\tilde{L}_\sigma(\omega) \equiv L_\sigma(\omega-h\sigma)$ and $\tilde{\Omega}_\sigma(\omega) \equiv \Omega_\sigma(\omega-h\sigma)$, and rewrite eq.(4.2.13), (4.2.15), and (4.3.1) in terms of $\tilde{L}_\sigma(\omega)$ and $\tilde{\Omega}_\sigma(\omega)$, as

$$\tilde{L}_\sigma(\omega) = \frac{1}{n_{-\sigma}^-}\left[\omega + \mu - n_{-\sigma}\tilde{\Omega}_\sigma(\omega) - \frac{n_{-\sigma}}{n_\sigma^-}\tilde{\Omega}_{-\sigma}(\omega)\right], \quad (4.3.2)$$

and

$$\tilde{\Omega}_\sigma(\omega) = \tilde{L}_\sigma(\omega) - \tilde{G}_\sigma(\omega)^{-1}, \quad (4.3.3)$$

$$\tilde{G}_\sigma(\omega) = N^{-1}\sum_{\mathbf{k}}(\tilde{L}_\sigma(\omega) - \varepsilon_{\mathbf{k}})^{-1}, \quad (4.3.4)$$

It should be noted here that the magnetic field does not appear explicitly in the self-consistent equations except the condition:

$$\frac{n}{2} + \sigma m = -\frac{1}{\pi}\int d\omega\, f(\omega)\ \mathrm{Im}\ G_\sigma(\omega)$$
$$= -\frac{1}{\pi}\int d\omega\, f(\omega)\ \mathrm{Im}\ \tilde{G}_\sigma(\omega+h\sigma)\ . \qquad (4.3.5)$$

Hence eqs.(4.3.2)~(4.3.4) determine $\tilde{G}_\sigma(\omega)$ as a function of ω, n, and m, so we expand $\tilde{G}_\sigma(\omega)$ and $\tilde{L}_\sigma(\omega)$ up to the first order of m:

$$\tilde{G}_\sigma(\omega) = \tilde{G}^{(0)}(\omega) + \sigma m\, \tilde{G}^{(1)}(\omega)\ , \qquad (4.3.6)$$
$$\tilde{L}_\sigma(\omega) = \tilde{L}^{(0)}(\omega) + \sigma m\, \tilde{L}^{(1)}(\omega)\ . \qquad (4.3.7)$$

Thus the condition (4.3.5) is written as

$$\frac{n}{2} = -\frac{1}{\pi}\int d\omega\, f(\omega)\ \mathrm{Im}\ \tilde{G}^{(0)}(\omega)\ , \qquad (4.3.8)$$
$$m = -\frac{1}{\pi}\int d\omega\, f(\omega)\ \mathrm{Im}\left[h\frac{\partial}{\partial\omega}\tilde{G}^{(0)}(\omega) + m\,\tilde{G}^{(1)}(\omega)\right]\ . \qquad (4.3.9)$$

Obviously $\tilde{G}^{(0)}(\omega)$ ($\tilde{L}^{(0)}(\omega)$) is nothing but the Green's function (the locator) of h=0 system, and will be written as $G(\omega)$ ($L(\omega)$) from now on. Equation (4.3.8) gives

$$m = h\,A + m\,B\ , \quad \text{i.e.} \quad m = \frac{\mu_B H\, A}{1 - B}\ , \qquad (4.3.10)$$

with

$$A \equiv -\frac{1}{\pi}\int d\omega\, f(\omega)\ \mathrm{Im}\ G'(\omega)\ , \qquad (4.3.11)$$
$$B \equiv -\frac{1}{\pi}\int d\omega\, f(\omega)\ \mathrm{Im}\ \tilde{G}^{(1)}(\omega)\ . \qquad (4.3.12)$$

The susceptibility χ is given by

$$\chi = \frac{g\mu_B m}{H} = \frac{2\mu_B^2 A}{1 - B}\ . \qquad (4.3.13)$$

Next we express $\tilde{G}^{(1)}(\omega)$ in terms of $G(\omega)$. From eq.(4.3.2) we have

$$L(\omega) = \bar{n}\ (\omega+\mu) + \frac{n(4-n)}{4}\ \frac{1}{G(\omega)}\ , \tag{4.3.14}$$

$$\frac{1-n}{\bar{n}}\ \tilde{L}^{(1)} - \frac{n^2}{4\ \bar{n}}\ \frac{\tilde{G}^{(1)}}{G^2} = \frac{1-n}{\bar{n}^2}\ L - \left(1+\frac{1-n}{\bar{n}^2}\right)\frac{1}{G}\ , \tag{4.3.15}$$

and from eq.(4.3.4)

$$\tilde{G}^{(1)}(\omega) = \tilde{L}^{(1)}(\omega)\ \chi_0(\omega)\ ,\ \text{and}\ \ G'(\omega) = L'(\omega)\ \chi_0(\omega)\ , \tag{4.3.16}$$

with $\chi_0(\omega)\equiv -N^{-1}\sum_{k} G_{k\sigma}(\omega)^2$ and $\bar{n}\equiv 1-n/2$. Differentiating each side of eq.(4.3.14) and using eqs.(4.3.15) and (4.3.16), we obtain

$$\chi_0(\omega) = G'/\ \left[\ \bar{n} - \frac{n(4-n)}{4}\ \frac{G'}{G^2}\ \right]\ , \tag{4.3.17}$$

and

$$G^{(1)}(\omega) = G'\ \frac{(1-n)\ (\omega+\mu) - 2\ \bar{n}^2\ G^{-1}}{\bar{n}\ \left[\ (1-n) + n\ \bar{n}\ \partial(G^{-1})/\partial\omega\ \right]}\ . \tag{4.3.18}$$

In the limit of $n\to 1$, the susceptibility in the case of $J=0$ shows the Curie law $\chi=\mu_B^2/T$, since

$$A = \beta\ (1-n) + O((1-n)^2)\ , \tag{4.3.19}$$

$$B = 1 - 2(1-n) + O((1-n)^2)\ , \tag{4.3.20}$$

around $n=1$ (see Appendix 4.B). This means that in the present approximation the localized free spin behaviour in the half-filled limit is correctly reproduced.

The case of $J \neq 0$ also reproduces the localized spin behaviour as following. We illustrate this within the mean field approximation of the exchange term in the Hamiltonian (4.1.1):

$$2J \sum_{i,j} (S_i \cdot S_j - \frac{1}{4} n_i n_j) \longrightarrow 2zJm \sum_{i\sigma} \sigma \, n_{i\sigma} \ . \qquad (4.3.21)$$

with the number of the nearest neighbour site z. In this way the Green's function is obtained by replacing h with $h_m \equiv h - 2zJm$ in the above treatment of J=0. Thus we found from eq.(4.3.9) and (4.3.10)

$$m = h_m A + m B \ , \quad \text{i.e.} \quad m = \frac{\mu_B H \, A}{1 - B + 2zJA} \ , \qquad (4.3.22)$$

$$\chi = \frac{2 \, \mu_B^2 \, A}{1 - B + 2zJA} \ . \qquad (4.3.23)$$

This leads to the Curie-Weiss law in the $n \to 1$ limit using eq.(4.3.19) and (4.3.20):

$$\chi = \frac{\mu_B^2}{T + zJ} \ . \qquad (4.3.24)$$

as was pointed out by Kawabata.[2] Our proof is more rigorous than that of Kawabata in the way of taking limit of $n \to 1$ and introducing J in the Green's function. As a result, we find that the analyticity of the Green's function is needed to prove, and it is also clarified that the Curie-Weiss form is derived reasonably in a mean field approximation.

In Fig.4.2, we plot the numerical results of the magnetic susceptibilities (4.3.23) for various J and n_h: J=0, J≠0, and $n_h \equiv 1-n=0$, 0.01, ···etc. It is found in both J=0 and J≠0 cases that the susceptibilities exhibit a gradual change from the Curie-Weiss law of the localized spins to the behaviour of itinerant electrons as Pauli-paramagnetic susceptibility, as doping electron holes, although the quasi-particle does not have the Fermi-surface in the crystal momentum space, as we have discussed in the end of §4.2.

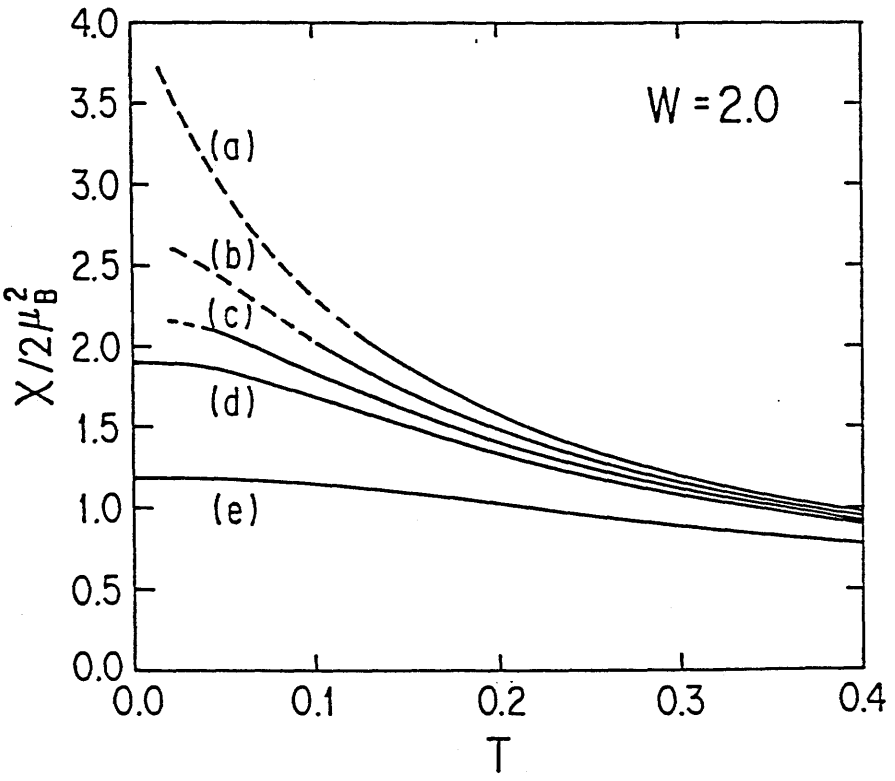

Fig.4.2. The temperature dependence of the magnetic susceptibility χ/μ_B^2 for the analytically solvable case given by DOS (4.2.16). The solid line and the broken line denotes the zJ=0 case and the zJ=0.12 case, respectively. (a) n_h=0, (b) n_h=0.01, (c) n_h=0.02, (d) n_h=0.03, (e) n_h=0.1, and zJ=0. (f) n_h=0, (g) n_h=0.1, and zJ=0.12. The unit is taken as W=2. The dotted line denotes the line given by eq.(4.3.23) below T_{AF}.

§4.4 Antiferromagnetism

In this section we study the antiferromagnetism of the t-J model. We divide the whole lattice into two sublattices A and B. The operator $c_{i\sigma}$, $n_{i\sigma}$, $\tilde{c}_{i\sigma}$, and $\varepsilon_{i\sigma}$ are denoted by $a_{i\sigma}$, $A_{i\sigma}$, $\tilde{a}_{i\sigma}$, and ε^A_σ, respectively (or $b_{i\sigma}$, $B_{i\sigma}$, $\tilde{b}_{i\sigma}$, and ε^B_σ, respectively), where the site i is belonging to the A- (or the B-) sublattice. Moreover we define $A_\sigma \equiv \langle A_{i\sigma}\rangle = n/2+\sigma m$, $\bar{A}_\sigma \equiv 1-A_\sigma$, $B_\sigma \equiv \langle B_{i\sigma}\rangle = n/2-\sigma m$, and $\bar{B}_\sigma \equiv 1-B_\sigma$. In the presence of a staggered magnetic field H, the Hamiltonian (4.1.2) is modified by putting $\varepsilon^A_\sigma = -\mu-h\sigma$ and $\varepsilon^B_\sigma = -\mu+h\sigma$ with $h \equiv \mu_B H$.

The equations of motion in the case of J=0 is

$$(\omega-\varepsilon^A_\sigma)\langle\tilde{a}_{i\sigma}|\tilde{a}^\dagger_{j\sigma}\rangle_\omega = \bar{A}_{-\sigma}(\delta_{ij} + \sum_k t_{ik}\langle\tilde{a}_{k\sigma}|\tilde{a}^\dagger_{j\sigma}\rangle_\omega)$$
$$+ \sum_k t_{ik}\langle \delta\bar{A}_{i-\sigma}\tilde{b}_{k\sigma}|\tilde{a}^\dagger_{j\sigma}\rangle_\omega + \sum_k t_{ik}\langle \tilde{b}_{k-\sigma}\tilde{a}^\dagger_{i-\sigma}\tilde{a}_{i\sigma}|\tilde{a}^\dagger_{j\sigma}\rangle_\omega , \quad (4.4.1)$$

$$(\omega-\varepsilon^B_\sigma)\langle\tilde{b}_{k\sigma}|\tilde{b}^\dagger_{j\sigma}\rangle_\omega = \bar{B}_{-\sigma}\sum_l t_{kl}\langle\tilde{b}_{l\sigma}|\tilde{a}^\dagger_{j\sigma}\rangle_\omega$$
$$+ \sum_l t_{kl}\langle \delta\bar{B}_{k-\sigma}\tilde{a}_{l\sigma}|\tilde{a}^\dagger_{j\sigma}\rangle_\omega + \sum_l t_{kl}\langle \tilde{a}_{l-\sigma}\tilde{b}^\dagger_{k-\sigma}\tilde{b}_{k\sigma}|\tilde{a}^\dagger_{j\sigma}\rangle_\omega . \quad (4.4.2)$$

Similarly to §4.2, the scattering correction in eq.(4.4.1) is calculated from the equations of motion:

$$\langle\delta\bar{A}_{i-\sigma}\tilde{b}_{k\sigma}|\tilde{a}^\dagger_{j\sigma}\rangle_\omega = 1^B_\sigma(\omega)^{-1}\sum_l t_{kl}\langle\delta\bar{A}_{i-\sigma}\tilde{a}_{l\sigma}|\tilde{a}^\dagger_{j\sigma}\rangle_\omega , \quad \text{for } i\neq k,$$
$$\langle\delta\bar{A}_{i-\sigma}\tilde{a}_{l\sigma}|\tilde{a}^\dagger_{j\sigma}\rangle_\omega = 1^A_\sigma(\omega)^{-1}\sum_m t_{lm}\langle\delta\bar{A}_{i-\sigma}\tilde{b}_{m\sigma}|\tilde{a}^\dagger_{j\sigma}\rangle_\omega , \quad \text{for } i\neq l, \quad (4.4.3)$$

with

$$1^A_\sigma(\omega) \equiv \frac{\omega - \varepsilon^A_\sigma}{A^-_{-\sigma}} \quad \text{and} \quad 1^B_\sigma(\omega) \equiv \frac{\omega - \varepsilon^B_\sigma}{B^-_{-\sigma}} \ . \tag{4.4.4}$$

They can be easily solved with the result:

$$\sum_k t_{ik} \langle \delta A_{i-\sigma}^- \tilde{b}_{k\sigma} | \tilde{a}^\dagger_{j\sigma} \rangle_\omega = A_{-\sigma} \Omega^A_\sigma(\omega) \langle \tilde{a}_{i\sigma} | \tilde{a}^\dagger_{j\sigma} \rangle_\omega \ , \tag{4.4.5}$$

where

$$\Omega^A_\sigma(\omega) \equiv 1^A_\sigma(\omega) - g^A_\sigma(\omega)^{-1} \ , \tag{4.4.6}$$

and $$g^A_\sigma(\omega) \equiv N^{-1} \sum_{\mathbf{k}} 1^B_\sigma(\omega)/(1^A_\sigma(\omega)\, 1^B_\sigma(\omega) - \varepsilon^2_{\mathbf{k}})^{-1} \ . \tag{4.4.7}$$

The resonance broadening correction is similarly calculated from the equations of motion:

$$\begin{aligned} &(\omega - \varepsilon^A_\sigma + \varepsilon^A_{-\sigma} - \varepsilon^B_{-\sigma}) \langle \tilde{b}_{k-\sigma} \tilde{a}^\dagger_{i-\sigma} \tilde{a}_{i\sigma} | \tilde{a}^\dagger_{j\sigma} \rangle_\omega \\ &\equiv B^-_\sigma \sum_l t_{kl} \langle \tilde{a}_{l-\sigma} \tilde{a}^\dagger_{i-\sigma} \tilde{a}_{i\sigma} | \tilde{a}^\dagger_{j\sigma} \rangle_\omega - t_{ik}(1-n) \langle \tilde{a}_{i\sigma} | \tilde{a}^\dagger_{j\sigma} \rangle_\omega \ . \end{aligned} \tag{4.4.8}$$

$$\begin{aligned} &(\omega - \varepsilon^A_\sigma + \varepsilon^A_{-\sigma} - \varepsilon^A_{-\sigma}) \langle \tilde{a}_{l-\sigma} \tilde{a}^\dagger_{i-\sigma} \tilde{a}_{i\sigma} | \tilde{a}^\dagger_{j\sigma} \rangle_\omega \\ &\equiv A^-_\sigma \sum_m t_{lm} \langle \tilde{b}_{m-\sigma} \tilde{a}^\dagger_{i-\sigma} \tilde{a}_{i\sigma} | \tilde{a}^\dagger_{j\sigma} \rangle_\omega \ , \end{aligned} \tag{4.4.9}$$

which leads to

$$\sum_k t_{ik} \langle \tilde{b}_{k-\sigma} \tilde{a}^\dagger_{i-\sigma} \tilde{a}_{i\sigma} | \tilde{a}^\dagger_{j\sigma} \rangle_\omega = \frac{B_{-\sigma}}{B^-_\sigma} \Omega^A_{-\sigma}(\omega - \varepsilon^A_\sigma + \varepsilon^A_{-\sigma}) \langle \tilde{a}_{i\sigma} | \tilde{a}^\dagger_{j\sigma} \rangle_\omega \ . \tag{4.4.10}$$

The correction terms in eq.(4.4.2) are obtained in the same way. Next, by replacing $l^A_\sigma(\omega)$, $l^B_\sigma(\omega)$, $g^A_\sigma(\omega)$, and $g^B_\sigma(\omega)$ with $L^A_\sigma(\omega)$, $L^B_\sigma(\omega)$, $G^A_\sigma(\omega)$, and $G^B_\sigma(\omega)$, in eq.(4.2.6), respectively, as discussed in §4.2, we have self-consistent equations from eqs.(4.4.1), (4.4.2), (4.4.5), (4.4.10):

$$G^A_\sigma(\omega) \equiv G^A_{ii\sigma}(\omega) = N^{-1}\sum_{\mathbf{k}} \frac{L^A_{-\sigma}(\omega)}{L^A_\sigma(\omega)\, L^A_{-\sigma}(\omega) - \varepsilon^2_{\mathbf{k}}} , \tag{4.4.11}$$

$$L^A_\sigma(\omega) \equiv \frac{1}{A^-_{-\sigma}} \left[\omega - \varepsilon^A_\sigma - A_{-\sigma}\Omega^A_\sigma(\omega) - \frac{A_\sigma}{A^-_{-\sigma}}\, \Omega^A_{-\sigma}(\omega-\varepsilon^A_\sigma+\varepsilon^A_{-\sigma})\right] , \tag{4.4.12}$$

$$\Omega^A_\sigma(\omega) \equiv L^A_\sigma(\omega) - G^A_\sigma(\omega)^{-1} , \tag{4.4.13}$$

and

$$A_\sigma = -\frac{1}{\pi}\int d\omega\, f(\omega)\, \mathrm{Im}\, G^A_\sigma(\omega) . \tag{4.4.14}$$

Here we have used the fact that $L^A_\sigma(\omega)=L^B_{-\sigma}(\omega)$, $G^A_\sigma(\omega)=G^B_{-\sigma}(\omega)$, and $A_\sigma=B_{-\sigma}$.

Equation (4.4.12) can be written in terms of $\tilde{L}^A_\sigma(\omega)\equiv L^A_\sigma(\omega-h\sigma)$, $\tilde{G}^A_\sigma(\omega)\equiv G^A_\sigma(\omega-h\sigma)$, and $\tilde{\Omega}^A_\sigma(\omega)\equiv\Omega^A_\sigma(\omega-h\sigma)$ as

$$\tilde{L}^A_\sigma(\omega) \equiv \frac{1}{A^-_{-\sigma}} \left[\omega + \mu - A_{-\sigma}\tilde{\Omega}^A_\sigma(\omega) - \frac{A_\sigma}{A^-_{-\sigma}}\, \tilde{\Omega}^A_{-\sigma}(\omega)\right] , \tag{4.4.15}$$

where the magnetic field does not appear explicitly.

Now we calculate the staggered magnetization. First we expand $\tilde{G}^A_\sigma(\omega)$ and $\tilde{L}^A_\sigma(\omega)$ up to the first order of m and h

$$\begin{aligned} \tilde{G}^A_\sigma(\omega) &= G(\omega) + \sigma\, \tilde{G}^{(1)}(\omega) + O(m^2, h^2) , \\ \tilde{L}^A_\sigma(\omega) &= L(\omega) + \sigma\, \tilde{L}^{(1)}(\omega) + O(m^2, h^2) , \end{aligned} \tag{4.4.16}$$

$$\tilde{\Omega}^{A}_{\sigma}(\omega) = \Omega(\omega) + \sigma\, \tilde{\Omega}^{(1)}(\omega) + O(m^2,\ h^2)\ ,$$

where the functions $G(\omega)$, $L(\omega)$, $\Omega(\omega)$ are those in the case of $m=0$ and $h=0$. Thus we find

$$L(\omega) = \bar{n}(\omega+\mu) + \frac{n(4-n)}{4}\,\frac{1}{G(\omega)}\ , \tag{4.4.17}$$

$$\tilde{L}^{(1)}(\omega) - (\frac{n}{2\bar{n}})^2\, \tilde{\Omega}^{(1)}(\omega) = -\frac{m}{\bar{n}}\,(\tilde{L}^{(0)}(\omega) - (\frac{n}{2\bar{n}})^2\, \tilde{\Omega}^{(0)}(\omega)\ )\ , \tag{4.4.18}$$

from eqs.(4.4.15) and (4.4.16). Furthermore, we expand $L^{A}_{\sigma}(\omega)$, $G^{A}_{\sigma}(\omega)$, $\Omega^{A}_{\sigma}(\omega)$ as

$$\begin{aligned} G^{A}_{\sigma}(\omega) &= G(\omega) + \sigma\, G^{(1)}(\omega) + O(m^2,\ h^2)\ , \\ L^{A}_{\sigma}(\omega) &= L(\omega) + \sigma\, L^{(1)}(\omega) + O(m^2,\ h^2)\ , \\ \Omega^{A}_{\sigma}(\omega) &= \Omega(\omega) + \sigma\, \Omega^{(1)}(\omega) + O(m^2,\ h^2)\ . \end{aligned} \tag{4.4.19}$$

Thus we have from eq.(4.4.14)

$$\frac{n}{2} = -\frac{1}{\pi}\int d\omega\ f(\omega)\ \mathrm{Im}\ G(\omega)\ , \tag{4.4.20}$$

$$m = -\frac{1}{\pi}\int d\omega\ f(\omega)\ \mathrm{Im}\ G^{(1)}(\omega)\ , \tag{4.4.21}$$

where $G^{(1)}(\omega)$ is obtained as

$$G^{(1)}(\omega) = h\,\frac{\partial}{\partial\omega}\,G(\omega) + \tilde{G}^{(1)}(\omega) \tag{4.4.22}$$

from the definition of $\tilde{G}^{A}_{\sigma}(\omega)$ and eqs.(4.4.16) and (4.4.19).

For simplicity, we define $I^A_\sigma(\omega)\equiv L^A_\sigma(\omega)-(\frac{n}{2\bar{n}})^2\Omega^A_\sigma(\omega)$, $\tilde{I}^A_\sigma(\omega)\equiv I_\sigma(\omega-h\sigma)$ and also their expansion factors by $I(\omega)$, $\tilde{I}^{(1)}(\omega)$ and $I^{(1)}(\omega)$, similarly to eqs.(4.4.16) and (4.4.19). Thus we have

$$\tilde{I}^{(1)}(\omega) = -\frac{m}{\bar{n}} I(\omega) , \quad h\frac{\partial}{\partial\omega} I(\omega) + \tilde{I}^{(1)}(\omega) = I^{(1)}(\omega) ,$$
$$I^{(1)}(\omega) = -\frac{I(\omega)}{G(\omega)} G^{(1)}(\omega) , \qquad (4.4.23)$$
$$I(\omega) = L(\omega) - (\frac{n}{2\bar{n}})^2\Omega(\omega) = \frac{1-n}{\bar{n}} [\omega + \mu + \frac{n\bar{n}}{1-n}\frac{1}{G(\omega)}] ,$$

where we use the fact that $G^{(1)}(\omega) = -\frac{G(\omega)}{L(\omega)} L^{(1)}(\omega)$. From these equations, it is easily derived that

$$G^{(1)}(\omega) = -G(\omega) [h\frac{\partial}{\partial\omega} \ln I(\omega) - \frac{m}{\bar{n}}] . \qquad (4.4.24)$$

Substituting this into eq.(4.4.21), and using eq.(4.4.20), we obtain

$$m = -hC + \frac{m}{\bar{n}}\frac{n}{2} , \qquad (4.4.25)$$

with

$$C = -\frac{1}{\pi}\int d\omega\, f(\omega)\, \mathrm{Im}[G\frac{\partial}{\partial\omega} \ln I(\omega)] . \qquad (4.4.26)$$

Thus the staggered magnetic susceptibility χ_{AF} is given by

$$\chi_{AF} = -\mu_B^2\frac{2-n}{1-n} C , \qquad (4.4.27)$$

This reduces to the form of that of the localized spin system: $\chi_{AF}=\mu_B^2/T$ in the limit of $n\to1$, as expected. This form is derived

from the expansion $C = -\beta(1-n) + O((1-n)^2)$ which is easily obtained from eq.(4.B.2).

Next we calculate the staggered susceptibility in the case of $J\neq 0$, in the mean field approximation of the exchange term. This is performed by putting $\varepsilon_\sigma^A=-\mu-h_m\sigma$ and $\varepsilon_\sigma^B=-\mu+h_m\sigma$ with $h_m\equiv h+M$ and $M\equiv 2zJm$. Thus the staggered magnetization is obtained by replacing h with h_m in eq.(4.4.25):

$$m = - h_m C + \frac{m}{n} \frac{n}{2} , \tag{4.4.28}$$

which leads to

$$\chi_{AF} = \frac{- (1-n/2)\ \mu_B^2\ C}{(1-n) + (2-n)zJC} . \tag{4.4.29}$$

If we take the limit $n\to 1$, we have

$$\chi_{AF} = \frac{\mu_B^2}{T - zJ} . \tag{4.4.30}$$

On the other hand, the AF transition temperature T_{AF} is given by the condition in which spontaneous magnetization appears:

$$\frac{1-n}{2-n} = zJ \frac{1}{\pi} \int d\omega\ f(\omega)\ \mathrm{Im}[G(\omega) \frac{\partial}{\partial\omega} \ln I(\omega)] . \tag{4.4.31}$$

In the $n\to 1$ limit, we again obtain the mean field result $T_{AF}=zJ$.

For various hole concentrations, T_{AF} is numerically calculated from eqs.(4.4.20) and (4.4.31). We show T_{AF} as a function of $n_h\equiv 1-n$, in Fig.4.3. It is found that doped itinerant holes

destroy the AF order very effectively, and T_{AF} vanishes even for very small hole concentration. The critical hole concentration n_h^c, at which T_{AF} vanishes, are shown in Fig.4.8 as well as in Fig.4.3. For example $n_h^c \cong 0.022$ in the case of zJ=0.06W. This behaviour is consistent with the experimental results of the high T_c oxides which shows the rapid distruction of the AF phase with slight hole-doping.

Lastly, we examine the equation of the magnetization for $T<T_{AF}$. First we examine that in the limit of $n\to 1$. We begin with the relation:

$$1-n = \langle \tilde{c}_{i\sigma} \tilde{c}_{i\sigma}^{\dagger} \rangle = -\frac{1}{\pi} \int_{-\infty}^{\infty} d\omega \, (1-f(\omega-\mu)) \, \mathrm{Im} \, G_{\sigma}^{A}(\omega-\mu) \, . \quad (4.4.32)$$

Here we note that the Green's function can be written as

$$\tilde{G}_{\sigma}^{A}(\omega-\mu) = A_{-\sigma}^{-} g(\omega-\mu) + O(1-n) \, , \quad (4.4.33)$$

near n=1 with a spin independent function $g(\omega-\mu)$ defined by

$$g(\omega-\mu) = [\, \omega + \tilde{G}_{\sigma}^{A}(\omega)^{-1} + \tilde{G}_{-\sigma}^{A}(\omega)^{-1} - (\tilde{L}_{\sigma}^{A}(\omega) + \tilde{L}_{-\sigma}^{A}(\omega)) \,]^{-1} \, . \quad (4.4.34)$$

This relation is obtained from eqs.(4.4.12) and (4.4.13). Substituting eq.(4.4.33) into eq.(4.4.32), we have

$$1 - n = e^{-\beta M \sigma} (\frac{1}{2} + \sigma m) \, D \, , \quad (4.4.35)$$

$$\text{with} \quad D \equiv -\frac{1}{\pi} \int d\omega \, e^{\beta(\omega-\mu)} \, \mathrm{Im} \, g(\omega) \, , \quad (4.4.36)$$

that is

$$2(1-n) = -\left(\cosh(\beta M) - 2m\sinh(\beta M)\right) D ,$$

$$0 = \left(\sinh(\beta M) - 2m\cosh(\beta M)\right) D , \qquad (4.4.37)$$

up to the order of 1-n. Therefore in the limit of n→1, we obtain

$$m = \frac{1}{2}\tanh(2zJm\beta) . \qquad (4.4.38)$$

The behaviour of the solution of m of this equation, i.e. the average value of S^z are shown in Fig.4.4. Equations (4.4.30) and (4.4.38) coincide with the mean field result of Heisenberg model as was pointed out by Kawabata,[2] in the large U Hubbard model, with some assumptions.

Second we examine the sublattice magnetization in the non-half-filled band case. The self-consistent equations (4.4.11) ~ (4.4.14) are solved numerically for zJ=0.1W, n=0.96, using the DOS given by eq.(4.2.16) conventionally. The results are shown in Fig.4.4. It is found that the spin moment shrinks by ~13% because of the hole-doping and that the temperature dependence is essentially the same with the half-filling case.

In addition, we calculate the momentum distribution in the AF phase and the result are shown in Fig.4.5, where we found that the electrons are more localized in the AF phase than in the normal phase. However, we should note that our treatments are within the mean field approximation on the exchange interaction J, in which the low lying excitations such as a spin-wave are neglected.

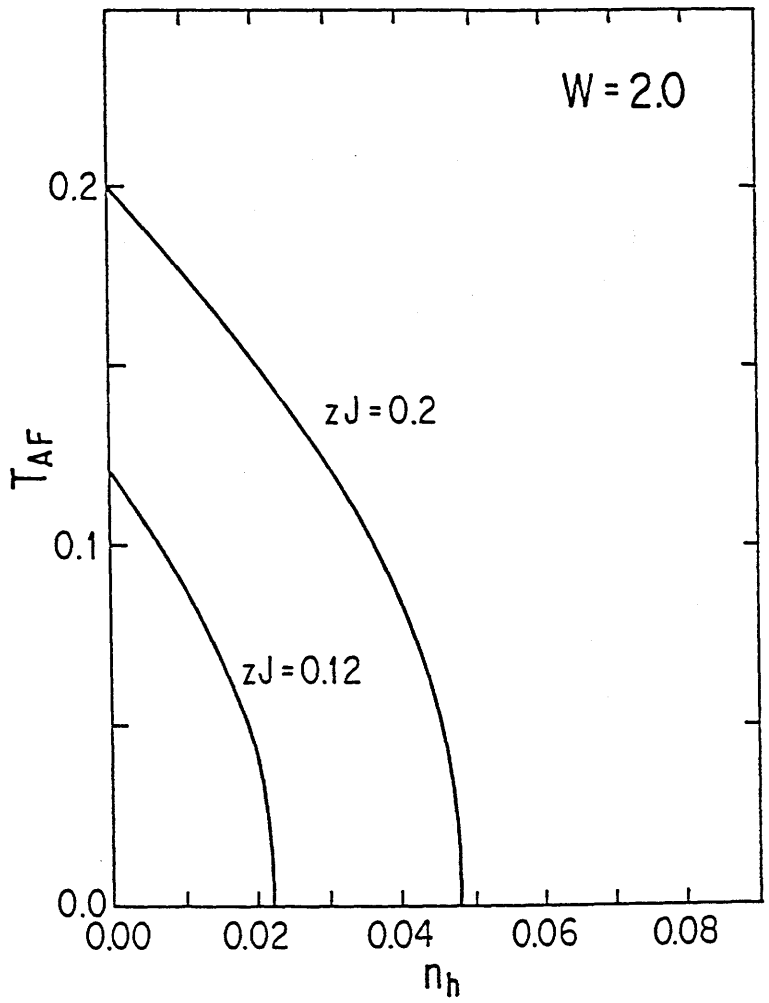

Fig.4.3. The AF transition temperature T_{AF} plotted to the hole densities n_h. The unit is taken as W=2.

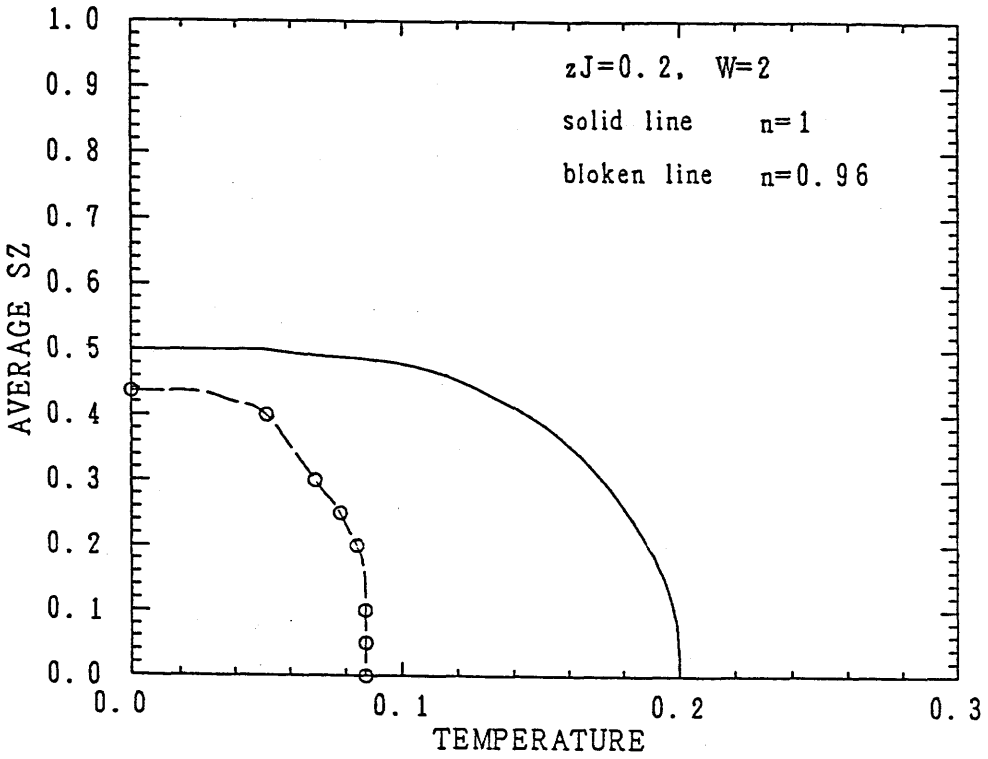

Fig.4.4. Temperature dependence of the staggered spin moment $m=\langle S_i^z \rangle$, for the half-filled band case (the solid line) and for the non-half-filled band case (n=0.96, the circle), with zJ=0.2. The broken line is to guide for eyes.

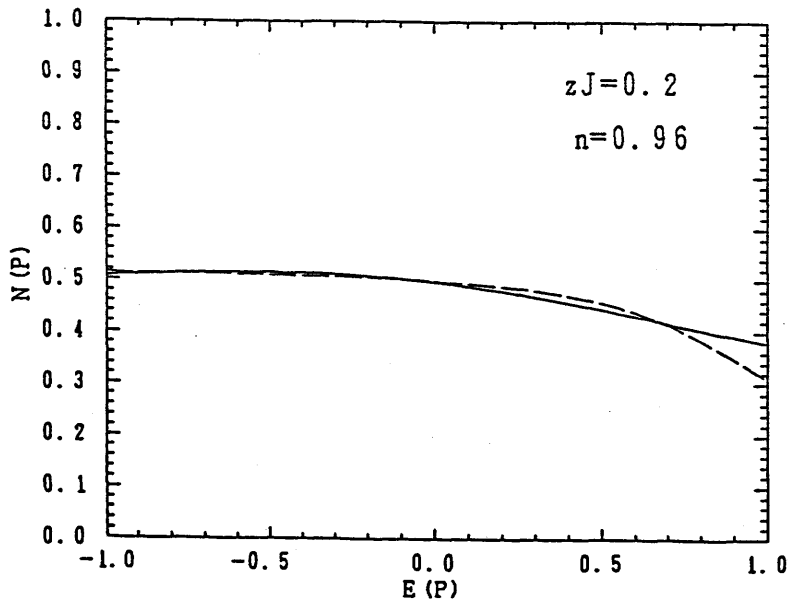

Fig.4.5. Momentum distribution in AF phase. We take zJ= 0.2, W=2.0, and n= 0.96.

§4.5 Superconductivity

In this section, we study the superconductivity induced by the exchange interaction given by the second term of eq.(4.1.1). Corresponding to the normal Green's function $G_{ij\sigma}(\omega)\equiv\langle\tilde{c}_{i\sigma}|\tilde{c}^{\dagger}_{j\sigma}\rangle_{\omega}$, we define the anomalous Green's function $F_{kj\sigma}(\omega)\equiv\langle\tilde{c}^{\dagger}_{k-\sigma}|\tilde{c}^{\dagger}_{j\sigma}\rangle_{\omega}$. We regard the average:

$$\Delta^{*}_{kj\sigma} \equiv 4J\langle\tilde{c}^{\dagger}_{j\sigma}\tilde{c}^{\dagger}_{k-\sigma}\rangle$$

$$= -\frac{4J}{\pi}\int_{-\infty}^{\infty}d\omega\, f(\omega)\, \mathrm{Im}[F_{kj\sigma}(\omega+i\delta)]\ , \qquad (4.5.1)$$

as an order-parameter of the superconductivity, which actually coincides with $4J\langle c^{\dagger}_{j\sigma}c^{\dagger}_{k-\sigma}\rangle$ in the t-J model.

First we study the s-wave pairing:

$$\Delta^{*}_{p\sigma} \equiv \sum_{k} e^{-ip\cdot R_{kj}}\,\Delta^{*}_{kj\sigma} = \frac{\sigma\Delta^{*}_{0}}{-t}\,\varepsilon_{p}\ , \qquad (4.5.2)$$

where ε_{p} is the bare electron dispersion defined by $\varepsilon_{p}\equiv\sum_{i}e^{-ip\cdot R_{ij}}\cdot t_{ij}$. For example, $\varepsilon_{p}=-2t(\cos(p_{x})+\cos(p_{y})+\cos(p_{z}))$ for the cubic lattice.

Now we note that the identity

$$\langle\tilde{c}^{\dagger}_{j\sigma}\tilde{c}^{\dagger}_{k-\sigma}\rangle = -\langle\tilde{c}^{\dagger}_{k-\sigma}\tilde{c}^{\dagger}_{j\sigma}\rangle \qquad (4.5.3)$$

requires the $F_{kj\sigma}(\omega+i\delta)$ to satisfy the condition:

$$\int_{-\infty}^{\infty} d\omega \; \mathrm{Im}[F_{kj\sigma}(\omega+i\delta)] = 0 \; . \tag{4.5.4}$$

The employed approximation scheme should not destroy such an identity. However a straightforward application of a decoupling approximation scheme sometimes destroys the above identity. Thus we propose the modified approximation scheme, in which the $F_{kj\sigma}(\omega+i\delta)$ satisfies the relation:

$$F_{kj\sigma}(\omega+i\delta) = F_{kj\sigma}(-\omega-i\delta) \; , \tag{4.5.5}$$

which guarantees the condition (4.5.4). We apply the decoupling theory studied in the preceding sections to each term of the equation of motion of the symmetrized form:

$$\begin{aligned} i\frac{\partial}{\partial t} F_{kj\sigma}(t) &\equiv i\frac{\partial}{\partial t}[-i\theta(t)\langle[\tilde{c}^{\dagger}_{k-\sigma}(\tfrac{t}{2}), \tilde{c}^{\dagger}_{j\sigma}(-\tfrac{t}{2})]_{+}\rangle] \; , \\ &= \frac{1}{2}\,[\langle[\tilde{c}^{\dagger}_{k-\sigma}, H]|\tilde{c}^{\dagger}_{j\sigma}\rangle - \langle\tilde{c}^{\dagger}_{k-\sigma}|[\tilde{c}^{\dagger}_{j\sigma}, H]\rangle] \; . \end{aligned} \tag{4.5.6}$$

This procedure makes no difference in the application to the normal Green's function compared to the treatment in §4.3 and §4.4. Under the assumptions mentioned above, we have

$$\begin{aligned} &\omega\, F_{kj\sigma}(\omega) \\ &= \frac{1}{2}\,[\,\{\,-\mu\,\langle\tilde{c}^{\dagger}_{k-\sigma}|\tilde{c}^{\dagger}_{j\sigma}\rangle_{\omega} - \bar{n}\sum_{l} t_{kl}\,\langle\tilde{c}^{\dagger}_{l-\sigma}|\tilde{c}^{\dagger}_{j\sigma}\rangle_{\omega} \\ &\quad - \sum_{l} t_{kl}\,\langle\,\delta n^{-}_{k\sigma}\tilde{c}^{\dagger}_{l-\sigma}\,|\tilde{c}^{\dagger}_{j\sigma}\rangle_{\omega} - \sum_{l} t_{kl}\,\langle\,\tilde{c}^{\dagger}_{k-\sigma}\tilde{c}_{k\sigma}\tilde{c}^{\dagger}_{l\sigma}|\tilde{c}^{\dagger}_{j\sigma}\rangle_{\omega} \\ &\qquad + \sum_{l} \Delta^{*}_{lk-\sigma}\,\langle\tilde{c}_{l\sigma}|\tilde{c}^{\dagger}_{j\sigma}\rangle_{\omega}\,\} \end{aligned}$$

$$- \{ - \mu \langle \tilde{c}^{\dagger}_{k-\sigma} | \tilde{c}^{\dagger}_{j\sigma} \rangle_{\omega} - \bar{n} \sum_{k'} t_{jk'} \langle \tilde{c}^{\dagger}_{k-\sigma} | \tilde{c}^{\dagger}_{k'\sigma} \rangle_{\omega}$$

$$- \sum_{k'} t_{jk'} \langle \tilde{c}^{\dagger}_{k-\sigma} | \delta n^{-}_{j-\sigma} \tilde{c}^{\dagger}_{k'\sigma} \rangle_{\omega} - \sum_{k'} t_{jk'} \langle \tilde{c}^{\dagger}_{k-\sigma} | \tilde{c}^{\dagger}_{j\sigma} \tilde{c}_{j-\sigma} \tilde{c}^{\dagger}_{k'-\sigma} \rangle_{\omega}$$

$$+ \sum_{k'} \Delta^{*}_{jk'\sigma} \langle \tilde{c}^{\dagger}_{k-\sigma} | \tilde{c}_{k'-\sigma} \rangle_{\omega} \}] \ . \qquad (4.5.7)$$

Here the decoupling $[\tilde{c}^{\dagger}_{k-\sigma}, H_{ex}] \cong \sum_{l} \Delta^{*}_{lk-\sigma} \tilde{c}^{\dagger}_{l-\sigma}$ has been used, where H_{ex} is the exchange term in eq.(4.1.1). Our approximation on H_{ex} resembles a mean field approximation, although it is different from the usual mean-field treatment of H_{ex} in treating the projection operator $n^{-}_{k\sigma}=1-n_{k\sigma}$. The scattering correction in the first term of eq.(4.5.7) is calculated from the equation of motion:

$$(\omega-\mu) \langle \delta n^{-}_{k\sigma} \tilde{c}^{\dagger}_{l-\sigma} | \tilde{c}^{\dagger}_{j\sigma} \rangle_{\omega}$$

$$\cong \bar{n} \sum_{m} t_{lm} \langle \delta n^{-}_{k\sigma} \tilde{c}^{\dagger}_{m-\sigma} | \tilde{c}^{\dagger}_{j\sigma} \rangle_{\omega} + \sum_{m} \Delta^{*}_{lm\sigma} \langle \delta n^{-}_{k\sigma} \tilde{c}_{m\sigma} | \tilde{c}^{\dagger}_{j\sigma} \rangle_{\omega}$$

$$+ \Delta^{*}_{lk\sigma} \langle \tilde{c}_{k\sigma} | \tilde{c}^{\dagger}_{j\sigma} \rangle_{\omega} \ , \qquad (4.5.8)$$

$$(\omega+\mu) \langle \delta n^{-}_{k\sigma} \tilde{c}_{m\sigma} | \tilde{c}^{\dagger}_{j\sigma} \rangle_{\omega}$$

$$\cong \bar{n} \sum_{n} t_{mn} \langle \delta n^{-}_{k\sigma} \tilde{c}_{n\sigma} | \tilde{c}^{\dagger}_{j\sigma} \rangle_{\omega} - \frac{n}{2} t_{km} \langle \tilde{c}_{k\sigma} | \tilde{c}^{\dagger}_{j\sigma} \rangle_{\omega} \ , \qquad (4.5.9)$$

where $k \neq l$ and $k \neq m$. Here we neglect the inhomogeneous terms and fluctuation terms including $\tilde{c}^{\dagger}_{m\sigma} \tilde{c}^{\dagger}_{l-\sigma} - \langle \tilde{c}^{\dagger}_{m\sigma} \tilde{c}^{\dagger}_{l-\sigma} \rangle$ in the present mean field like treatment. These equations are solved with use of $\langle \delta n^{-}_{k\sigma} \tilde{c}^{\dagger}_{k-\sigma} | \tilde{c}^{\dagger}_{j\sigma} \rangle = \frac{n}{2} F_{kj\sigma}$ and $\langle \delta n^{-}_{k\sigma} \tilde{c}_{k\sigma} | \tilde{c}^{\dagger}_{j\sigma} \rangle = \frac{n}{2} G_{kj\sigma}$. We have the expression of the scattering correction up to the first order of Δ_0:

$$\sum_l t_{kl}\langle \delta n^-_{k\sigma}\tilde{c}^\dagger_{l-\sigma}|\tilde{c}^\dagger_{j\sigma}\rangle_{\omega+i\delta}$$

$$\cong \frac{n}{2}\,\Omega^{(-)}F_{kj\sigma} - \frac{2-n}{2\bar{n}}\,\frac{\sigma\Delta_o^*}{-t}\,\Omega^{(-)}G_{kj\sigma}$$

$$- \frac{n}{2\bar{n}}\left(1-\frac{1}{\bar{n}}\right)\frac{\sigma\Delta_o^*}{-t}\,\frac{L^{(-)}\Omega^{(-)} - L\,\Omega}{L^{(-)} - L}\,G_{kj\sigma}\ , \qquad (4.5.10)$$

where $\Omega^{(-)}\equiv\Omega(-\omega-i\delta)$, $\Omega\equiv\Omega(\omega+i\delta)$, $L^{(-)}\equiv L(-\omega-i\delta)$, $L\equiv L(\omega+i\delta)$, etc. The scattering correction in the second term of eq.(4.5.7) is similarly calculated as

$$\sum_{k'} t_{jk'}\langle\tilde{c}^\dagger_{k-\sigma}|\delta n^-_{j-\sigma}\tilde{c}^\dagger_{k'\sigma}\rangle_{\omega+i\delta} = -\sum_{k'} t_{jk'}\langle\delta n^-_{j-\sigma}\tilde{c}^\dagger_{k'\sigma}|\tilde{c}^\dagger_{k-\sigma}\rangle_{-\omega-i\delta}$$

$$\cong -\frac{n}{2}\,\Omega\,F^{(-)}_{jk-\sigma} + \frac{2-n}{2\bar{n}}\,\frac{-\sigma\Delta_o^*}{-t}\,\Omega\,G^{(-)}_{jk-\sigma}$$

$$+ \frac{n}{2\bar{n}}\left(1-\frac{1}{\bar{n}}\right)\frac{-\sigma\Delta_o^*}{-t}\,\frac{L^{(-)}\Omega^{(-)} - L\,\Omega}{L^{(-)} - L}\,G^{(-)}_{jk-\sigma}\ . \qquad (4.5.11)$$

The resonance broadening correction in the first term in eq.(4.5.6) is calculated from the equation of motion:

$$(\omega-\mu)\ \langle\tilde{c}^\dagger_{k-\sigma}\tilde{c}_{k\sigma}\tilde{c}^\dagger_{l\sigma}|\tilde{c}^\dagger_{j\sigma}\rangle_\omega$$

$$\cong \bar{n}\sum_m t_{lm}\langle\tilde{c}^\dagger_{k-\sigma}\tilde{c}_{k\sigma}\tilde{c}^\dagger_{m\sigma}|\tilde{c}^\dagger_{j\sigma}\rangle_\omega + (1-n)\,t_{kl}\langle\tilde{c}^\dagger_{k-\sigma}|\tilde{c}^\dagger_{j\sigma}\rangle_\omega +$$

$$+ \sum_m \Delta^*_{lm\sigma}\langle\tilde{c}^\dagger_{k-\sigma}\tilde{c}_{k\sigma}\tilde{c}_{m-\sigma}|\tilde{c}^\dagger_{j\sigma}\rangle_\omega + \Delta^*_{kl\sigma}\langle\tilde{c}_{k\sigma}|\tilde{c}^\dagger_{j\sigma}\rangle_\omega\ ,$$

$$(\omega+\mu)\ \langle\tilde{c}^\dagger_{k-\sigma}\tilde{c}_{k\sigma}\tilde{c}_{m-\sigma}|\tilde{c}^\dagger_{j\sigma}\rangle_\omega$$

$$\cong \bar{n}\sum_n t_{mn}\langle\tilde{c}^\dagger_{k-\sigma}\tilde{c}_{k\sigma}\tilde{c}_{n-\sigma}|\tilde{c}^\dagger_{j\sigma}\rangle_\omega + \frac{n}{2}\,t_{km}\langle\tilde{c}_{k\sigma}|\tilde{c}^\dagger_{j\sigma}\rangle_\omega\ ,$$

where $k \neq l$ and $k \neq m$. The resulting expression for the resonance broadening correction is

$$\sum_l t_{kl} \langle \tilde{c}^{\dagger}_{k-\sigma} \tilde{c}_{k\sigma} \tilde{c}^{\dagger}_{l\sigma} | \tilde{c}^{\dagger}_{j\sigma} \rangle_{\omega+i\delta}$$

$$= \frac{n}{2\bar{n}} \Omega^{(-)} F_{kj\sigma} - \frac{1}{\bar{n}} \frac{\sigma\Delta_0^*}{-t} \Omega^{(-)} G_{kj\sigma}$$

$$+ \frac{n}{2\bar{n}^2} \frac{\sigma\Delta_0^*}{-t} \frac{L^{(-)}\Omega^{(-)} - L\,\Omega}{L^{(-)} - L} G_{kj\sigma} \,. \qquad (4.5.12)$$

Similarly, that of the second term in eq.(4.5.6) is calculated with the results:

$$\sum_{k'} t_{jk'} \langle \tilde{c}^{\dagger}_{k-\sigma} | \tilde{c}^{\dagger}_{j\sigma} \tilde{c}_{j-\sigma} \tilde{c}^{\dagger}_{k'-\sigma} \rangle_{\omega+i\delta} = - \sum_{k'} t_{jk'} \langle \tilde{c}^{\dagger}_{j\sigma} \tilde{c}_{j-\sigma} \tilde{c}^{\dagger}_{k'\sigma} | \tilde{c}^{\dagger}_{k-\sigma} \rangle_{-\omega-i\delta}$$

$$\equiv - \frac{n}{2\bar{n}} \Omega F^{(-)}_{jk-\sigma} + \frac{1}{\bar{n}} \frac{-\sigma\Delta_0^*}{-t} \Omega G^{(-)}_{jk-\sigma}$$

$$+ \frac{n}{2\bar{n}^2} \frac{-\sigma\Delta_0^*}{-t} \frac{L^{(-)}\Omega^{(-)} - L\,\Omega}{L^{(-)} - L} G^{(-)}_{jk-\sigma} \,. \qquad (4.5.13)$$

Inserting eqs.(4.5.10)~(4.5.13) into eq.(4.5.7), we obtain an expression for the Fourier transform $F_{p\sigma}(\omega+i\delta) \equiv \sum_k e^{-ip\cdot R_{kj}} F_{kj\sigma}(\omega+i\delta)$ up to the first order of Δ_0^*:

$$F_{p\sigma}(\omega+i\delta)$$

$$\equiv \frac{1}{\bar{n}} \left[\Delta^*_{p\sigma} + \frac{n(2+n)}{(2-n)^2} \frac{L^{(-)}\Omega^{(-)} - L\,\Omega}{L^{(-)} - L} \frac{\sigma\Delta_0^*}{-t} \right] G_{p\sigma} G^{(-)}_{-p-\sigma}$$

$$+ \frac{\sigma\Delta_0^*}{-t} \frac{4-n}{2-n} \frac{\Omega^{(-)} G_{p\sigma} - \Omega\, G^{(-)}_{-p-\sigma}}{L^{(-)} - L} \,. \qquad (4.5.14)$$

The first term in the bracket gives an anomalous Green's function with vertex correction $1/\bar{n}$ in an analogy of a diagramatic technique with the renormalized Green's function $G_{p\sigma}$. The imaginary part of this expression is an odd function of ω, and satisfies the condition (4.5.4) and (4.5.5), as is expected. The T_c equation for the nearest-neighbour s-wave superconductivity is obtained as

$$1 = -\frac{2J}{\bar{n}dt^2\pi}\int d\omega\, f(\omega)\, \mathrm{Im}\Big[-\frac{L^{(-)}G^{(-)}\Omega^{(-)} - L\,G\,\Omega}{L^{(-)}-L} - \frac{n(2+n)}{(2-n)^2}\frac{(L^{(-)}\Omega^{(-)}-L\,\Omega)(L^{(-)}G^{(-)}-L\,G)}{(L^{(-)}-L)^2} + \frac{4-n}{2-n}\frac{\Omega^{(-)}\Omega\,(G^{(-)}-G)}{L^{(-)}-L}\Big], \qquad (4.5.15)$$

where $d\equiv N^{-1}\sum_{p}\varepsilon_p^2/2t^2$ is the dimension of the system for the cubic lattice (d=3), square lattice (d=2), and 1D chain (d=1). Then since z=2d and band width W=4dt, the prefactor of the integral in eq.(4.5.15) becomes $2J/\bar{n}dt^2\pi=16zJ/\bar{n}W^2\pi$.

On the other hand, for the d-symmetry superconductivity, the last two terms vanish because of the symmetry. Thus we obtain the T_c equation for the d-symmetry superconductivity:

$$1 = -\frac{4J}{\bar{n}\pi}\int d\omega\, f(\omega)\, \mathrm{Im}[N^{-1}\sum_{p}\gamma_p^2\, G_{p\sigma}G^{(-)}_{-p-\sigma}], \qquad (4.5.16)$$

where we set $\Delta_{p\sigma}=\sigma\Delta_0\gamma_p$ with d-symmetry real function γ_p. For the nearest neighbour pairing, we have $\gamma_p=\cos(p_x)-\cos(p_y)$.

The detailed structure of the DOS does not seem to influence the estimation of eqs.(4.5.15) and (4.5.16) very much, since the

damping of the quasi-particle is rather large as is seen in §4.2. Thus we assume the DOS given by (4.2.16) for numerical estimation of T_c, and moreover set $\gamma_p^2 \cong 1$ in the integrand of eq.(4.5.16). The results are shown in Fig.4.6 for the d-wave case and in Fig.4.7 for the s-wave case. We find that the superconductivity does not appear near $n_h=0$ in the both two cases. This is due to the presence of the damping of the quasi-particle, which becomes more remarkable as one approaches $n_h=0$, as seen in §4.2. This effect is remarkable in s-wave superconductivity owing to the last two terms in eq.(4.5.14), which corresponds to the contribution from the vertex corrections in a diagramatic technique. Therefore the d-wave superconductivity is more favourable than the s-wave superconductivity, as seen in Figs.4.6 and 4.7. Moreover we show the numerical estimation of the critical J values for the superconductivity and the antiferromagnetism at ground state in Fig.4.8. It is found that for the weak J ($\lesssim 0.7t$) case, the t-J model does not exhibit the superconductivity for any n_h.

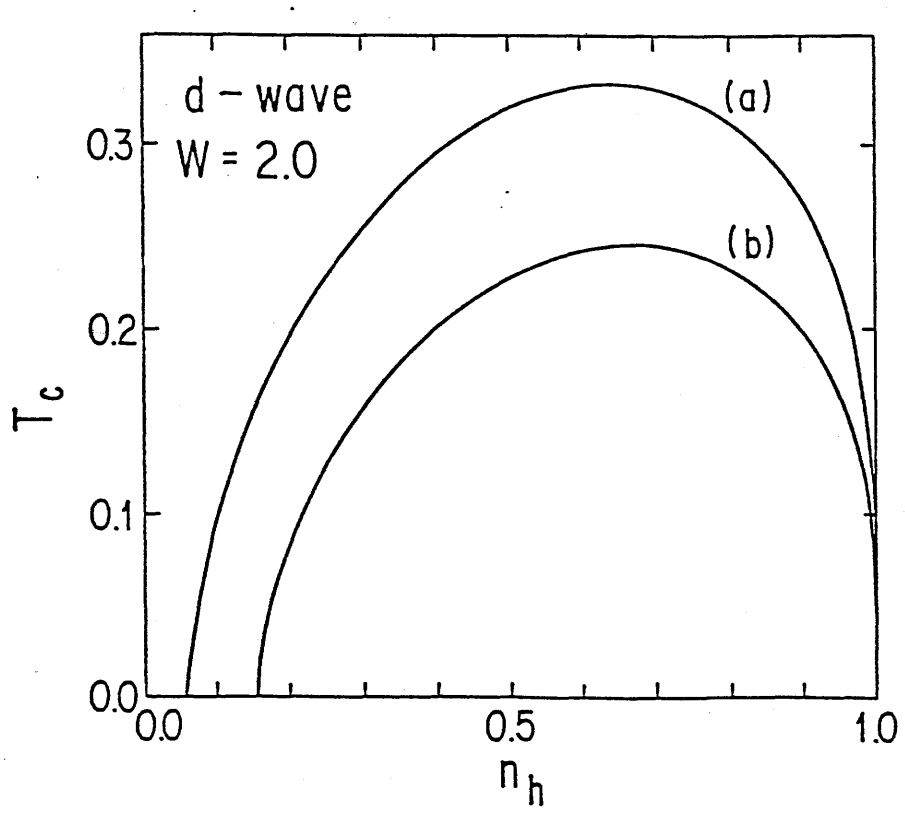

Fig.4.6. The hole concentration n_h dependence of T_c for d-pairing. (a) zJ=2.2, (b) zJ=1.8. The unit is taken as W=2. We put z=4 as an example.

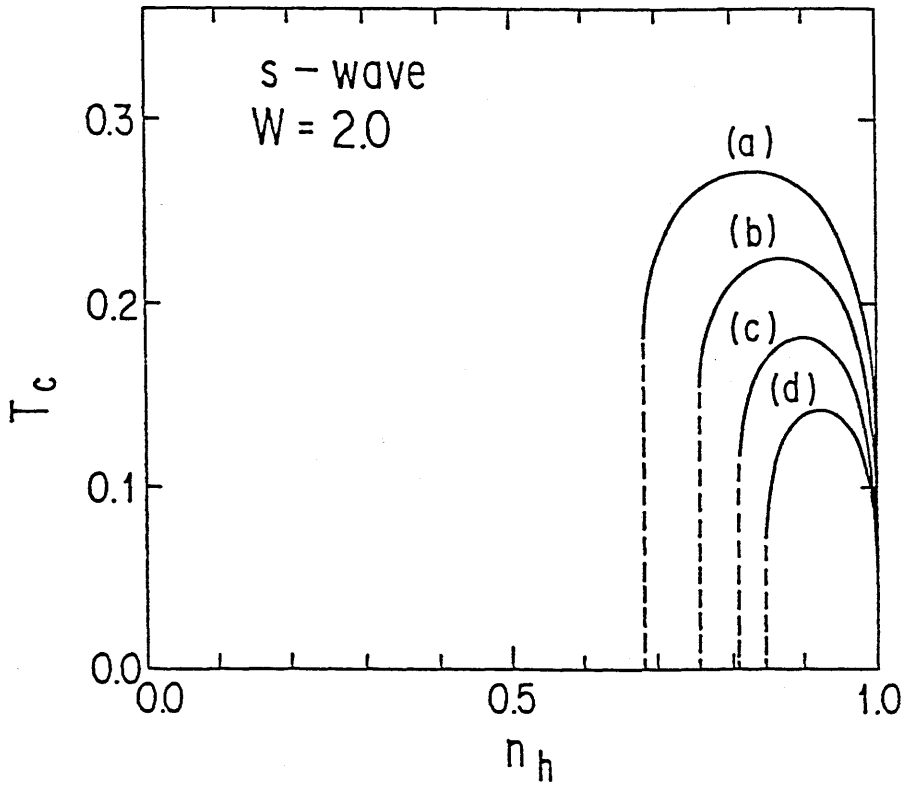

Fig.4.7. The hole concentration n_h dependence of T_c for s-pairing. (a) zJ=2.4, (b) zJ=2.2, (c) zJ=2.0, and (d) zJ=1.8. The unit is taken as W=2. z=2d, W=4td. d denotes the dimension of the system. The broken lines are conventionally drawn, in parallel with T_c axis. Here we omit unphysical solutions of the T_c equation, since they corresponds to transitions from the superconducting phase to the normal phase as decreasing temperatures.

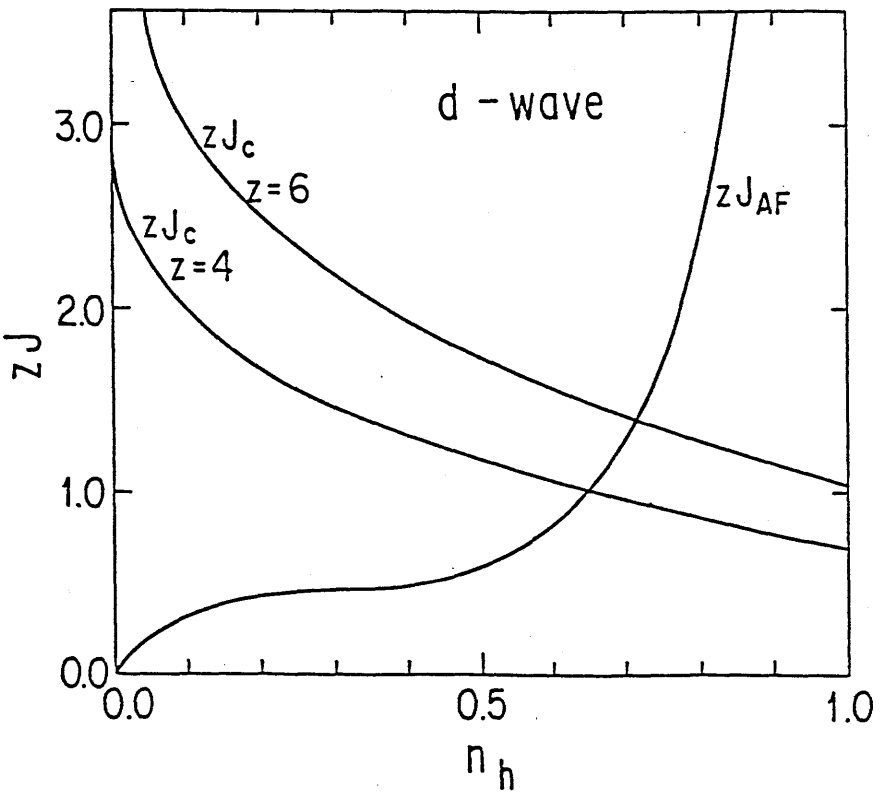

Fig.4.8. The hole concentration n_h dependence of the critical J value for the appearance of the antiferromagnetism J_{AF} and the (d-symmetry) superconductivity J_c, at T=0. The unit is taken as W=2. (a) zJ_c for z=6. (b) zJ_c for z=4. (c) zJ_{AF}.

§4.6 Green's function for Other Band Structures

The numerical calculation in the preceeding sections are based on the particular choise of the DOS given by eq.(4.2.16), which gives the analytical solution of the self-consistent equations of the Green's function. We expected that this costs little error at least qualitatively, because the imaginary part of the Green's function is necessarily large owing to the structure of the self-consistent equations. The purpose of this chapter is to verify this point.

First, we calculate the Green's function in the paramagnetic case, for electron systems on the cubic lattice, the square lattice, and 1D chain with n.n. hopping. We solve the self-consistent equations (4.2.11)~(4.2.15) numerically or analytically using the DOS for each band structure for n=0.95. Figs.4.9 ~4.10 show the results for the imaginary part of the Green's function, i.e. the one particle spectrum multiplied by π. It is found that for the cubic lattice the band width narrows into about 0.883W with that in the free case W, while for the square lattice the band width does not change from the free case. The band width narrowed in the former case is very close to the value calculated by Kubo[30] in the system of only one hole doped to half-filling. For the 1D chain, the band width is unreasonably broadened because of the unusual original band structure. Neverthless we find from this calculation that any sharp peaks and edges are smeared out as expected, and that the resulting spectrums are essentially of the same shape with that of the solvable DOS case if the band width are scaled. Therefore it is

obvious that our result obtained in the preceeding sections are almost unchanged for other band structures if we only scale the all energies by the band width taking into the band narrowing, which is found not to be so sensitive to the electron number.

In fact, we found from Fig.4.12 that the critical J values for the AF transition for the cubic lattice case are not different from that for the solvable DOS case qualitatively and even quantitatively if we scale the band width. In other words, the result for the cubic lattice with t=1 and n=0.95 is almost the same with that for the solvable DOS with the band width W=10.6, quantitatively. Moreover our consequence on the hole concentration dependence are not change even if we use the realistic band structures, because the extent of the band narrowing is not so sensitive to the hole concentration.

Now we comment on the ferromagnetism. The above result indicates that the magnetic susceptibility does not diverge for any hole concentration, since susceptibility for the realistic DOS hass almost the same behaviour with the susceptibility of the solvable DOS case with appropriate band width, which does not divergence as seen in §4.4. This is consistent with the CPA result.[3)]

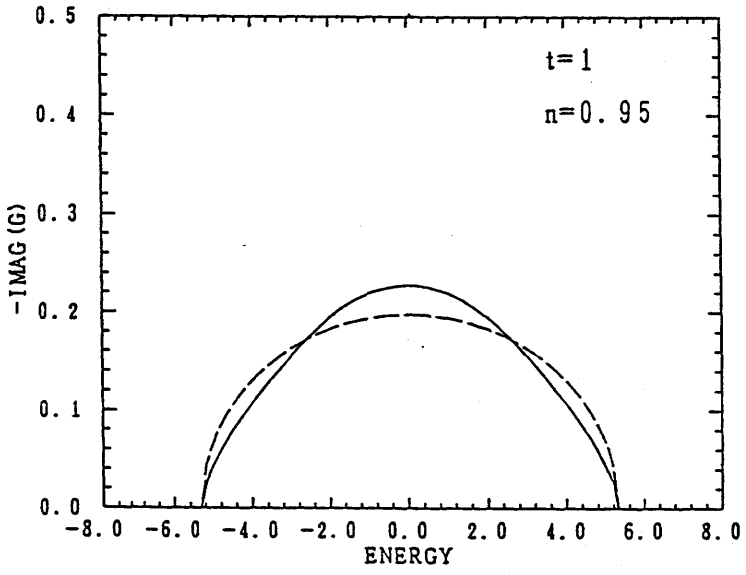

Fig.4.9.
Imaginary part of the Green's function for the cubic lattice band structure with t=1 (the solid line), and for the solvable DOS with W=10.6 (the broken line) in the case of n=0.95.

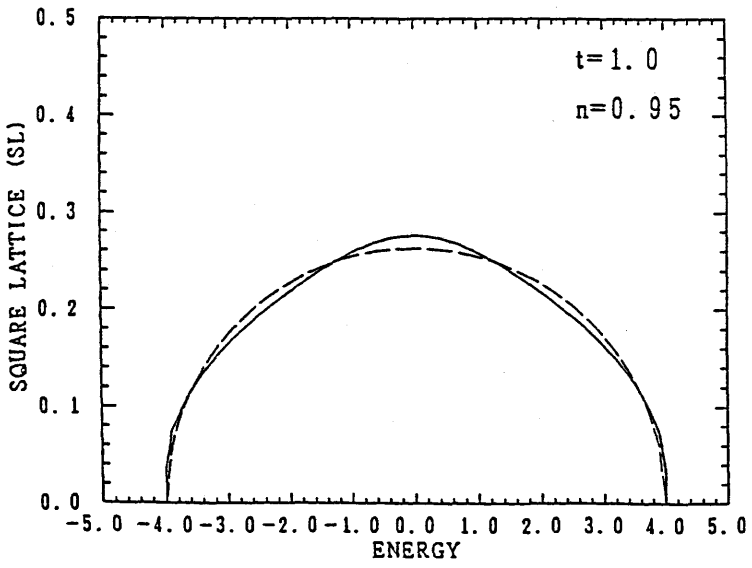

Fig.4.10.
Imaginary part of the Green's function, for the square lattice band structure with t=1 (the solid line), and for the solvable DOS with W=8 (the broken line) in the case of n=0.95.

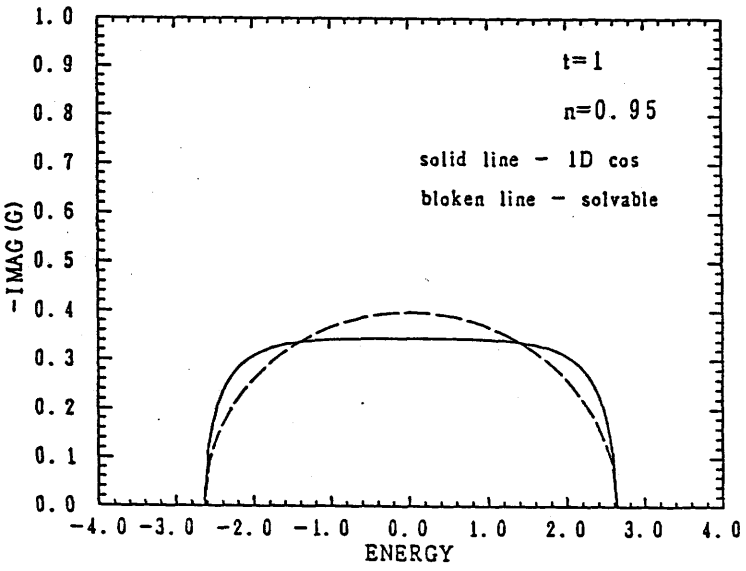

Fig.4.11.
Imaginary part of the Green's function, for the 1D cosin band with t=1 (the solid line), and for the solvable DOS with W=4 (the broken line) in the case of n=0.95.

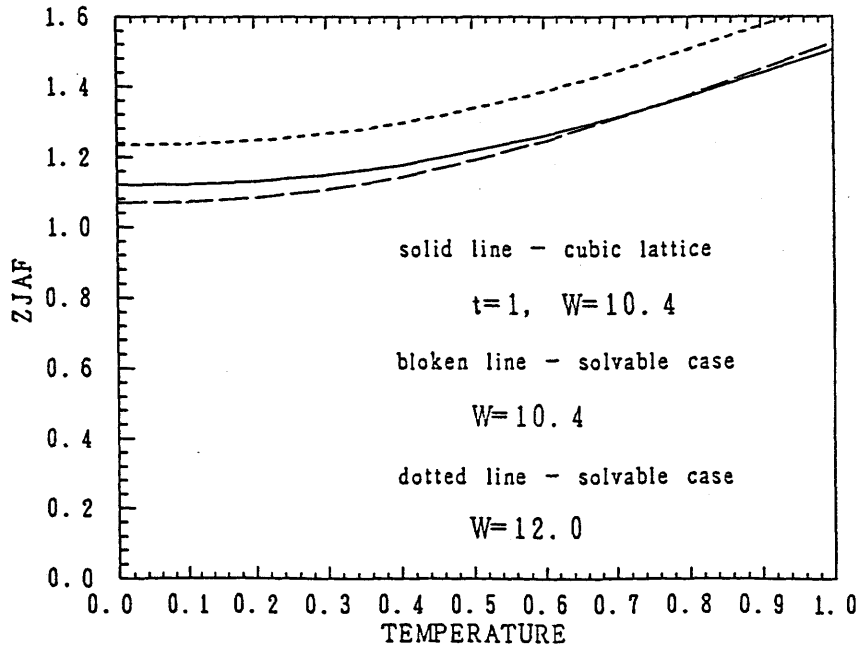

Fig.4.12. The critical J value multiplied by z for the cubic lattice band structure with t=1 (the solid line), for the solvable DOS with W=10.6 (the broken line), with W=12 (the dotted line), in the case of n=0.95.

§4.7 Summary and Discussion

Now we summarize and discuss the results which we have obtained in the previous sections. In §4.2, the normal electron Green's function in the case of J=0 has been examined. For the analytically solvable case given by the DOS (4.2.16), the Green's function and the momentum distribution of the quasi-particles are explicitly obtained. We found there that the Fermi-surface does not appear as can be seen in Fig.4.1, because of the damping of the quasi-particle resulting from the scattering and resonance broadening corrections.

However, in §4.3, we have found that the magnetic susceptibility changes from the Curie-Weiss law of the localized spin system to a Pauli-paramagnetism-like behaviour of the itinerant electrons with slight hole-doping, while the quasi-particle damping is still large, which indicates the localized character of the quasi-particles. This seems to well-reproduce the properties of the high-T_c superconductors in which the magnetic susceptibility seems to be that of itinerant electrons,[15,16] while the localized character of the electrons is indicated by the photo-emission studies.[13] We have also proved the Curie-Weiss form of the susceptibility in the $n_h \to 0$ limit of the t-J model, within the mean field approximation on H_{ex}.

In §4.4, we have calculated the AF transition temperatures and the staggered spin moment in the half-filled and the non-half-filled band case. At the half-filling our result coincides with the mean-field result of the AF Heisenberg model, reproducing the localized nature of electrons. In the non-half-filled

band case, the spin moment shrinks and the AF phase is found to vanish at a very small hole concentration, in which feature the t-J model also seems to well-reproduce the high-T_c superconductors.

Thus our approximation would be appropriate for describing the localized properties of the electrons and its change to the itinerant character, and the t-J model seems to describe the essential character of the high-T_c superconductors, at least with respect to the magnetic properties. Thus in §4.5 we have treated the correlation effect on the superconductivity through the first term of eq.(4.1.1) within the same approximation while the exchange term H_{ex} in eq.(4.1.1) is treated within the mean field approximation, and have calculated the superconducting transition temperatures T_c for the s- and d-symmetry cases, with the results of Figs.4.6~4.8. However, although the mean field approximation on H_{ex} is sufficient to illustrate the above argument, it might be insufficient for the quantitative arguments of T_{AF} and T_c for the high-T_c superconductors, since in such compounds the inter-CuO_2-plane coupling of J may be so weak that our resulting T_{AF} and T_c should be modified into smaller values. Moreover it is worthwhile noting that the superconductive quasi-long-range order remains below its Kosterlitz-Thouless temperature while the T_{AF} vanishes, in two dimensions. Therefore it is naturally expected that the suppression of T_{AF} is much larger than that of T_c, in the case in which the quasi-two-dimensionality is taken into account with an appropriate treatment. Thus we should be careful if we apply our theory to the quasi-two-dimensional systems such as high-T_c superconductors.

Nevertheless our theory gives the following qualitative results for the superconductivity in the t-J model:

(1) The superconductivity is found to be very difficult to obtain in the strong coupling Hubbard model ($J \ll t$), and near the half-filled band case, at least except below the very low temperatures mentioned above. The former result is consistent with the recent quantum simulation by Imada[8] and that of our perturbation theory in weak coupling Hubbard model.[23]

(2) The d-wave superconductivity is more favourable than the s-wave superconductivity in the t-J model of the rather large J case, or the strong coupling Hubbard model with some additional n.n. attractive interaction. This is because in the s-symmetry pairing case the damping of the quasi-particle seriously suppresses the superconductivity through the vertex correction which vanishes by symmetry in the d-wave pairing case. Such a tendency of the t-J model is consistent with the recent result of the variational Monte-Carlo studies by Yokoyama and Shiba.[9]

Lastly we calculated Green's function and critical J value for the antiferromagnetism for various DOS. We verified that the details of the band structure are smeared out due to the damping of the quasi-particle and does not affect the physical properties. As a result, for example, we found that the magnetic susceptibility does not diverge.

Appendix 4.A

Now we show the solution of f_{ik} which satisfies that

$$L\, f_{ik} = \sum_{l} t_{kl}\, f_{il} + A_{ik}\,, \qquad \text{for } k\neq i, \tag{4.A.1}$$

in terms of f_{ii}, $G=N^{-1}\sum_{p}(L-\varepsilon_p)^{-1}$, $\varepsilon_p \equiv \sum_{k} e^{-ip\cdot R_{kl}}\, t_{kl}$, L and $\bar{A}_{ip} \equiv \sum_{k(\neq i)} e^{-ip\cdot R_k}\, A_{ik}$. First we define the Fourier transform $\bar{f}_{ip} \equiv \sum_{k(\neq i)} e^{-ip\cdot R_k}\, f_{ik}$. From eq.(4.A.1), we have

$$\bar{f}_{ip} = \frac{\varepsilon_p}{L-\varepsilon_p}\, e^{-ip\cdot R_i}\, f_{ii} + \frac{\bar{A}_{ip}}{L-\varepsilon_p} - e^{-ip\cdot R_i} \sum_{l} t_{il} f_{il}\, \frac{1}{L-\varepsilon_p}\,. \tag{4.A.2}$$

On the other hand

$$\sum_{l} t_{il} f_{il} = N^{-1} \sum_{p} e^{ip\cdot R_i}\, \varepsilon_p \bar{f}_{ip}\,. \tag{4.A.3}$$

From eq.(4.A.2) and (4.A.3), we have

$$\sum_{l} t_{il} f_{il} = \Omega\, f_{ii} + \frac{1}{LG}\, N^{-1} \sum_{p} \frac{e^{ip\cdot R_i}\, \varepsilon_p \bar{A}_{ip}}{L-\varepsilon_p}\,, \tag{4.A.4}$$

with $\Omega=L-1/G$. Inserting eq.(4.A.4) to eq.(4.A.2), we obtain the solution:

$$\bar{f}_{ip} = \left(-1+ \frac{1}{G\cdot(L-\varepsilon_p)}\right) e^{-ip\cdot R_i}\, f_{ii}$$

$$+\frac{1}{L-\varepsilon_p}\left[\bar{A}_{ip}-\frac{1}{LG}e^{-ip\cdot R_i}N^{-1}\sum_{p'}\frac{e^{ip'\cdot R_i}\,\varepsilon_{p'}A_{ip'}}{L-\varepsilon_{p'}}\right], \quad (4.A.5)$$

Appendix 4.B

Now we prove the expansion (4.3.19) and (4.3.20) in the vicinity of n=1. First we note that

$$1-n=\langle\tilde{c}_{i\sigma}\tilde{c}_{i\sigma}^{\dagger}\rangle=-\frac{1}{\pi}\int_{-\infty}^{\infty}d\omega\,(1-f(\omega-\mu))\,\mathrm{Im}[G_{\sigma}(\omega-\mu)]\,. \quad (4.B.1)$$

Since $-\frac{1}{\pi}\mathrm{Im}[G_{\sigma}(\omega-\mu)]$ and $1-f(\omega-\mu)$ is positive definite and $G_{\sigma}(\omega-\mu)$ does not depend on μ, μ becomes very large in comparison with the band width in the limit of $n\to1$, so that $1-f(\omega-\mu)=e^{(\omega-\mu)\beta}/(e^{(\omega-\mu)\beta}+1)$ vanishes. In the vicinity of this limit $f(\omega-\mu)$ can be expanded as $f(\omega-\mu)=1-e^{(\omega-\mu)\beta}+\cdots$. Thus it is found that $e^{-\mu\beta}$ is order of (1-n) from (4.B.1).

Equation (4.3.19) is easily derived from above argument. Substituting $f(\omega-\mu)=1-e^{(\omega-\mu)\beta}+O((1-n)^2)$ into eq.(4.3.11) and partially integrating the right-hand-side of it, we have

$$A=-\beta\frac{1}{\pi}\int_{-\infty}^{\infty}d\omega\,e^{\beta(\omega-\mu)}\,\mathrm{Im}[G(\omega-\mu)]=\beta(1-n)+O((1-n)^2)\,. \quad (4.B.2)$$

Lastly we prove eq.(4.3.20). We rewrite eq.(4.3.18) as

$$\tilde{G}^{(1)}(\omega) = \frac{2}{n} G(\omega) + \frac{1-n}{\bar{n}^2} G(\omega)^2 \frac{-(\omega+\mu) + \frac{2\bar{n}}{n}\frac{G}{G'}}{n - \frac{1-n}{\bar{n}}\frac{G^2}{G'}} , \quad (4.B.3)$$

and eq.(4.3.12) as

$$B = \frac{2}{n}\left[-\frac{1}{\pi}\int_{-\infty}^{\infty} d\omega\, f(\omega)\, \mathrm{Im}\, G(\omega) \right]$$
$$- \frac{1}{\pi}\int_{-\infty}^{\infty} d\omega\, f(\omega-\mu)\, \mathrm{Im}\left[\tilde{G}^{(1)}(\omega-\mu) - \frac{2}{n} G(\omega-\mu)\right] . \quad (4.B.4)$$

This first term gives 1 from eq.(4.3.8). On the other hand, since Im[···] in the second term is O(1-n) from eq.(4.B.3), we put $f(\omega-\mu)=1$ there, correctly up to O(1-n) in eq.(4.B.4). Thus the second term of (4.B.4) is

$$-\frac{1}{\pi}\int_{-\infty}^{\infty} d\omega\, \mathrm{Im}\left[\tilde{G}^{(1)}(\omega-\mu) - \frac{2}{n} G(\omega-\mu)\right]$$
$$= -\frac{1}{\pi}\int_{C} dz \left[\tilde{G}^{(1)}(z) - \frac{2}{n} G(z)\right] , \quad (4.B.5)$$

where C is the infinite circle of the complex z space, and the function $\tilde{G}^{(1)}(z)$ and G(z) is analytic continuation to the upper (lower) half plane of the retarded (advanced) Green's function $\tilde{G}^{(1)}(\omega)$ and $G(\omega)$ ($\tilde{G}^{(1)}(\omega)^*$ and $G(\omega)^*$), respectively. Here we used the fact that the function $\tilde{G}^{(1)}(z)$ and G(z) are analytic except on the real axis. Noting that

$$G(z) \longrightarrow \frac{\bar{n}}{z} , \quad \text{as } |z|\to\infty , \quad (4.B.6)$$

we have

$$\tilde{G}^{(1)}(z) - \frac{2}{n} G(z) = - \frac{2(1-n)}{z} + O((1-n)^2) . \qquad (4.B.7)$$

Substituting this into eq.(4.B.5) and integrating it explicitly, we obtain

$$B = 1 - 2(1-n) + O((1-n)^2) . \qquad (4.B.8)$$

References 4.

1. J.Hubbard: Proc.Roy.Soc. A**276**(1963)283; **281**(1964)401.
2. A.Kawabata: Prog.Theor.Phys. **48**(1972)1793
3. H.Fukuyama and H.Ehrenreich: Phys.Rev.B **7**(1973)3266.
4. D.R.Penn: Phys.Rev. **142**(1966)350.
5. J.E.Hirsch: Phys.Rev.B **31**(1985)4403; **35**(1987)1851.
6. H. Yokoyama and H. Shiba: J.Phys.Soc.Jpn. **56** (1987)1490; **56** (1987)3570; **56**(1987)3582.
7. P.W.Anderson: Science **235**(1987)1196.
8. M. Imada: J. Phys. Soc. Jpn. **56** (1987) 3793; M. Imada and Y. Hatsugai: J.Phys.Soc.Jpn. **58**(1989)3752.
9. H.Yokoyama and H.Shiba: J.Phys.Soc.Jpn. **57**(1988)2482.
10. H.Fukuyama and K.Yoshida: Jpn.J.Appl.Phys. **26**(1987)L371.
11. J.G.Bednorz and K.A.Muller: Z.Phys.B **64**(1986)189.
12. C.W.Chu, P.H.Hor, R.L.Meng, L.Gao, Z.J.Huang and Y.Q. Wang: Phys.Rev.Lett. **58**(1987)405.
13. A.Fujimori, E.Takayama-Muromachi, Y.Uchida and B.Okai: Phys. Rev.B **35**(1987)8814.
14. T.Fujita, Y.Aoki, Y.Maeno, J.Sakurai, H.Fukuba and H.Fujii: Jpn.J.Appl.Phys. **26**(1987)L368.
15. H.Takagi, S.Uchida, H.Obara, K.Kishio, K.Kitazawa, K. Fueki and S.Tanada: Jpn.J.Appl.Phys. **26**(1987)L434.
16. N.P.Ong, Z.Z.Wang, J.Clayhold, J.M.Tarascon, L.H.Greene and W.R. McKnnon: Phys.Rev.B **35**(1987)8807.
17. N. Nishida, H. Miyatake, D. Shimada, S.Okuma, M.Ishikawa, T. Takabatake, Y.Nakazawa, Y. Kuno, R.Keitel, J.H. Brewer, T.M. Riseman, D.L.Williams, Y.Watanabe, T.Yamazaki, K. Nishiyama,

K.Nagamine, E.J.Ausaldo and E.Torikai: Jpn. J. Appl.Phys. **26** (1987)1856.

18. F.C.Zhang and T.M.Rice: Phys.Rev. B**37**(1988)3759.
19. H.Fukuyama, H.Matsukawa and Y.Hasegawa: J.Phys.Soc. Jpn. **58** (1989)364.
20. H.Shimahara and S.Takada: Jpn.J.Appl.Phys. **26**(1987)1674.
21. D.J.Scalapino, E.Loh,Jr. and J.E.Hirsch: Phys.Rev.B **34**(1986) 8190.
22. K.Miyake, S.Schmitt-Rink and C.M.Varma: Phys.Rev.B **34**(1986) 6554.
23. H.Shimahara and S.Takada: J.Phys.Soc.Jpn. **57**(1988)1044.
24. H.Shimahara: J.Phys.Soc.Jpn. **58**(1989)1735; in Proceeding of the Physics and Chemistry of Organic superconductors, edited by G. Saito and S. Kagoshima (Springer-Verlag, Berlin, Heidelberg, New York, to be published).
25. F.J.Ohkawa: Jpn.J.Appl.Phys. **26**(1987)L652; J.Phys.Soc.Jpn.**56** (1987)2267.
26. H.Shimahara, S.Misawa and S.Takada: J.Phys.Soc.Jpn. **58**(1989) 801; **58**(1989)4168; Proceeding of the Tsukuba Seminar on High T_c Superconductivity, edited by K. Masuda, T.Arai, I.Iguchi, and R.Yoshizaki (Univ. Tsukuba, Tsukuba, 1989), pp.73~78.
27. C.Mehrotra and K.S.Viswanathan: Solid State Commun. **12**(1973) 129.
28. C.Bastide and C.Lacroix: preprint.
29. S. Misawa: preprint. See also H. Fukuyama and Y. Hasegawa: Physica **148B**(1987)204.
30. K.Kubo: J.Phys.Soc.Jpn. **33**(1972)929.

Chapter 5.

Summary and Discussion

In this thesis, we have studied the electron systems with short range repulsive interaction in the weak coupling regime and in the strong coupling one, and discussed the relation to the quasi-one-dimensional (quasi-1D) organic superconductors and the copper oxide superconductors. We have examined the magnetism and superconductivity of the weak coupling Hubbard model in chapter 2 and 3, and those of the strong coupling Hubbard model and the t-J model in chapter 4. Our method used for the weak coupling model is a perturbation theory, and that for the strong coupling model is a decoupling scheme of the equation of motion of Green's function in real space. The specific features of the quasi-2D and the quasi-1D band structure have been examined in chapter 2 and 3, respectively.

The antiferromagnetic (AF) susceptibility of the half-filled non-interacting electron system on the square lattice exhibits the square logarithmic behaviour at low temperatures reflecting the logarithmic van Hove singularity and the perfect nesting of the Fermi-surface, as was shown in chapter 2. This means the strong correlation exists in the half-filled electron systems on a square lattice, even in the weakly interacting systems. Thus even a weak repulsive interaction causes an AF instability at low

temperatures and leads to the SDW state. Moreover uniform susceptibility exhibits logarithmic enhancement at half-filling as the temperature is lowered. However, such an enhancement of the AF susceptibility and uniform susceptibility are sensitively suppressed by slight hole-doping. Then the SDW phase vanishes and the uniform susceptibility becomes Pauli-paramagnetic.

Such crossover is seen in the strong coupling Hubbard model and t-J model as well. At half-filling, the susceptibility obeys the Curie-Weiss law reflecting the localized nature of the electrons. However the susceptibility becomes to show the temperature dependence like Pauli-susceptibility with slightly hole-doping. The doped holes move around and destroy the localized AF long-range-order very effectively. The sensitive but continuous change of the susceptibility and the antiferromagnetism have been shown in chapter 4. This behaviour is similar to that of the SDW, although their mechanisms are different. In the intermediate coupling regime, the AF transition temperature takes its maximum, but it would vanish with hole-doping.

The antiferromagnetism is also suppressed by introducing some kind of frustration such as next-nearest-neighbour (n.n.n.) hopping in the quasi-2D case. In itinerant electron systems, the n.n.n. hopping distorts the Fermi-surface and worsens the Fermi-surface nesting. As a result the AF correlation is suppressed. On the other hand, in the localized electron system, the n.n.n. hopping leads to the kinetic or super exchange interaction between spins on the n.n.n. sites, which is nothing but the frustration to the antiferromagnetism. The sensitive suppression of the SDW due to the n.n.n. hopping has been shown in chapter 2.

The SDW in the quasi-1D organic compounds is also suppressed by the distortion of the Fermi-surface with the pressure increased, as many authors argued. The same effect for the localized antiferromagnetism has not been demonstrated in this thesis, but it is quite plausible from the above arguments.

These similar behaviours of the magnetic quantities in the weak and the strong coupling regime seem to suggest the continuous change of the magnetic properties in intermediate coupling regime in the Hubbard model. However near half-filling, this problem is closely related to the Mott-Hubbard transition, which occurs in the intermediate coupling regime. The quantum simulation study by Hirsch supports the continuous change of the AF transition temperature.[1)]

After the suppression of the AF transition, AF correlations remain strong and may lead to an attractive interaction between the electrons on the different sublattice sites, as many authors argued.[2,3,4)] The long-range nature of the AF correlation leads to the same nature of the attractive interaction. Such nature enhances the superconductivity remarkably in the itinerant electron case, because in this case the contribution from the electrons near the Fermi-surface is large. We have examined this behaviour in quasi-1D systems in chapter 3, and obtained the the phase diagram which qualitatively agrees with that of the organic superconductors, by taking into account the long-range SDW fluctuations along the conductive chains. On the other hand, in the localized electron case, in which the Fermi-liquid description breaks down, or even in the Fermi-liquid systems in which the

Fermi-jump is small, the major contribution to the superconductivity would arise from the n.n. interaction, such as the kinetic exchange interaction J in the t-J model. This case was studied in chapter 4, and it was found that the superconductivity is difficult to appear in the Hubbard model with only n.n. hopping, consistently with the result of the quantum simulation by Imada et al.[5,6] Moreover, we found that the d-wave pairing is more favourable than the s-wave pairing in the t-J model, consistently with the result of the variational Monte-Carlo by Yokoyama et al.[7]

Futhermore we have studied the superconductivity in the weak coupling 2D Hubbard model in chapter 2. We have obtained the vanishingly small but finite transition temperature of d-wave superconductivity in the model with only n.n. hopping. However it was also found that the n.n.n. hopping integral does not only suppress the SDW transition but also enhances the superconductivity remarkably. Such tendency was also found in recent quantum simulation study by dos Santos,[8] in which they have studied the 2D Hubbard model with n.n. and n.n.n. hoppings, and showed that the d-wave pairing susceptibility enhances as temperature is lowered and becomes larger than that in the non-interacting case. On the other hand, in the strong coupling Hubbard model, we have not examined the same effect of the n.n.n. hopping. However we conjecture that the n.n.n. hopping may enhance the superconductivity in the strong coupling case as well, from the above argument on the relation of the weak and the strong coupling model.

Lastly we should comment on the low-dimensionality. We have examined the specific features of the quasi-low-dimensional band structures in chapter 2 and 3. However, in our present theories, we have assumed the three dimensionality enough to suppress the thermal fluctuations and to make the long-range-ordering possible. Such an assumption may be invalid for the copper oxide superconductors, which may have extremely small three dimensional coupling between CuO_2 planes.[9] In this case the quasi-long-range order is formed, and then the exchange of low energy spin-wave like excitation may lead attractive interaction between electrons. This remains for future studies.

References 5.

1. J.E.Hirsch: Phys.Rev.B **35**(1987)1851; Phys.Rev.Lett. **51**(1983) 1900; Phys.Rev.B **31**(1985)4403.
2. V.J.Emery: Synth.Met.13(1986)21.
3. D.J.Scalapino, E.Loh,Jr., and J.E.Hirsch: Phys.Rev.B**34**(1986) 8190; Phys.Rev. B**35**(1987)6694.
4. K.Miyake, S.Schmitt-Rink, and C.M.Varma: Phys.Rev.B **34**(1986) 6554.
5. M.Imada: J.Phys.Soc.Jpn. **56**(1987)3793.
6. M.Imada and Y.Hatsugai: J.Phys.Soc.Jpn. **58**(1989)3752.
7. H.Yokoyama and H.Shiba: J.Phys.Soc.Jpn. **57**(1988)2482.
8. R.R.dos Santos: Phys. Rev. B **39**(1989)7259; See also K.Saito and S.Takada: J.Phys.Soc.Jpn. **58**(1989)783.
9. S.Chakravaty, B.I.Halperin, and D.R.Nelson: Phys.Rev.Lett. **60**(1988)1057.